CHAPTER IV
RESULTS AND DISCUSSION

1. Rifampicin Precipitates by Supercritical Fluid Technique

Scanning electron microscope images of the raw material rifampicin are shown in Figure 4-1 (a). The starting material consisted of larger polygon particles that were up to 10 μm in size and with a broad size distribution. Supercritical antisolvent (SAS) precipitation had been used to produce supercritical-processed rifampicin. Rifampicin was dissolved in methylene chloride and sprayed into supercritical carbon dioxide at 2500 psi, 40 °C, solution concentration of 2 % w/v and solution feed rate of 0.5 ml/min were employed. SEM images of the powder precipitated from this experiment show that rifampicin was precipitated in form of long needles of crystals (Figure 4-1 (b)). Dimethyl sulfoxide (DMSO) was also used as a solvent of rifampicin and sprayed into supercritical carbon dioxide at the same operating condition. The solution of rifampicin in DMSO did not precipitate in the pressure chamber. The product could not be obtained. The same results were obtained from the rifampicin in DMSO: methylene chloride solution at ratio of 1:9, 1:4, 3:7, 2:3, 1:1, 3:2, 7:3, 4:1 and 9:1.

This result was in contrast to the previous SAS precipitation experiment by Reverchon et al. (2002), which performed using *N*-methyl 2-pyrrolidone (NMP), methyl alcohol (MeOH), and methylene chloride (MeC), rifampicin was precipitated in form of tightly networked nanoparticles while using ethyl acetate (EtAc) mostly obtained some millimeters long needlelike crystals. In addition, they could prepare spherical single microparticles with mean diameters ranged from 2.5 to 5 μm using dimethyl sulfoxide (DMSO), operating at 40 °C and a pressure between 90 and 110 bar. When they increased pressure to 120 bar (~1740 psi) or more, rifampicin was precipitated in form of nanoparticles coalesced in small groups. The difference in the product obtained, it might be that not only the apparatus used was different but also the operating conditions used. Specifically, amount of carbon dioxide and its flow rate used in this research (1.5 g/min) were lower than in the previous work (20 g/min). So, it was not sufficient to induce precipitation of rifampicin from the solution of DMSO and its mixture with methylene chloride.

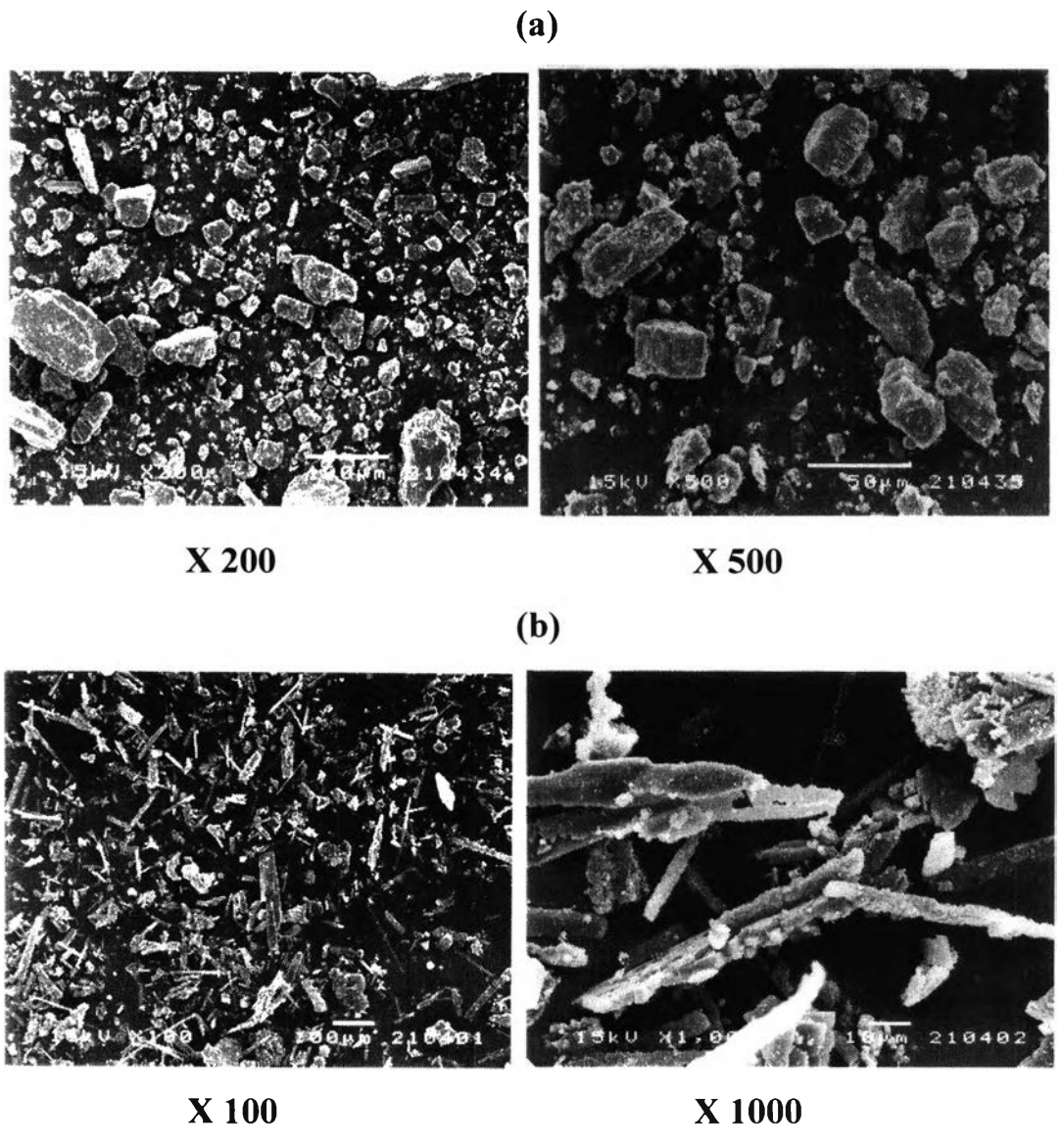

Figure 4-1 SEM of unprocessed rifampicin (a) processed rifampicin (b) using supercritical antisolvent precipitation from methylene chloride at 2500 psi, 40 ^{o}C, 2% w/v solution and solution feed rate of 0.5 ml/min.

2. The Co-Precipitation of Rifampicin and Various Biodegradable Polymers by Supercritical Fluid Technique

The supercritical anti-solvent method was carried out in order to design controlled release systems. This study focused on the co-precipitation of rifampicin and various biodegradable polymers.

2.1 Effect of Polymer Type and Polymer Content

2.1.1 PLGA

The morphology of rifampicin-DL PLGA microparticles at various polymer drug ratios is summarized in Table 4-1. In the production of drug loaded DL-PLGA microparticles, 2% w/v solution of rifampicin and DL-PLGA in methylene chloride, an operating pressure of 2500 psi, temperature of 33 °C and solution feed rate of 0.5 ml/min were used. Biodegradable rifampicin microparticles were observed using a scanning electron microscope (SEM) to determine particle morphology. In this experiment, it was observed that film was formed at the base and on the wall of the high-pressure vessel when using high polymer content. The products from SAS process of 100 %, 90 % and 80 % DL-PLGA were films having 1-3 μm pores which tightly adhered on the bottom of vessel (Figure 4-2). The pores might be due to the penetration of supercritical carbon dioxide into the film. The products containing 90 % and 80 % polymer contents provided smoother surface and continuously porous films than those containing 100 % polymer content. The precipitates generated from 70 % and 60% PLGA were films adhering to the bottom of the vessel. SEM photomicrographs show that their fine structure was microparticles coalescing in large groups and network (Figure 4-3). The network consisted of fused agglomerates. At 1:1 polymer-drug ratio (50% DL-PLGA), the discontinuous film was obtained and fused agglomerates was observed in fine microstructure. It was likely that the tendency for rifampicin-PLGA microparticles to flocculate and fuse together had decreased when increased % drug loading and decreased percent polymer content. At low polymer content (20-40%), products with irregular and highly agglomerated particles were produced (Figure 4-4). In addition, at 1:4 polymer-drug ratio (20% DL-

PLGA), drug crystals was observed. This result showed that amount of polymer was insufficient to encapsulate the drug.

Polymer had the ability to fuse and to form films or fibers instead of spherical particles, because of the complex phase separation involved in the precipitation pathway (Dixon et al. 1993 and Subra et al. 2000). Polymers could also absorb dense gases, including CO_2. The effect of this CO_2 sorption was swelling and plasticization (depression of the glass transition temperature) that affected the agglomeration of the primary particles and yielded softened or fused structure. So, the agglomerates and its fusion to form networks occurred by depression in the glass transition temperature (T_g) due to plasticization effect, especially at high polymer: drug ratio (>50% polymer content).

Table 4-1 The morphology rifampicin-DL-PLGA microparticles at various polymer drug ratios.

Polymer type	Polymer content	Rifampicin (%)	Polymer : drug ratio	Morphology
DL-PLGA	100 %	0 %	-	film
	90 %	10 %	9:1	film
	80 %	20 %	4:1	film
	70 %	30 %	7:3	film
	60 %	40 %	3:2	film
	50 %	50 %	1:1	film
	40 %	60 %	2:3	aggregated particles
	30 %	70 %	3:7	aggregated particles
	20 %	80 %	1:4	aggregated particles

100%PLGA

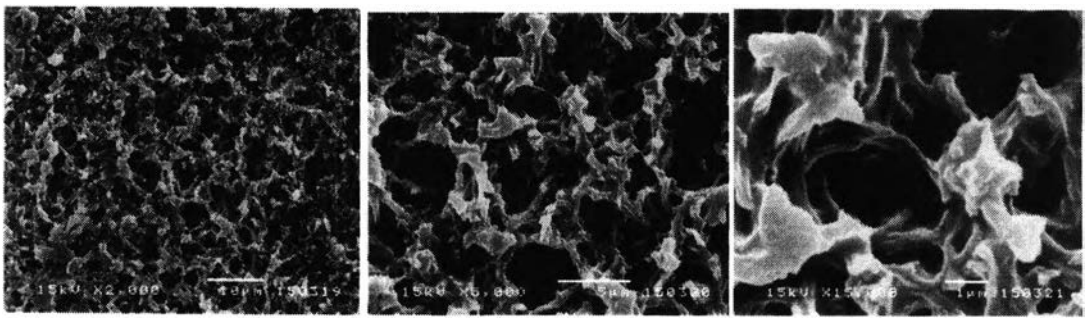

X 2000 **X 5000** **X 15000**

90%PLGA

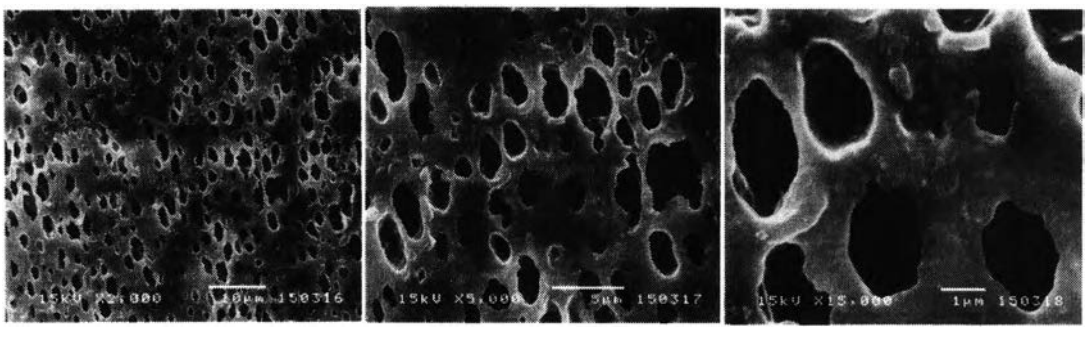

X 2000 **X 5000** **X 15000**

80%PLGA

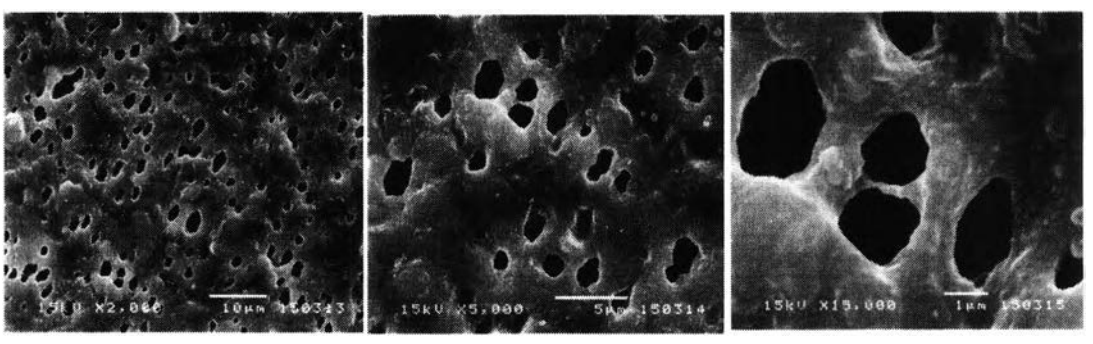

X 2000 **X 5000** **X 15000**

Figure 4-2 SEM photomicrographs of rifampicin-DL-PLGA co-precipitates produced from polymer content of 100 %-80 %.

70%PLGA

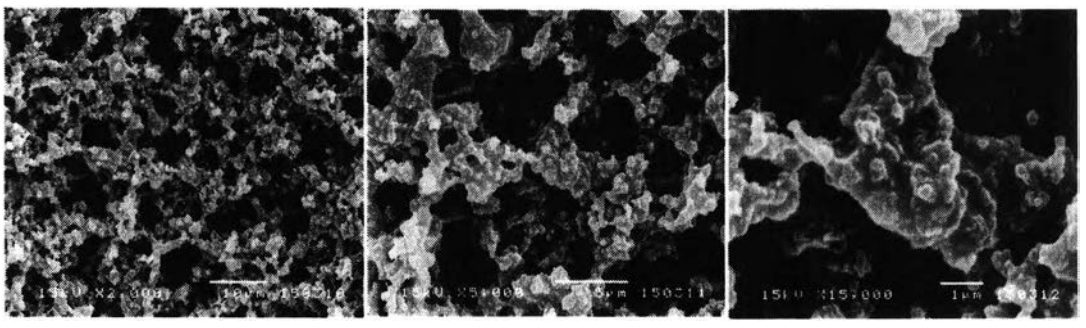

X 2000 **X 5000** **X 15000**

60%PLGA

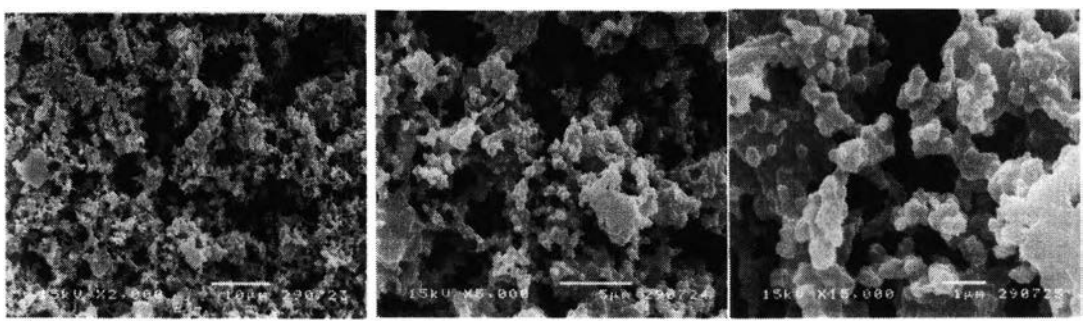

X 2000 **X 5000** **X 15000**

50%PLGA

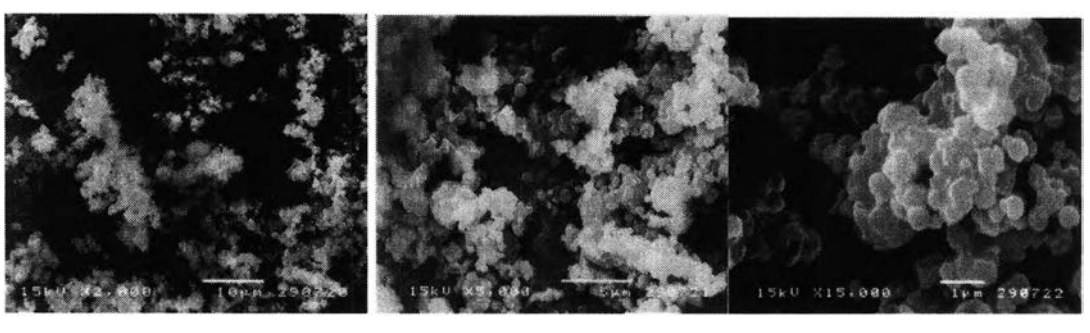

X 2000 **X 5000** **X 15000**

Figure 4-3 SEM photomicrographs of rifampicin-DL-PLGA co-precipitates produced from polymer content of 70 %-50 %.

40%PLGA

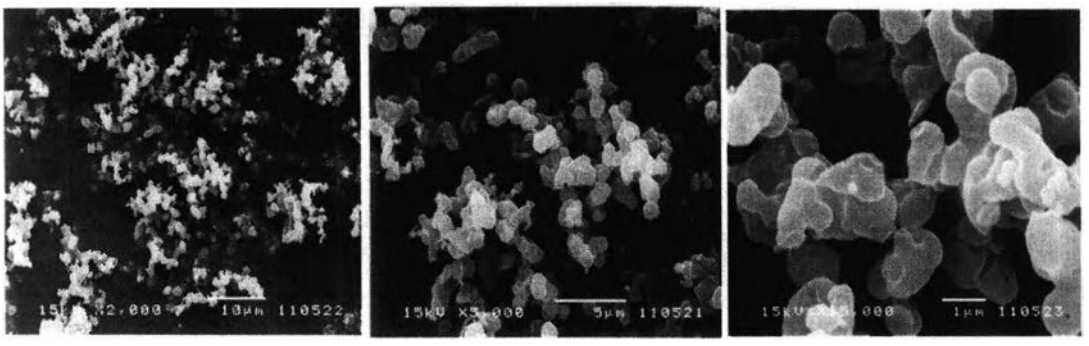

X 2000 **X 5000** **X 15000**

30%PLGA

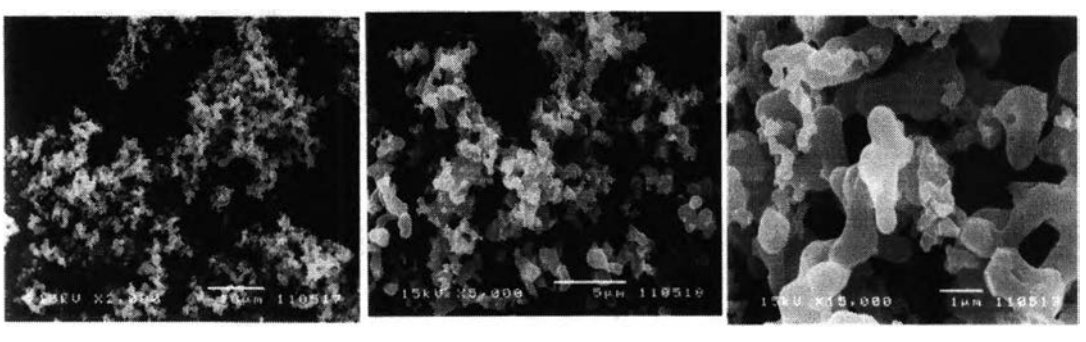

X 2000 **X 5000** **X 15000**

20%PLGA

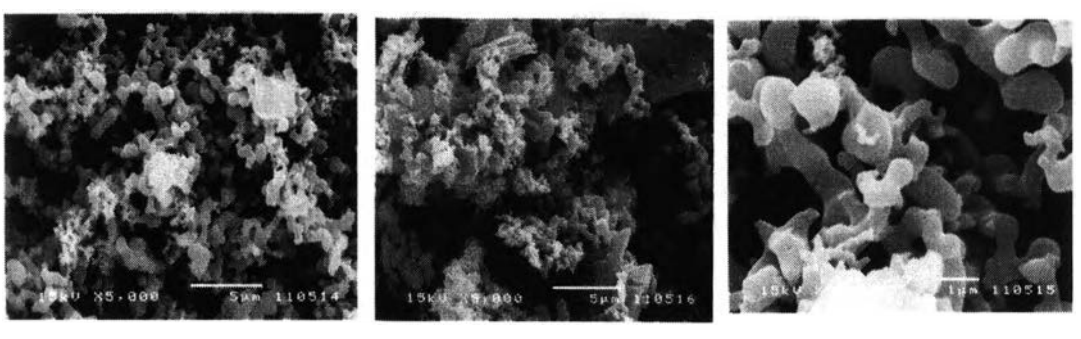

X 5000 **X 5000** **X 15000**

Figure 4-4 SEM photomicrographs of rifampicin-DL-PLGA microparticles produced from polymer content of 40%-20%.

This experiment gave similar results to earlier studies (Bleich et al. 1993 and Bodmeier et al. 1995) that films were found in pressure vessel when using pure DL-PLGA. On the contrary, Ghaderi et al. (1999), who prepared microparticles using solution-enhanced dispersion by supercritical fluid (SEDS) process, obtained discrete spherical microparticles of DL-PLGA with a volumetric median diameter of 130 μm. They reduced the flocculation of polymeric microparticles by using proper nozzle in SEDS process. One of the major difficulties is the interaction between the supercritical CO_2 and the amorphous polymers (DL-PLGA) due to the high solubility of the CO_2 in amorphous materials. The CO_2 might act as a plasticizer and the polymer swells while still inside the nozzle. This disturbed the atomization phase of processing of the polymer solution. This reason was supported by further study of Ghaderi et al. (2000) that modified the SEDS process by using the combination of supercritical N_2 and CO_2 which led to a more efficient dispersion of polymer solutions than CO_2 alone. They could reduce discrete spherical microparticles size with a volumetric median diameter of less than 10 μm from product of DL-PLGA. It was shown that it was able to decrease the interaction between the CO_2 and the amorphous polymers inside the nozzle and thereby increase the dispersive effect of the nozzle for the amorphous solutions. The use of N_2 in the process might also increase the solidification rate of the particles due to the lower solubility of the polymers in the CO_2–N_2 mixture than in CO_2 alone. In addition, they also used this process for incorporation of hydrocortisone into the DL-PLGA microparticles. There were no significant differences in particle size between loaded and unloaded particle. But loaded microparticles were more irregular in shape compared to empty ones. The entrapment efficiency (EE) for this drug was 22% and the production yield was almost 40 %.

Percent yield, percent drug loading and percent entrapment efficiency (EE) of powders produced from DL-PLGA are shown in Table 4-2 and Table 4-3, respectively. Percent yield of this experiment ranged from 31 to 45 %. It was increased when percent drug content in formulation increased. This similar result occurred for percent drug loading. Percent polymer content significantly influenced percent drug loading ($p < 0.05$) (Table 5-1 in Appendix). Whereas percent polymer content did not significantly influence percent EE (Table 5-2 in Appendix), percent

Table 4-2 The percent yield of rifampicin DL-PLGA microparticles at various polymer content.

Polymer type	Polymer content	Rifampicin (%)	Polymer : drug ratio	% Yield
DL-PLGA	100 %	0 %	-	-
	90 %	10 %	9:1	-*
	80 %	20 %	4:1	-
	70 %	30 %	7:3	-
	60 %	40 %	3:2	-
	50 %	50 %	1:1	-
	40 %	60 %	2:3	31.01
	30 %	70 %	3:7	39.29
	20 %	80 %	1:4	45.05

*- can not be determined because of adhesion of films at the wall of vessel

Table 4-3 The percent drug loading and percent entrapment efficiency (EE) of rifampicin-DL- PLGA microparticles at various polymer content.

Polymer type	Polymer content	Rifampicin (%)	Polymer : drug ratio	% Drug loading average (SD)	% EE average (SD)
DL-PLGA	100 %	0 %	-	-	-
	90 %	10 %	9:1	-*	-
	80 %	20 %	4:1	-	-
	70 %	30 %	7:3	-	-
	60 %	40 %	3:2	-	-
	50 %	50 %	1:1	-	-
	40 %	60 %	2:3	45.86 (7.15)	76.43 (11.92)
	30 %	70 %	3:7	62.86 (0.10)	89.80 (0.14)
	20 %	80 %	1:4	69.65 (6.37)	87.07 (7.96)

*- can not be determined because of adhesion of films at the wall of vessel

EE ranged from 76 to 89. It might be possible that the quantity of drug was higher than drug extraction by supercritical carbon dioxide at high drug loading (60 %-80 %).

Figure 4-5 and Figure 4-6 illustrate the volume particle size distribution and percent cumulative undersize of powders generated from rifampicin-DL-PLGA microparticles of 20 %- 40 % polymer content. It was found that rifampicin DL-PLGA microparticles were divided into two groups: primary microparticles had particle size between 0.5-1 μm and agglomerates of microparticles had particle size between 1-1000 μm. The amount of primary microparticles increased when % polymer content decreased. This result might be that lower quantity of polymer formed agglomerates of higher primary microparticles. Due to the CO_2 acted as a plasticizer for DL-PLGA, the agglomerates of primary microparticles were formed and tightly connected or fused together. Table 4-4 and 4-5 show the effect of polymer content on particle size of microparticles, % particle having size ranging from 1-5 μm and < 5 μm, respectively. The volume median diameter of those microparticles was larger than 18 μm. The percent polymer content significantly influenced $D_{50\%}$ ($p < 0.05$) (Table 5-3 in Appendix). The microparticles having size 1-5 μm using polymer content of 20 % and 30 % were very low (~ 3 %). It indicated that DL-PLGA microparticles were not appropriate for the use in pulmonary drug delivery.

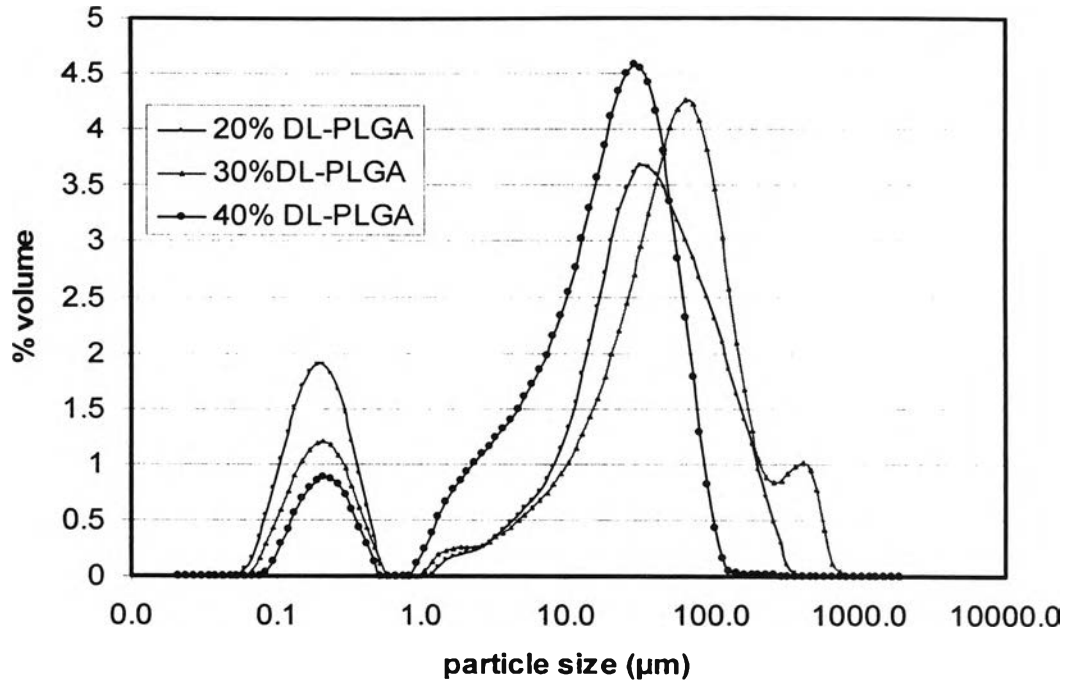

Figure 4-5 Particle size distribution by volume of rifampicin-DL-PLGA microparticles produced from polymer content of 20 %-40 %.

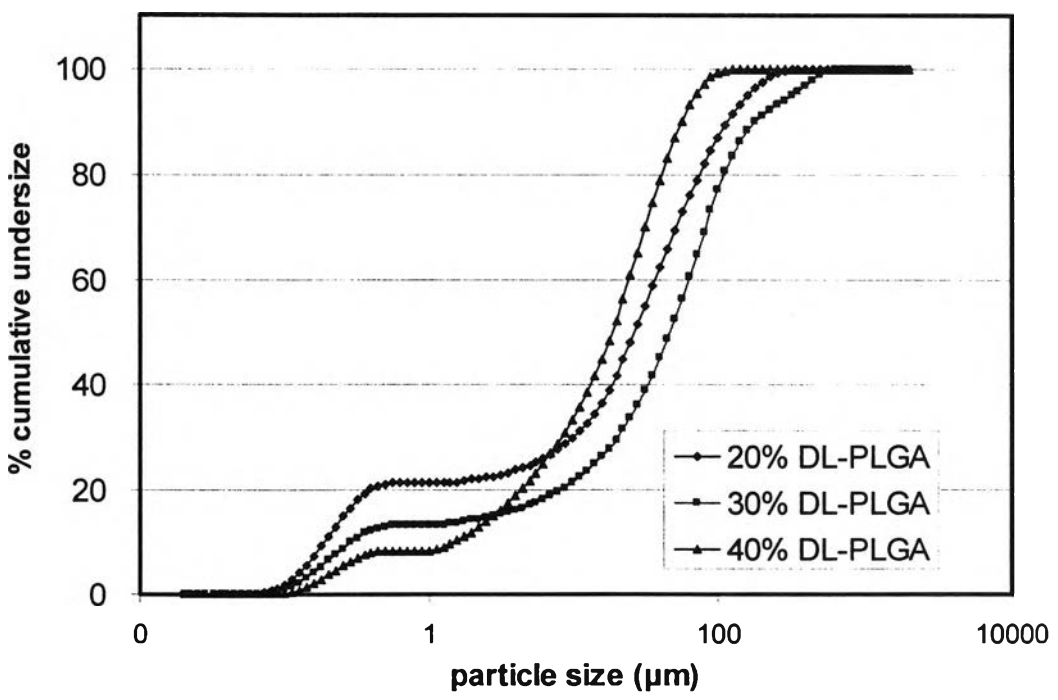

Figure 4-6 Percent cumulative undersize of rifampicin-DL-PLGA microparticles produced from polymer content of 20 %-40 %.

Table 4-4 Effect of polymer content on particle size of rifampicin-DL-PLGA microparticles.

Polymer content	**$D_{10\%}$** (μm)	**$D_{50\%}$** (μm)	**$D_{90\%}$** (μm)	**Span**
	average (SD)	average (SD)	average (SD)	average (SD)
20 % PLGA	0.19 (0.01)	27.00 (1.21)	117.18 (11.27)	4.33 (0.29)
30 % PLGA	0.28(0.02)	46.74 (0.90)	180.78 (8.47)	3.86 (0.11)
40 % PLGA	1.43 (0.47)	18.68 (0.49)	56.01(1.78)	2.92 (0.13)

Table 4-5 Effect of polymer content on % particle size of 1-5 μm and < 5 μm of rifampicin-DL-PLGA microparticles.

Polymer content	**% Particle** 1-5 μm	**% Particle** < 5 μm
	average (SD)	average (SD)
20 % PLGA	3.00 (0.13)	24.30 (1.45)
30 % PLGA	3.53 (0.16)	16.67 (0.91)
40 % PLGA	12.07 (0.68)	20.64 (1.41)

2.1.2 DL-PLA

In the production of drug loaded DL-PLA microparticles, 2 % w/v solution of rifampicin and DL-PLA in methylene chloride, operating pressure of 2500 psi, temperature of 33 °C and solution feed rate of 0.5 ml/min were used. Table 4-6 summarizes the morphology of rifampicin-DL-PLA microparticles at various polymer to drug ratios. This result was similar to rifampicin-DL-PLGA microparticles (in section 2.1.1.) as the film was formed at the base and on the wall of the high-pressure vessel when using high polymer content. The precipitates of 100 %, 90 % and 80 % DL-PLA were films generated from the particles fused together and formed the network (Figure 4-7). The pores of film might occur by supercritical carbon dioxide penetration. The products of 90 % and 80 % DL-PLA provided denser and continuous films with less porous than 100 % DL-PLA. The film of 70 % DL-PLA had fewer pores and completely fused to be a more continuous film. The product of 60 % DL-PLA showed its fine structure, partially coalescing together and forming film with rough texture (Figure 4-8). At 1:1 polymer-drug ratio (50 % DL-PLA), the sticky larger agglomerates was obtained. It was likely that the tendency for rifampicin-DL-PLA microparticles to flocculate and fuse together had decreased when increased % drug loading and decreased % polymer content. At low polymer content (40-20 % of DL-PLA), isolated small agglomerates were observed (Figure 4-9). The precipitates of 30 % and 20 % DL-PLA were microparticles partially connected together. This result might be that low polymer content decreased fused microparticles and the size of agglomerates.

DL-PLA is amorphous biodegradable as DL-PLGA is. So, it also absorbed dense gases CO_2. The glass transition temperature (T_g) of a polymer was lowered due to CO_2 sorption into the polymer/solvent matrix and the weakening of the inter-and intramolecular attractions between the polymer segments within the matrix. As a result, the T_g of the polymer was depressed in proportion to the amount of CO_2 absorbed, and typically caused the polymer to precipitate as a film (Tu et al. 2002). In addition, the effect of this CO_2 sorption was swelling and plasticization (depression of the glass transition temperature) that affected the agglomeration of the primary particles and yielded softened or fused structure (Dixon et al. 1993 and Subra et al. 2000). The tight agglomerates and their fusion to form networks occurred by

plasticization of the polymer, especially at high polymer: drug ratio (>50% polymer content).

The similar results by Bodmeier et al. (1995) showed that agglomerate mass of polymer was retained on the base of vessel when pure DL-PLA was used. The CO_2 might act as a plasticizer for amorphous polymer (DL-PLA). However, Ghaderi et al. (1999) could prepare DL-PLA-microparticles using SEDS process and obtained a mixture of discrete and agglomerated particles on the walls and the base of the vessel. The particles were porous and varied widely in size and shape. In a further study, Ghaderi et al. (2000) modified the SEDS process by using the combination of supercritical N_2 and CO_2. The particles produced by the modified SEDS process had a volumetric particle size between 9 and 10 μm. DL-PLA microparticles were almost spherical and the surface of these microparticles were very smooth and nonporous. It was shown that it was able to decrease the interaction between the CO_2 and the amorphous polymers inside the nozzle and thereby increase the dispersive effect of the nozzle for the amorphous solutions. The use of N_2 in the process might also increase the solidification rate of the particles due to the lower solubility of the polymers in the CO_2–N_2 mixture than in CO_2 alone.

Table 4-6 The morphology rifampicin-DL-PLA microparticles at various polymer content.

Polymer type	Polymer content	Rifampicin (%)	Polymer: drug : ratio	Morphology
DL-PLA	100 %	0 %	-	film
	90 %	10 %	9:1	film
	80 %	20 %	4:1	film
	70 %	30 %	7:3	film
	60 %	40 %	3:2	film
	50 %	50 %	1:1	Sticky large agglomerates
	40 %	60 %	2:3	aggregated particles
	30 %	70 %	3:7	aggregated particles
	20 %	80 %	1:4	aggregated particles

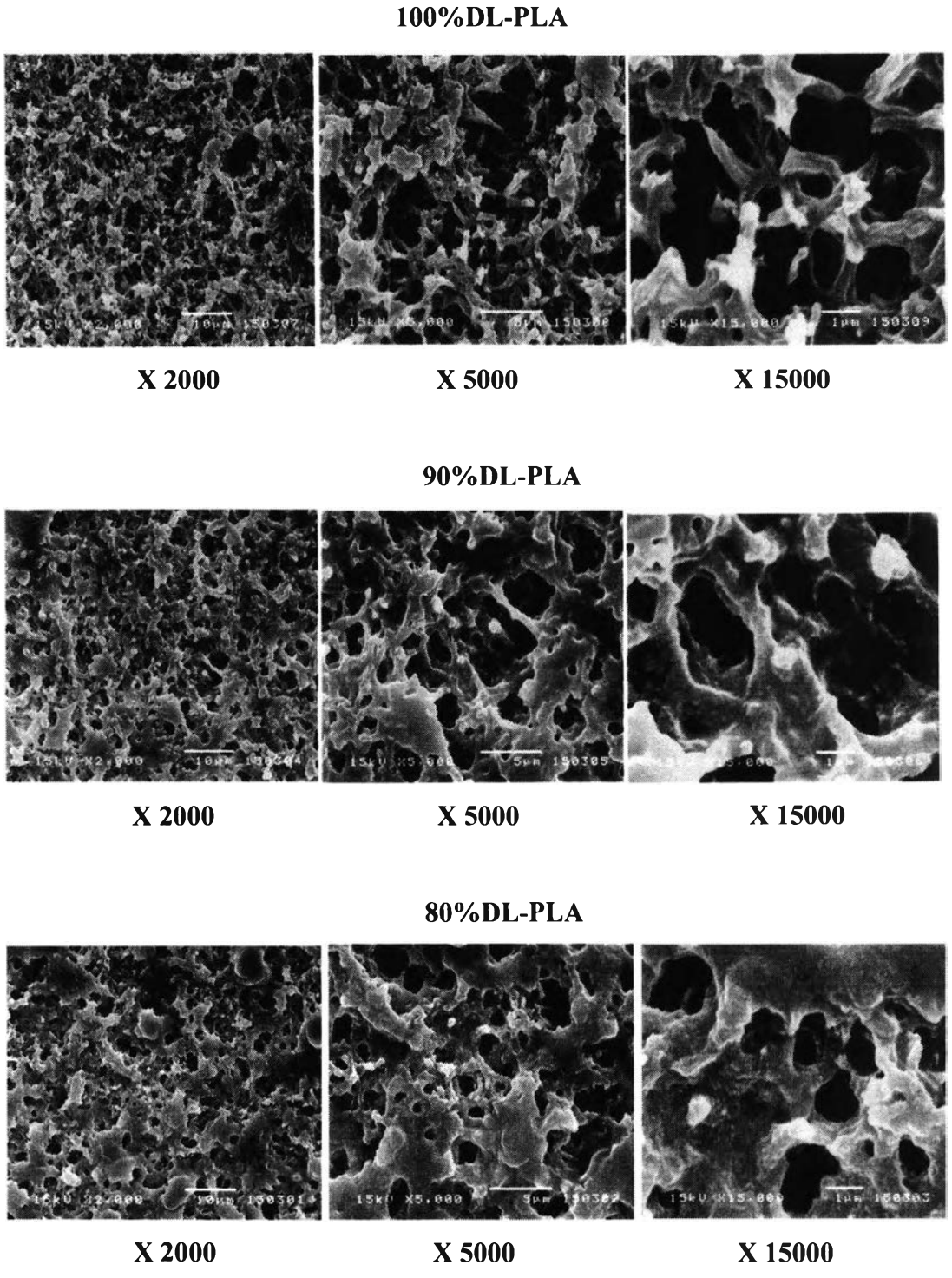

Figure 4-7 SEM photomicrographs of rifampicin-DL-PLA co-precipitates produced from polymer content of 100%-80%.

70%DL-PLA

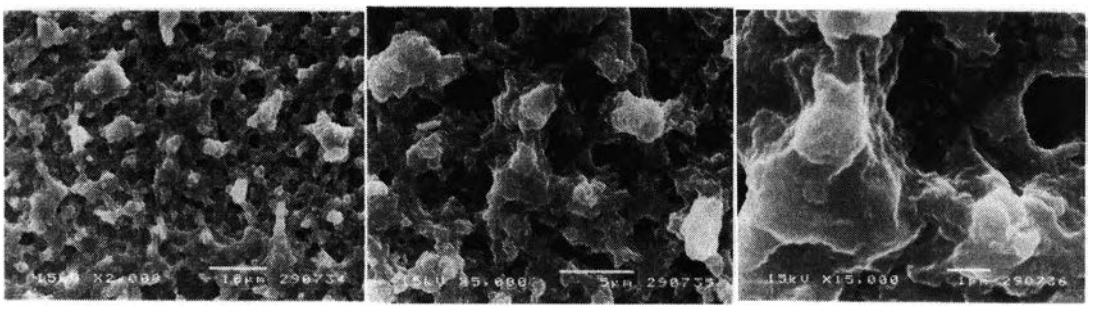

X 2000 **X 5000** **X 15000**

60%DL-PLA

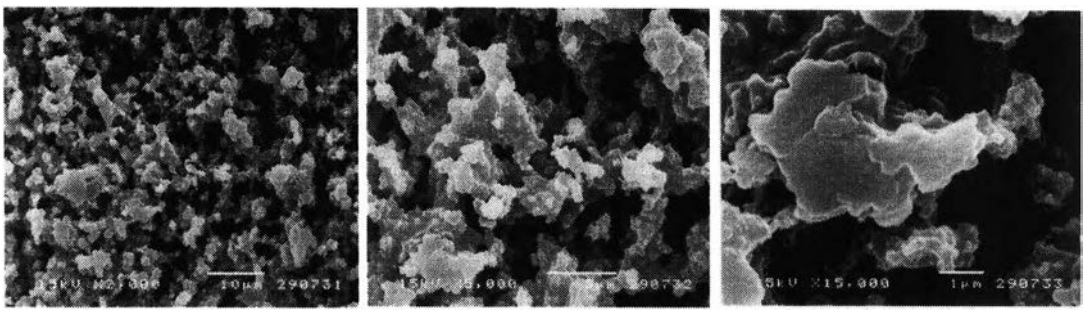

X 2000 **X 5000** **X 15000**

50%DL-PLA

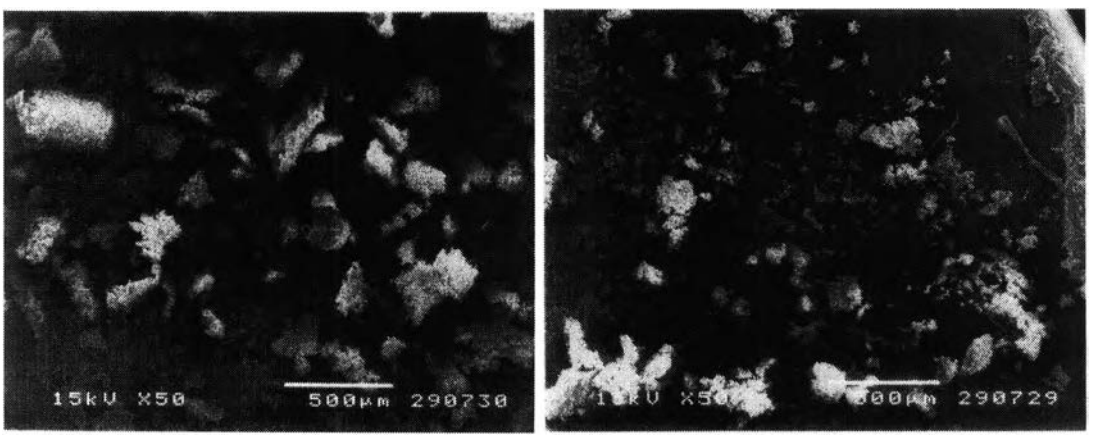

X 50 **X 50**

Figure 4-8 SEM photomicrographs of rifampicin-DL-PLA co-precipitates produced from polymer content of 70 %-50 %.

40% DL-PLA

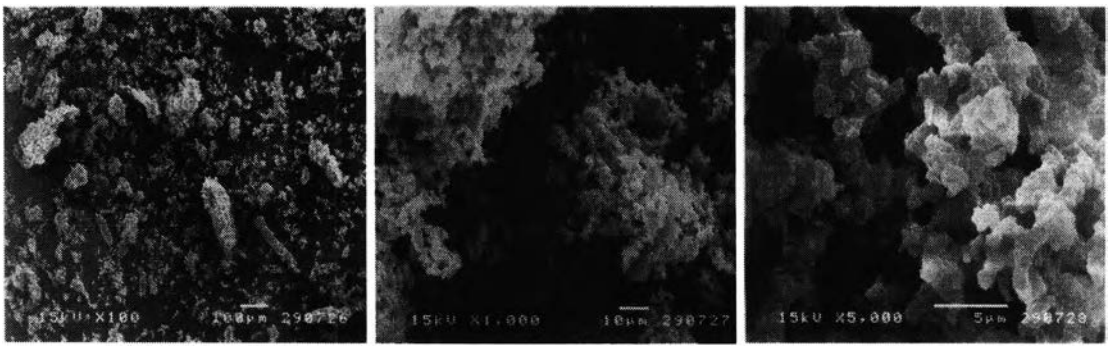

X 100 **X 1000** **X 5000**

30% DL-PLA

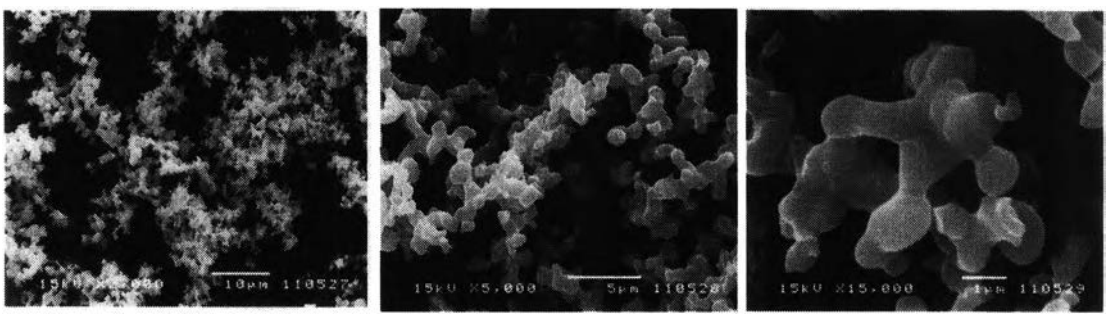

X 2000 **X 5000** **X 15000**

20% DL-PLA

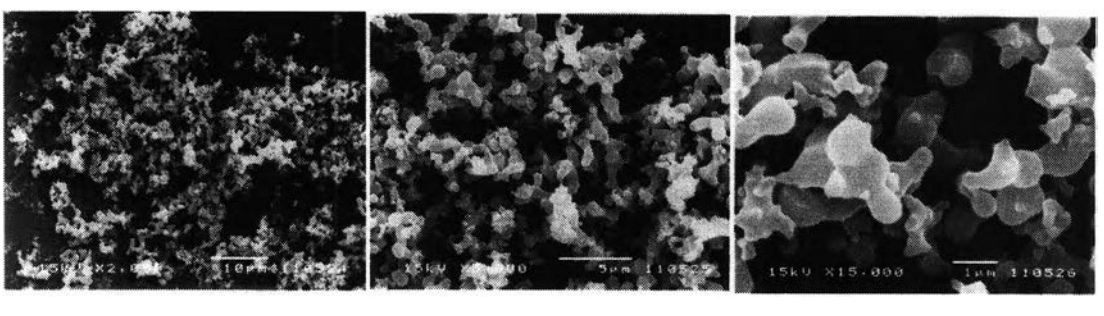

X 2000 **X 5000** **X 15000**

Figure 4-9 SEM photomicrographs of rifampicin-DL-PLA microparticles produced from polymer content of 40%-20%.

Percent yield, percent drug loading and percent entrapment efficiency (EE) of products using DL-PLA are shown in Table 4-7 and Table 4-8, respectively. Percent yields of this experiment ranged from 30 to 40 %. Percent polymer content significantly influenced percent drug loading ($p < 0.05$) (Table 5-4 in Appendix). Percent EE were ranging from 83 to 91 % which slightly higher than the products of DL-PLGA. Percent polymer content did not significantly influence percent EE (Table 5-5 in Appendix). It might be possible that the quantity of drug was higher than drug extraction by supercritical carbon dioxide at high drug loading (60 %-80 %).

Figure 4-10 and Figure 4-11 illustrate the particle size distribution by volume and percent cumulative undersize of rifampicin-DL-PLA microparticles at polymer content of 20%-40%, respectively. It was exhibited that rifampicin DL-PLA microparticles were divided into two groups: primary microparticles had particle size between 0.5-1 μm and agglomerates of microparticles had particle size between 1-1000 μm. The amount of primary microparticles increased when % polymer content decreased. This result might be that lower quantity of polymer formed more agglomerates of primary microparticles. Due to the CO_2 acted as a plasticizer for DL-PLA, the agglomerates were obtained from primary microparticles tightly connected or fused together. Table 4-9 and Table 4-10 show the effect of polymer content on particle size of microparticles, percent particle having size ranging from 1-5 μm and < 5 μm, respectively. The microparticles having size 1-5 μm using polymer content of 20 %-40 % were very low (~3-7 %). The volume median diameter of those microparticles was larger than 27 μm. The size of 20 % DL-PLA microparticles was larger than 30 and 40 % DL-PLA microparticles. Percent polymer content significantly influenced $D_{50\%}$ ($p < 0.05$) (Table 5-6 in Appendix). It might be that smaller microparticles having higher tendency to aggregate than larger microparticles. Similar to products of DL-PLGA, DL-PLA microparticles were not proper to be used for pulmonary drug delivery.

Table 4-7 The percent yield of rifampicin DL-PLA-microparticles at various polymer content.

Polymer type	Polymer content	Rifampicin (%)	Polymer : drug ratio	% Yield
DL-PLA	100 %	0 %	-	-
	90 %	10 %	9:1	-*
	80 %	20 %	4:1	-
	70 %	30 %	7:3	-
	60 %	40 %	3:2	-
	50 %	50 %	1:1	-
	40 %	60 %	2:3	33.09
	30 %	70 %	3:7	40.07
	20 %	80 %	1:4	38.06

*- can not be determined because of adhesion of films at the wall of vessel

Table 4-8 The percent drug loading of rifampicin-DL-PLA microparticles at various polymer content.

Polymer type	Polymer content	Rifampicin (%)	Polymer : drug ratio	% Drug loading average (SD)	% EE average (SD)
DL-PLA	100%	0%	-	-	-
	90%	10%	9:1	-*	-
	80%	20%	4:1	-	-
	70%	30%	7:3	-	-
	60%	40%	3:2	-	-
	50%	50%	1:1	-	-
	40%	60%	2:3	50.02 (1.45)	83.37 (2.42)
	30%	70%	3:7	58.14 (6.15)	83.06 (8.78)
	20%	80%	1:4	72.78 (1.34)	90.97 (1.67)

*- can not be determined because of adhesion of films at the wall of vessel

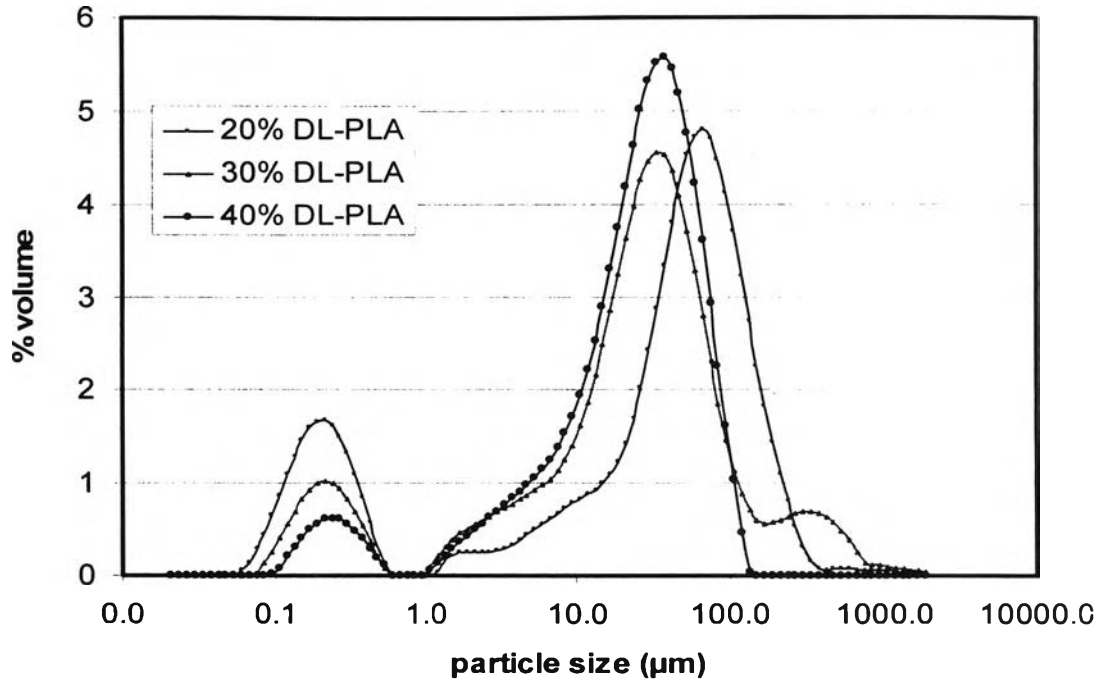

Figure 4-10 Particle size distribution by volume of rifampicin-DL-PLA microparticles produced from polymer content of 20 %-40 %.

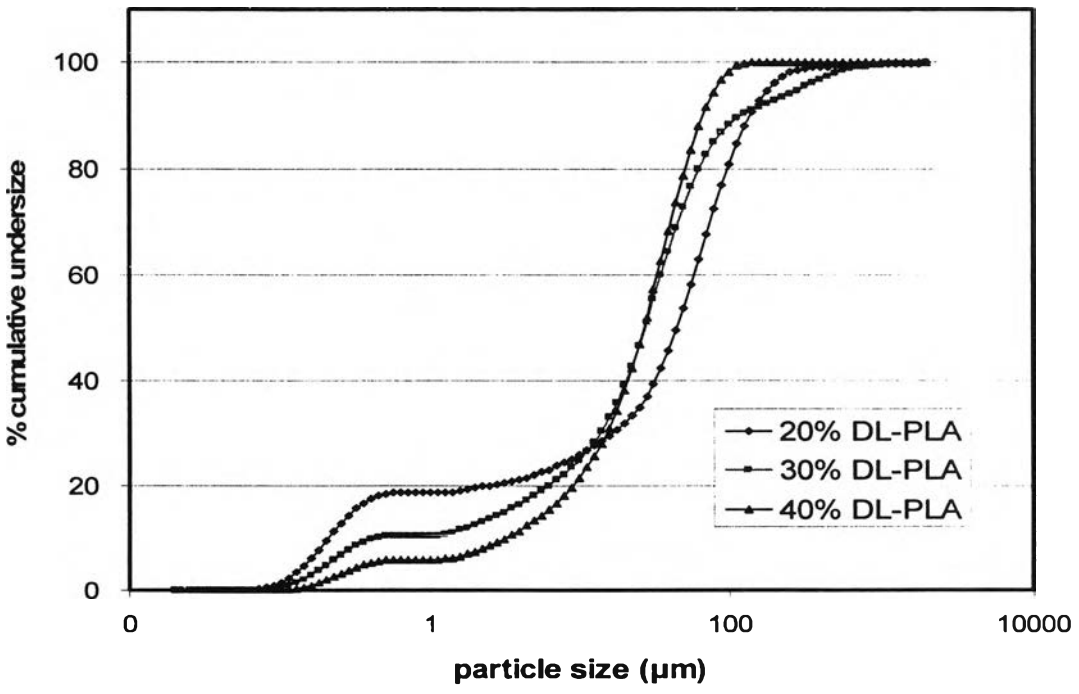

Figure 4-11 Percent cumulative undersize of Rifampicin-DL-PLA microparticles produced from polymer content of 20%-40 %.

Table 4-9 Effect of polymer content on particle size of rifampicin-DL-PLA microparticles.

Polymer content	**$D_{10\%}$** (μm)	**$D_{50\%}$** (μm)	**$D_{90\%}$** (μm)	**Span**
	average (SD)	average (SD)	average (SD)	average (SD)
20% DL-PLA	0.21 (0.01)	45.37 (0.32)	136.68 (5.60)	3.01 (0.14)
30% DL-PLA	0.66 (0.49)	27.49 (0.90)	118.59 (9.18)	4.29 (0.28)
40% DL-PLA	3.22 (0.15)	27.04 (0.95)	67.16 (2.57)	2.36 (0.02)

Table 4-10 Effect of polymer content on % particle size of 1-5 μm and < 5 μm of rifampicin-DL-PLA microparticles.

Polymer content	**% Particle** 1-5 μm	**% Particle** < 5 μm
	average (SD)	average (SD)
20% DL-PLA	3.11 (0.21)	21.81 (0.57)
30% DL-PLA	7.05 (0.37)	17.56 (0.71)
40% DL-PLA	6.73 (0.77)	12.74 (0.61)

2.1.3 L-PLA

The morphology of drug loaded L-PLA microparticles at various polymer-drug ratios obtained by spraying a 2 % solution of rifampicin and L-PLA in methylene chloride into supercritical fluid carbon dioxide at 2500 psi, 40 °C and solution feed rate of 0.5 ml/min is summarized in Table 4-11. Biodegradable rifampicin microparticles were analyzed with a scanning electron microscope (SEM) to determine their particle morphology. The products of L-PLA microparticles were discrete microparticles which retained on the walls and the base of the vessel. Rifampicin-L-PLA microparticles with polymer content ranging from 100 % to 70 % were almost spherical and the surface of these microparticles was very smooth and nonporous (Figure 4-12). But the microparticles of 60 % polymer content were a combination of less spherical and some irregular particles. The microparticles were more irregular in shape when % drug loading was more than 50 %. At 1:1 polymer: drug ratio (50 % polymer content), the spherical microparticles did not occur (Figure 4-13). The agglomerated particles were found when using 40-20 % polymer content in formulations. At low polymer content, it is possible that feed solution was atomized into droplets, but the amount of polymers was not enough for hardening the droplet into spherical microparticles and provided the irregular microparticles. Figure 4-14 is SEM photomicrographs that show coalescing microparticles in fine microstructure.

The similar results were obtained in previous studies (Bodmeier et al. 1995 and Bleich et al. 1993) which found that the use of L-PLA led to the formation of spherical microparticles. The semicrystalline polymer L-PLA provided small and spherical microparticles, while the amorphous DL-PLA and DL-PLGA copolymers gave agglomerated even at low temperatures (33 °C). The amorphous polymer had lower glass transition temperature than semicrystalline polymer, which could easily be lowered to that below operating temperature by CO_2. The semicrystalline polymer L-PLA had an ambient Tg of 65 °C. CO_2 might only slightly decrease the Tg of L-PLA due to the fact that DL-PLA and DL-PLGA were more amorphous polymers compared to L-PLA.

The morphology of microparticles significantly depended on both nature of drug and % drug loading. In this experiment, the agglomerated and irregular microparticles obtained at drug-to-polymer-ratio of 4:1, but Tu et al. (2002) could produce uniform and discrete microparticles of a *p*-HBA loaded L-PLA using ASES at drug-to-polymer-ratio of 5.

Table 4-11 The morphology rifampicin L-PLA microparticles at various polymer content.

Polymer type	Polymer content	Rifampicin (%)	Polymer : drug ratio	Morphology
L-PLA	100 %	0 %	-	Discrete microparticles
	90 %	10 %	9:1	Discrete microparticles
	80 %	20 %	4:1	Discrete microparticles
	70 %	30 %	7:3	Discrete microparticles
	60 %	40 %	3:2	Discrete microparticles
	50 %	50 %	1:1	Irregular microparticles
	40 %	60 %	2:3	Agglomerated microparticles
	30 %	70 %	3:7	Agglomerated microparticles
	20 %	80 %	1:4	Agglomerated microparticles

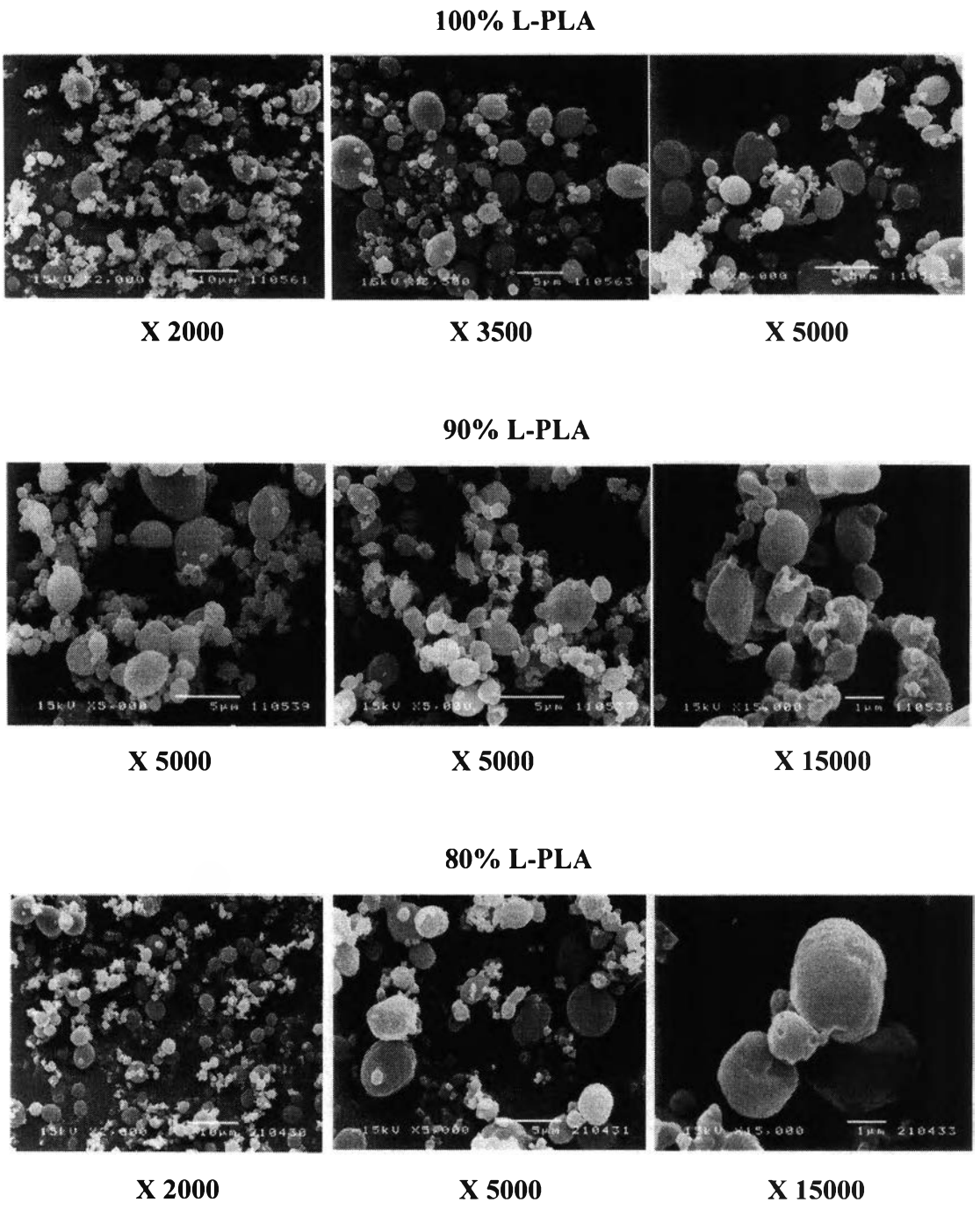

Figure 4-12 SEM photomicrographs of rifampicin-L-PLA microparticles produced from polymer content of 100 %-80 %.

70% L-PLA

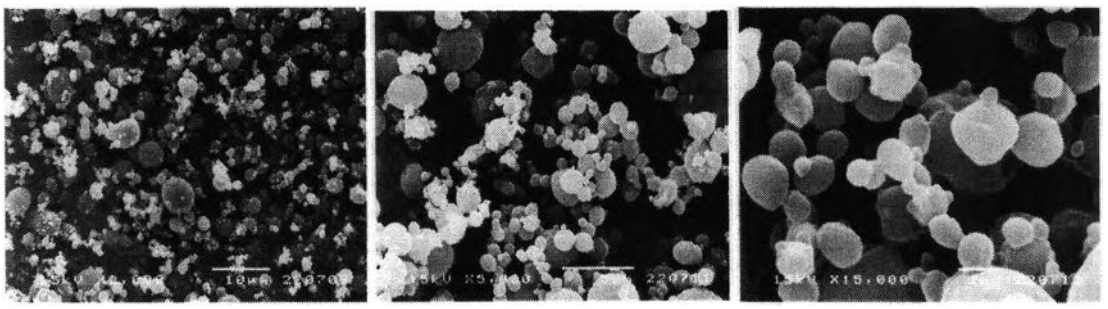

X 2000 **X 5000** **X 15000**

60% L-PLA

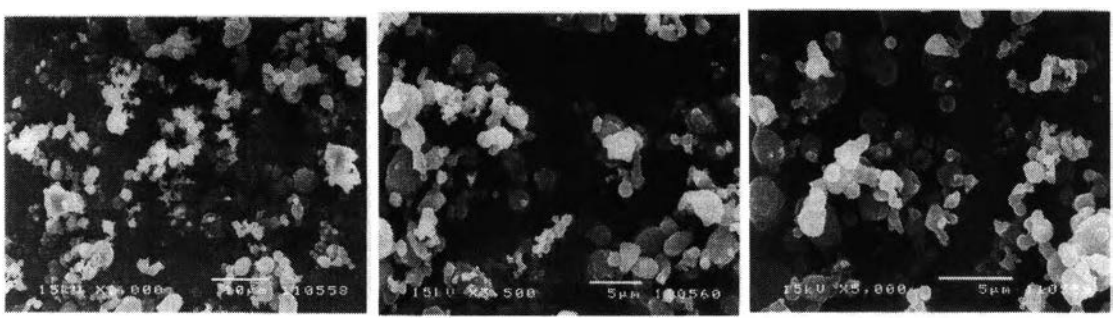

X 2000 **X 3500** **X 5000**

50% L-PLA

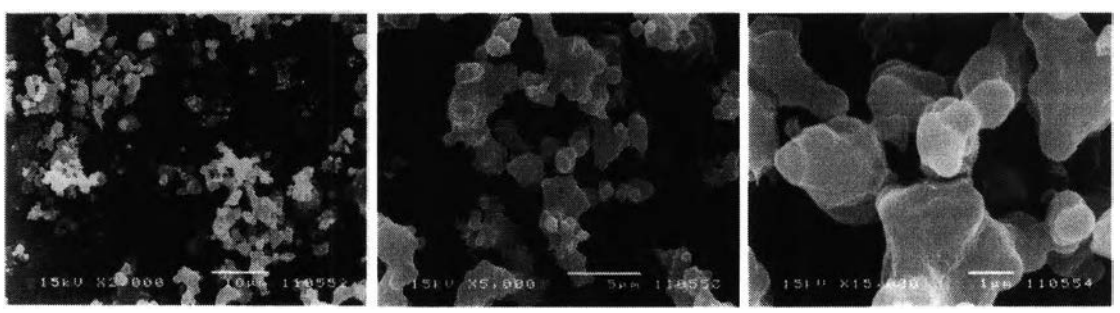

X 2000 **X 5000** **X 15000**

Figure 4-13 SEM photomicrographs of rifampicin-L-PLA microparticles produced from polymer content of 70 %-50 %.

40% L-PLA

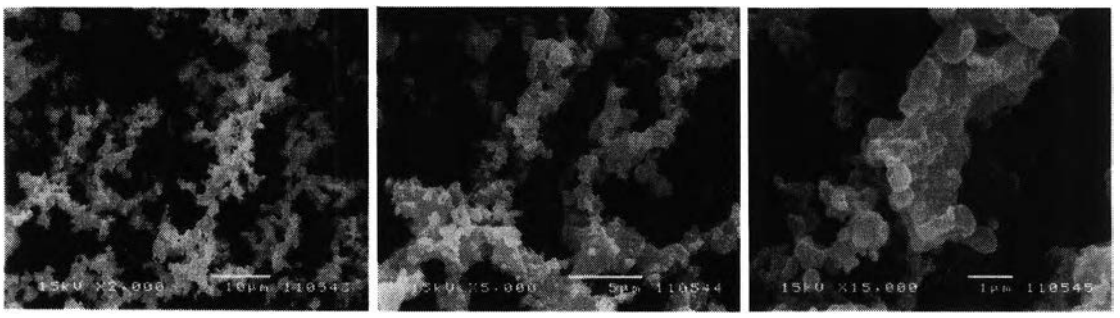

X 2000 **X 5000** **X 15000**

30% L-PLA

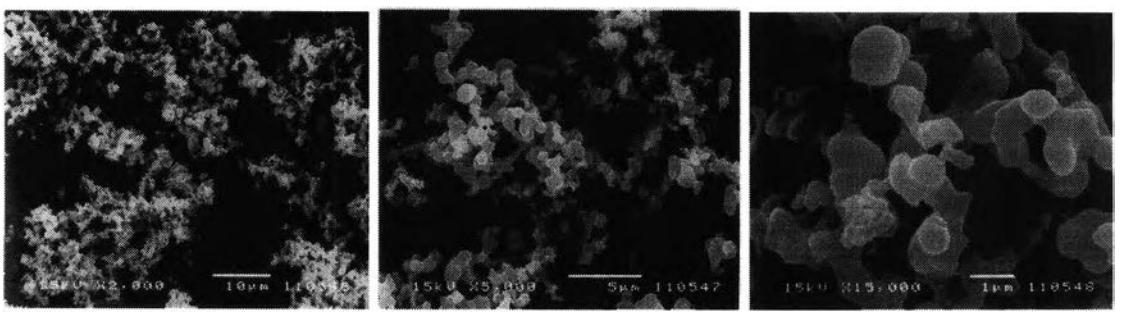

X 200 **X 5000** **X 15000**

20% L-PLA

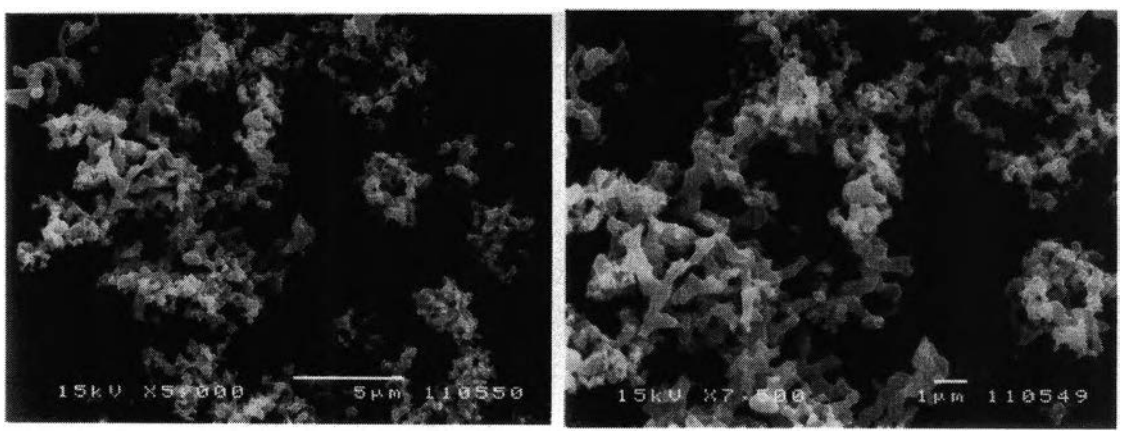

X 5000 **X 15000**

Figure 4-14 SEM photomicrographs of rifampicin-L-PLA microparticles produced from polymer content of 40 %-20 %.

Percent Yield of rifampicin microparticles were between 39-53 % (Table 4-12). Pure polymer provided the highest percent yield (53 %). Spraying a mixture of 10 % w/w rifampicin and 90 % w/w L-PLA from methylene chloride solution into supercritical carbon dioxide produced microparticles with a percent drug loading of 3.34 % (Table 4-13). Increasing the rifampicin concentration to 20 % (w/w) gave particles having 8.13 % rifampicin by weight. In statistical test, it found that percent polymer content significantly affected percent drug loading (see detail in appendix, Table 5-7). Therefore, drug incorporation was rather inefficient (only approximately 33-40 % of the drug was entrapped in the polymer). It might be that because rifampicin was very hydrophobic, and consequently was partially soluble in supercritical carbon dioxide. During particle formation, the L-PLA precipitated normally, but rifampicin remained in solution of the supercritical fluid carbon dioxide/methylene chloride mixture and did not co-precipitate with L-PLA until its solubility limit was reached. After saturation of supercritical carbon dioxide with rifampicin occurred, the percent encapsulation efficiency increased to higher than 80 %. Using one way ANOVA test, it was found that the products from high drug content (50 %-80 %) did not significantly influence the percent encapsulation efficiency (Table 5-8 in appendix). It could be observed that higher percent drug content higher percent encapsulation efficiency of microparticles (Table 4-13). Bodmeier et al. (1995) reached a similar conclusion regarding indomethacin being extracted from L-PLA particles by supercritical carbon dioxide due to the highly lipophilic nature of indomethacin. They sprayed both indomethacin and chlorpheniramine maleate at a theoretical drug loading of 10 % and retained only 0.73 and 3.73 %, respectively.

The encapsulation efficiency obtained by the SAS process was relatively low compared to other conventional processes, such as spray drying, where efficiencies in excess of 80 % had been reported (O'Hara et al. 2000). At the 70 % and 60 % polymer content in formulation provided discrete microparticles by SAS process which had percent encapsulation efficiency of 54 and 58 %, respectively (Table 4-12). However percent encapsulation efficiency of this experiment was higher than the other studies. The drug loading of the particles in other studies was determined to be 7.0% and percent encapsulation efficiency was only 8.4 % (Tu et al. 2002), which was comparable to the study of Bodmeier et al. (1995).

Table 4-12 The percent yield of rifampicin-L-PLA microparticles at various polymer content.

Polymer type	Polymer content	Rifampicin (%)	Polymer : drug ratio	% Yield
L-PLA	100 %	0 %	-	53.99
	90 %	10 %	9:1	39.86
	80 %	20 %	4:1	39.68
	70 %	30 %	7:3	39.75
	60 %	40 %	3:2	39.31
	50 %	50 %	1:1	35.50
	40 %	60 %	2:3	42.48
	30 %	70 %	3:7	39.82
	20 %	80 %	1:4	46.13

Table 4-13 The percent drug loading and percent encapsulation efficiency of rifampicin L-PLA microparticles at various polymer content.

Polymer type	Polymer content	Rifampicin (%)	Polymer : drug ratio	% Drug loading average (SD)	% EE average (SD)
L-PLA	100 %	0 %	-	-	-
	90 %	10 %	9:1	3.34 (1.42)	33.40 (14.18)
	80 %	20 %	4:1	8.13 (0.29)	40.64 (1.43)
	70 %	30 %	7:3	16.33 (0.21)	54.46 (0.70)
	60 %	40 %	3:2	23.30 (0.79)	58.25 (1.97)
	50 %	50 %	1:1	41.52 (2.31)	83.03 (4.62)
	40 %	60 %	2:3	53.80 (1.16)	89.67 (1.93)
	30 %	70 %	3:7	64.21 (0.98)	91.73 (1.40)
	20 %	80 %	1:4	66.42 (5.70)	83.02 (7.13)

The microencapsulation results achieved in this and other studies indicate that the encapsulation efficiency might be dependent on the type of polymer and drug in the system. However, the drug loading might depend more on the type of system, such as the crystallisation/precipitation behaviour of both the drug and the polymer.

Figure 4-15, 4-16, 4-17 and 4-18 illustrate the particle size distribution by volume and percent cumulative undersize of rifampicin-L-PLA microparticles at polymer content of 20 %-50 % and 60 %-100 %, respectively. At polymer content 20 and 30 %, it was exhibited that rifampicin L-PLA microparticles were divided into two groups: the cluster of microparticles were obtained from primary microparticles tightly fused together having particle size between 0.5 -1 μm and large agglomerates of microparticles had particle size between 1-1000 μm. However, at polymer content of 40 and 50 % provided only large agglomerates. The amount of small cluster of microparticles increased when percent polymer content decreased. In formulations of 40 and 50 % polymer content did not find the cluster of microparticles. Figure 4-16 shows that the curves of particles size distribution by volume of microparticles produced form 60 %-100 % polymer content almost superimposed. The effect of polymer content on particle size of rifampicin L-PLA microparticles and % particle having size ranging from 1-5 μm and < 5 μm by the supercritical process are listed in Table 4-14 and 4-15, respectively. The microparticles having size 1-5 μm using polymer content of 20 % and 30 % were very low (~2-5 %) and the volume median diameter of microparticles was larger than 18 μm. The size of 20 % and 30 % L-PLA microparticles was larger than 40-100 % L-PLA microparticles. The particles size of microparticles was reduced when % polymer content was higher. The unloaded L-PLA microparticles were spheres of less than 3.26 μm in diameter. The particles sizes of 70 to 90 % L-PLA loaded microparticles were comparable to unloaded particles and their % particles size of 1-5 μm was approximately 60 % (Table 4-15). It was shown that no statistically significant difference $D_{50\%}$ of the microparticles generating from 60 %-100 % polymer content (Table 5-9 in appendix).

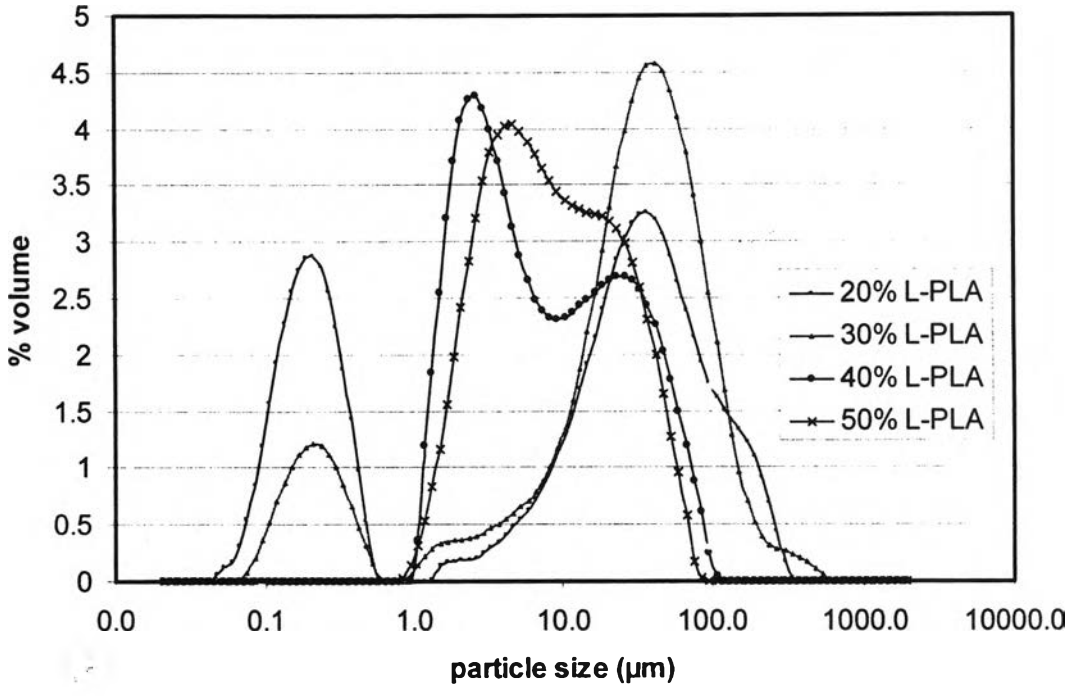

Figure 4-15 Particle size distributions by volume of rifampicin-L-PLA microparticles produced from polymer content of 20 %-50 %.

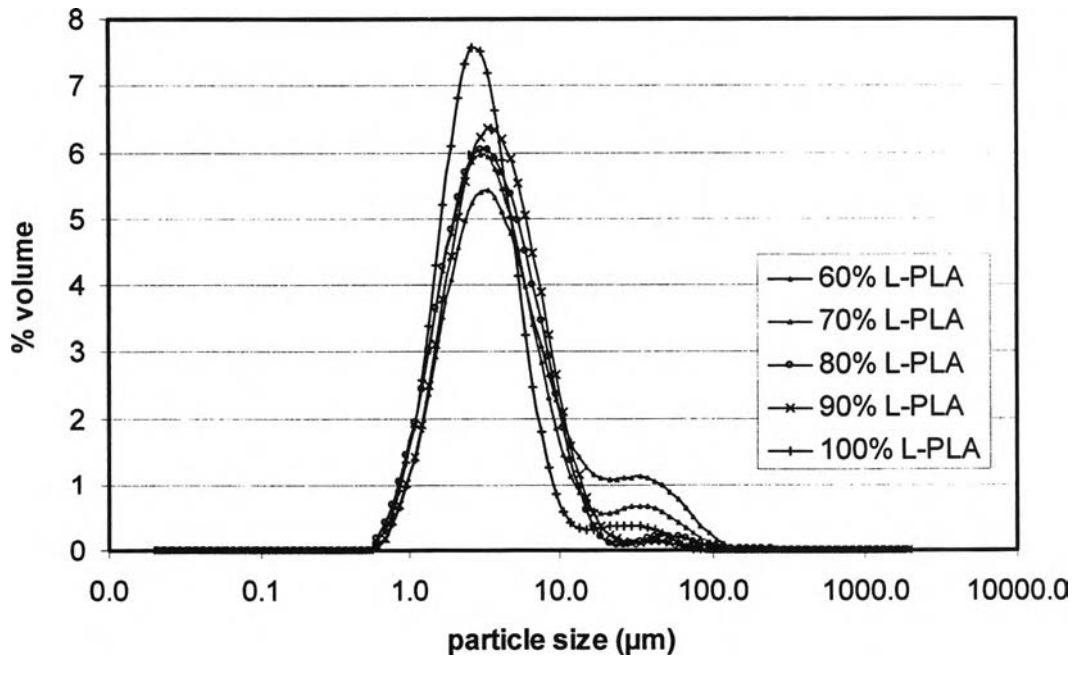

Figure 4-16 Particle size distributions by volume of rifampicin-L-PLA microparticles produced from polymer content of 60 %-100 %.

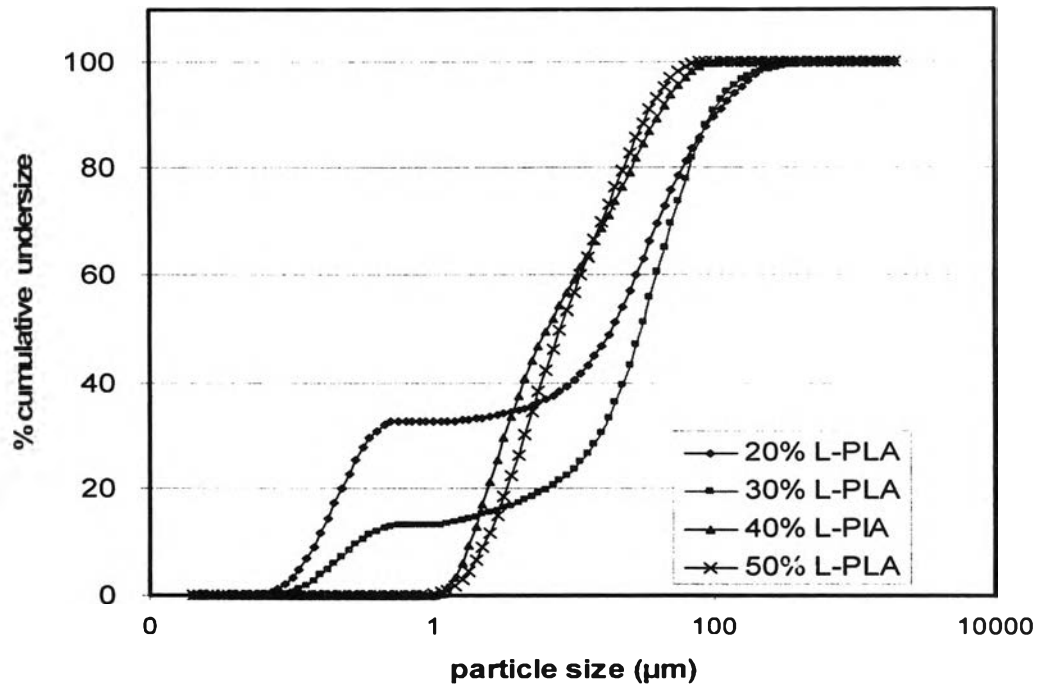

Figure 4-17 Percent cumulative undersize of rifampicin-L-PLA microparticles produced from polymer content of 20 %-50 %.

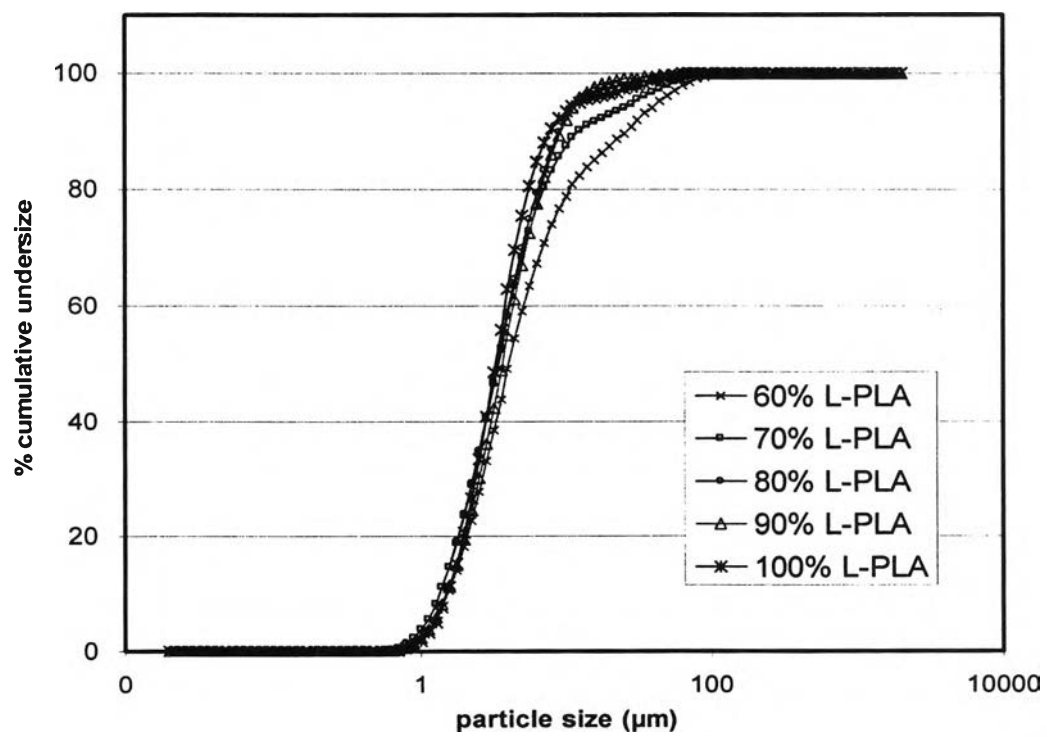

Figure 4-18 Percent cumulative undersize of rifampicin-L-PLA microparticles produced from polymer content of 60 %-100%.

Table 4-14 Effect of polymer content on particle size of rifampicin-L-PLA microparticles.

Polymer content	**$D_{10\%}$** (μm)	**$D_{50\%}$** (μm)	**$D_{90\%}$** (μm)	**Span**
	average (SD)	average (SD)	average (SD)	average (SD)
20% L-PLA	0.15 (0.00)	18.78 (1.02)	103.38 (4.09)	5.50 (0.09)
30% L-PLA	0.30 (0.01)	30.53 (0.33)	97.20 (2.87)	3.17 (0.11)
40% L-PLA	1.83 (0.03)	6.60 (1.08)	41.01 (1.96)	6.04 (1.05)
50% L-PLA	2.34 (0.02)	8.05 (0.04)	33.94 (0.68)	3.93 (0.07)
60% L-PLA	1.55 (0.05)	4.07 (0.21)	25.94 (3.09)	5.98 (0.44)
70% L-PLA	1.36 (0.01)	3.40 (0.04)	12.52 (0.77)	3.29 (0.25)
80% L-PLA	1.36 (0.06)	3.37 (0.28)	9.00 (1.07)	2.26 (0.20)
90% L-PLA	1.52 (0.11)	3.65 (0.26)	9.15 (0.55)	2.09 (0.03)
100% L-PLA	1.53 (0.04)	3.26 (0.18)	7.89 (1.55)	1.93 (0.39)

Table 4-15 Effect of polymer content on % particle size of 1-5 μm and < 5 μm of rifampicin-L-PLA microparticles.

Polymer content	**% Particle** 1-5 μm	**% Particle** < 5 μm
	average (SD)	average (SD)
20% L-PLA	2.53 (0.28)	35.24 (0.65)
30% L-PLA	5.00 (1.06)	18.12 (0.96)
40% L-PLA	41.73 (1.07)	41.73 (1.07)
50% L-PLA	31.44 (2.28)	31.62 (2.24)
60% L-PLA	53.63 (1.23)	55.82 (1.30)
70% L-PLA	61.44 (2.68)	65.20 (2.69)
80% L-PLA	62.43 (5.64)	66.24 (6.05)
90% L-PLA	60.65 (4.75)	63.08 (5.26)
100% L-PLA	69.66 (4.19)	71.56 (4.13)

It was shown that, using poly (L-lactic acid) (L-PLA) as polymer leading to a successful microparticles production. Other polymers except L-PLA were tested but did not give convincing results. The products were obtained as film or aggregated particles when used poly (DL-lactide-co-glycolide) copolymer composition 50:50 (PLGA) and poly (DL-lactide) (DL-PLA) as polymer. The polymer content had a pronounced influence on product of each preparation. The microparticles production results achieved in this and other studies indicating that the microparticles production might be dependent on the type of polymer and percent drug in the system. However, the drug loading might depend more on the type of system, such as the crystallization/precipitation behaviour of both the drug and the polymer (Lu et al. 2002).

The formulation containing 30 % rifampicin and 70 % L-PLA was used for future experiment, because it provided spherical and discrete microparticles consisting of high drug loading. In addition, the size of microparticles was 3.4 μm which could be used as powder inhalation and suitable for targeting drug to deep pulmonary system.

2.2 Effect of Solvent

DMSO and its mixture with methylene chloride were used as solvent for preparation rifampicin biodegradable microparticles and sprayed into supercritical carbon dioxide of 2500 psi, 40 °C, solution concentration of 2 % w/v and solution feed rate of 0.5 ml/min. The solution of rifampicin and L-PLA in DMSO did not precipitate in the pressure chamber, the powders did not occur. The same results obtained from the rifampicin and L-PLA in DMSO: methylene chloride solution at various ratios such as 1:9, 1:4, 3:7, 2:3, 1:1, 3:2, 7:3, 4:1 and 9:1. It might be possible that not only the type of apparatus but also operating conditions in experiment had dramatically influence on precipitation of solution. Especially, amount of carbon dioxide (400ml) and its flow rate (1.5 g/min) of this study were rather low. So, it might not be enough to precipitate rifampicin and polymer from the solution of DMSO and its mixture with methylene chloride.

2.3 Effect of Temperature

As it was shown in the previous experiment, operation pressure of 2500 psi, 2% w/v of 30% rifampicin and 70% L-PLA in methylene chloride solution, and feed solution rate of 0.5 ml/min at temperature of 40 °C were operating conditions which provided discrete microparticles in this experiment. The effect of temperature on the precipitation of drug and polymer solution by SAS process was studied by various operating temperature at 33 and 50 °C while maintaining all other variables constant.

The comparative morphology of microparticles obtained from various operating temperatures is illustrated in Figure 4-19. The characteristics of the rifampicin-polymer microparticles were slightly sensitive to temperature changes in the system. The microparticles processed at temperature of 33 and 40 °C were more spherical and slightly smaller size than the microparticle of 50 °C. The formation of these less spherical microparticles processing at 50 °C and a slightly increase in microparticles agglomeration at the higher temperatures might be due to more polymer plasticization effect of CO_2.

In previous study, Bleich et al. (1994) reported that the particles produced at higher temperatures lead to compact agglomerates by bridging (larger particle size). It had been shown in the literature that the temperature might greatly influence the precipitation of polymers. In particular, the morphology of the solid formed might differ depending on whether the operating temperature was higher or lower than the glassy transition point. The T_g of a polymer is lowered due to CO_2 sorption into the polymer/solvent matrix and the weakening of the inter-and intramolecular attractions between the polymer segments within the matrix. As a result, the T_g of the polymer is depressed in proportion to the amount of CO_2 absorbed (Tu et al. 2002).

Figure 4-20 and 4-21 show the volume particle size distribution and % cumulative undersize curves of rifampicin-L-PLA microparticles at various operating temperature, respectively. The volume particle size distribution and % cumulative undersize curves of rifampicin-L-PLA microparticles of 30 °C and 40 °C were superimposed each other, whereas those of 50 °C shifted to the right, lower in height and broader.

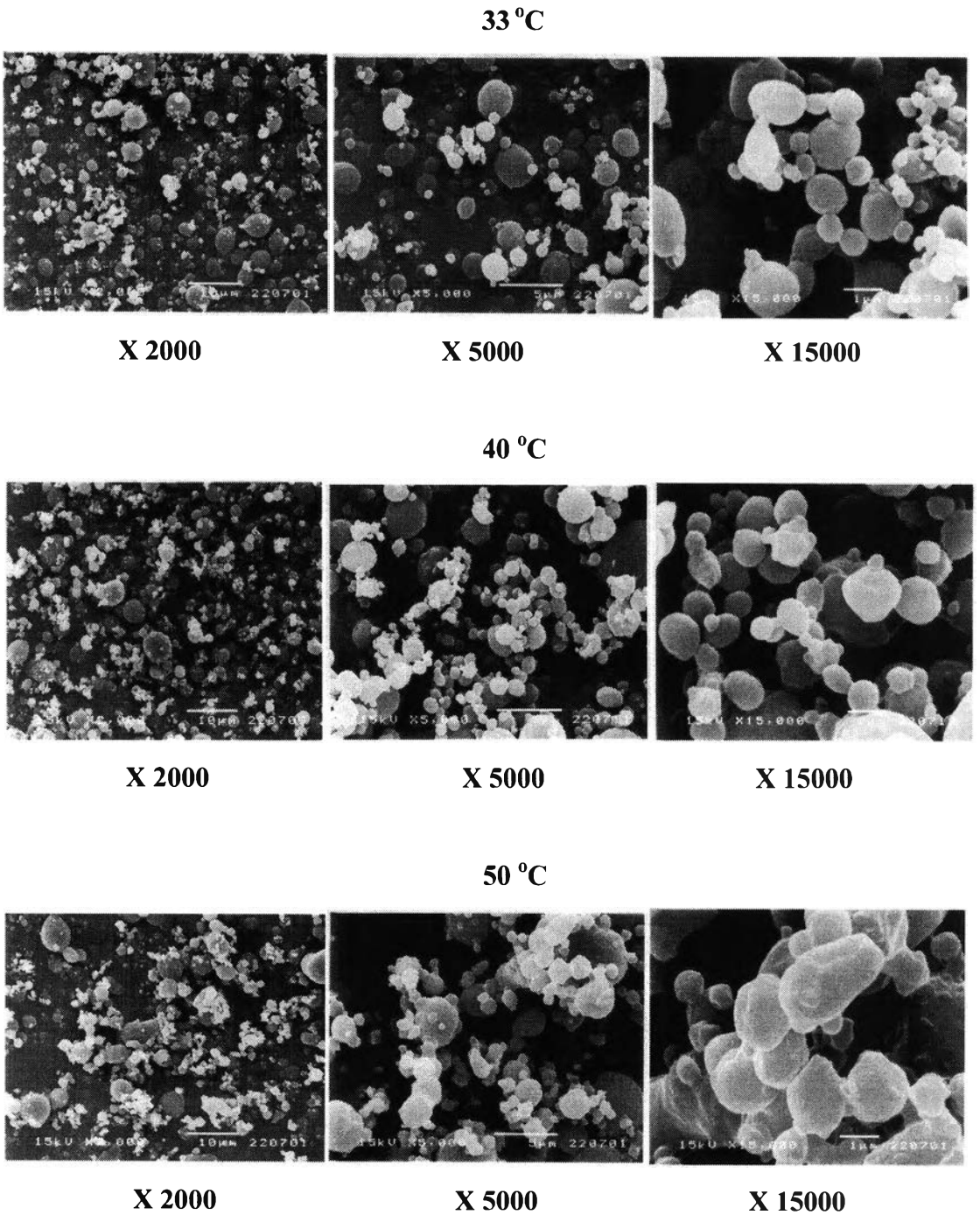

Figure 4-19 SEM photomicrographs of rifampicin-L-PLA microparticles produced at temperatures of 33, 40 and 50 °C.

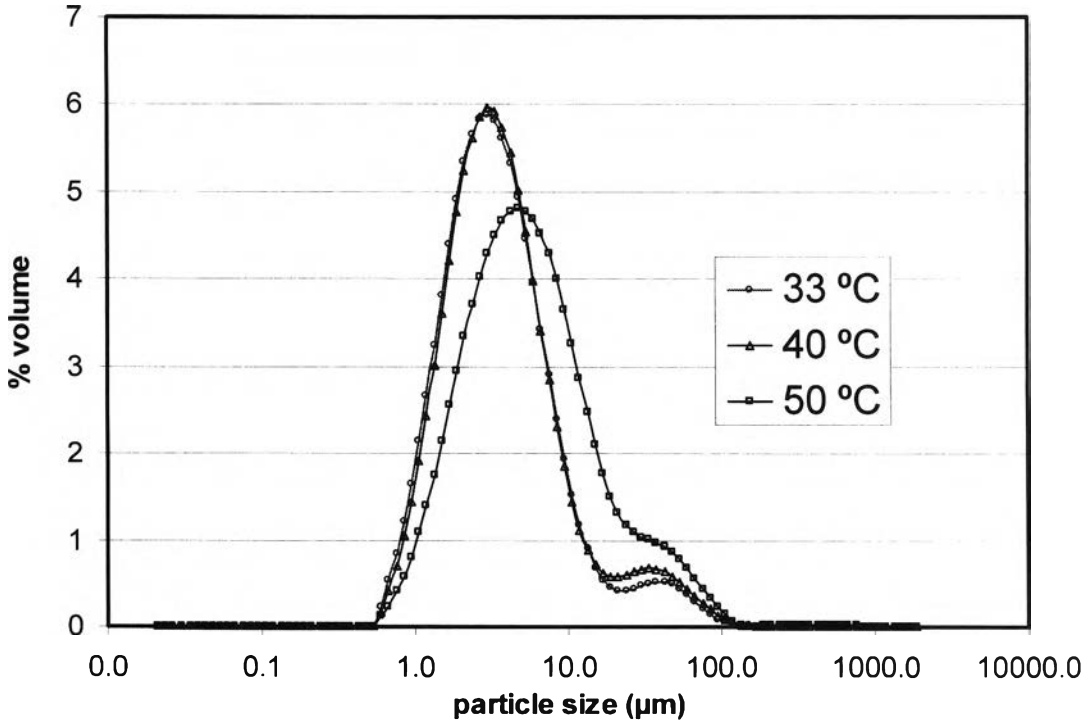

Figure 4-20 Effect of temperature on particle size distribution by volume of rifampicin-L-PLA microparticles.

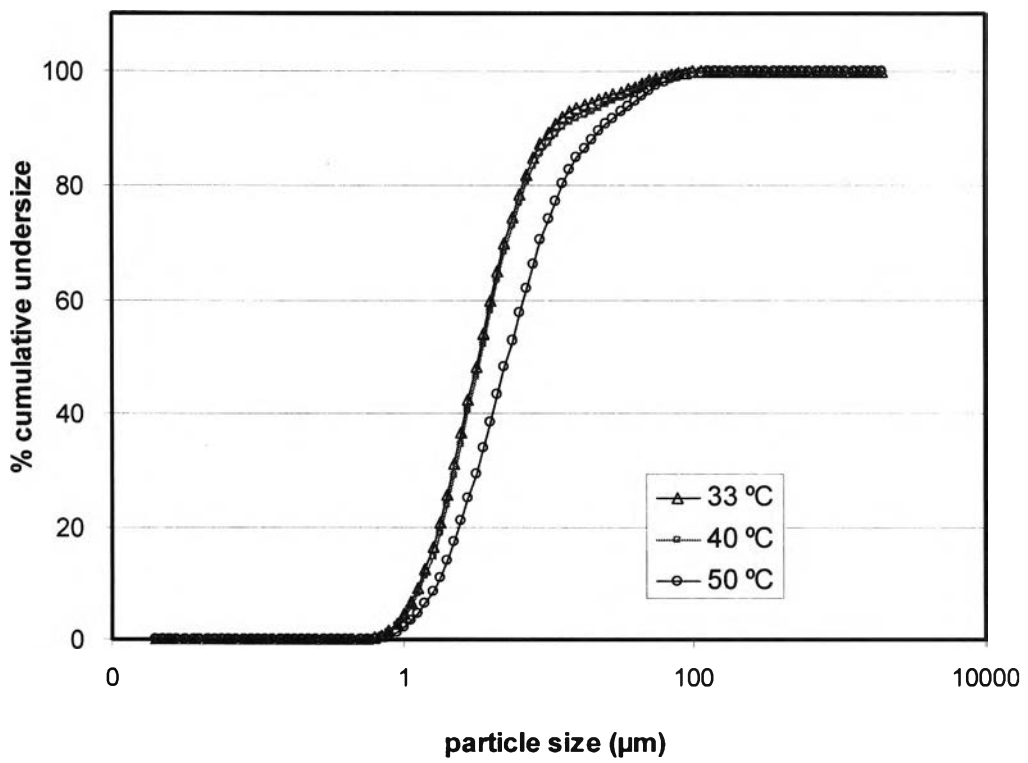

Figure 4-21 Effect of temperature on percent cumulative undersize of rifampicin-L-PLA microparticles.

Table 4-16 shows the value of $D_{10\%}$, $D_{50\%}$, $D_{90\%}$ and span of rifampicin L-PLA microparticles that measured by laser diffraction. By one way ANOVA test (Table 5-10 in Appendix), it was found that temperature did not significantly effect on $D_{50\%}$ of 33 °C and 40 °C. But $D_{50\%}$ of 33 °C and 40 °C were significantly different from $D_{50\%}$ of 50 °C ($p<0.05$). The percent 1-5 μm size of microparticles which operated at 33 °C and 40 °C were more than 60 % whereas at 50 °C operation condition was only approximately 45 % (Table 4-17). It was possible that more agglomerated microparticles were occurred at 50 °C.

Table 4-16 Effect of temperature on particle size of rifampicin-L-PLA microparticles.

Temp. (°C)	**$D_{10\%}$ (μm)**	**$D_{50\%}$ (μm)**	**$D_{90\%}$ (μm)**	**Span**
	average (SD)	average (SD)	average (SD)	average (SD)
33	1.30 (0.01)	3.27 (0.02)	10.59 (0.21)	2.84 (0.07)
40	1.36 (0.01)	3.40 (0.04)	12.52 (0.77)	3.29 (0.25)
50	1.70 (0.02)	5.25 (0.17)	23.70 (1.94)	4.19 (0.38)

Table 4-17 Effect of temperature on % particle size of 1-5 μm and < 5 μm of rifampicin-L-PLA microparticles.

Temp. (°C)	**% Particle 1-5 μm**	**% Particle < 5 μm**
	average (SD)	average (SD)
33	62.30 (2.98)	66.75 (2.99)
40	61.4 (2.68)	65.20 (2.69)
50	45.81 (1.35)	47.96 (1.36)

2.4 Effect of Operating Pressure

The effect of operating pressure on the precipitation of the drug and polymer by the SAS process was studied at 2000, 2500 and 3000 psi while maintaining all other variables constant. The experiments were conducted at a constant temperature of 40 °C to insure that the glass transition temperature of the polymer was higher than the carbon dioxide temperature.

The morphology of microparticles obtained from various operating pressures is illustrated in Figure 4-22. The characteristics of rifampicin-polymer microparticles were found to be slightly sensitive to pressure changes in the system. The microparticles processed at all operating pressures were spherical. Figure 4-23 and 4-24 show the particle size distribution by volume and percent cumulative undersize curves of rifampicin-L-PLA microparticles at various operating pressure, respectively. The volume particle size distribution curve of rifampicin-L-PLA microparticles at operating pressure of 2000 psi were slightly shifted to the right and broader than those of 2500 psi. As the operating pressure was increased to 3000 psi, a narrowing of the size distribution of drug loaded microparticles were achieved (Figure 4-23). However, the volumetric median microparticle size (Table 4-18) of all operating pressure was no statistically significant different (Table 5-11 in Appendix). However $D_{90\%}$ of microparticles produced at 3000 psi was the lowest. Table 4-19 reports the percent particle size of 1-5 μm and < 5 μm of rifampicin-L-PLA microparticles. It was observed that the percent 1-5 μm size using operating pressure at 2000 psi was approximately 56 %, but those of 2500 psi and 3000 psi were more than 60 %.

Dixon et al. (1993) found a decrease in particle size for the mixture of polystyrene in toluene solution and carbon dioxide if the density of the extracting gas was raised. The authors presumed the rapid atomization was controlled by inertial and interfacial forces. With increasing carbon dioxide density, the inertial force increased and the interfacial force decreased due to the higher miscibility of carbon dioxide and toluene. Hence it follows that the liquid jet disintegrates more rapidly and into smaller droplets if the carbon dioxide density is raised.

2000 psi

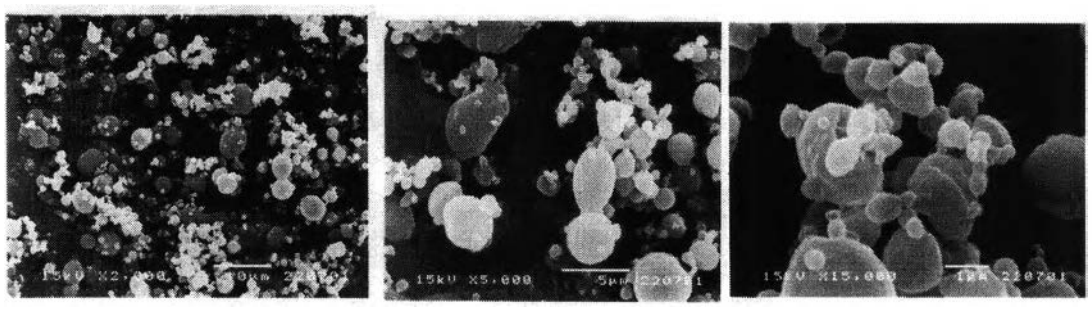

X 2000 **X 5000** **X 15000**

2500 psi

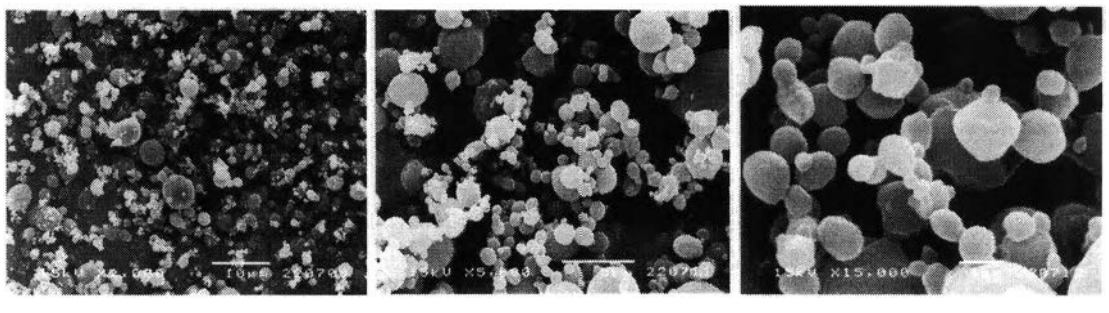

X 2000 **X 5000** **X 15000**

3000 psi

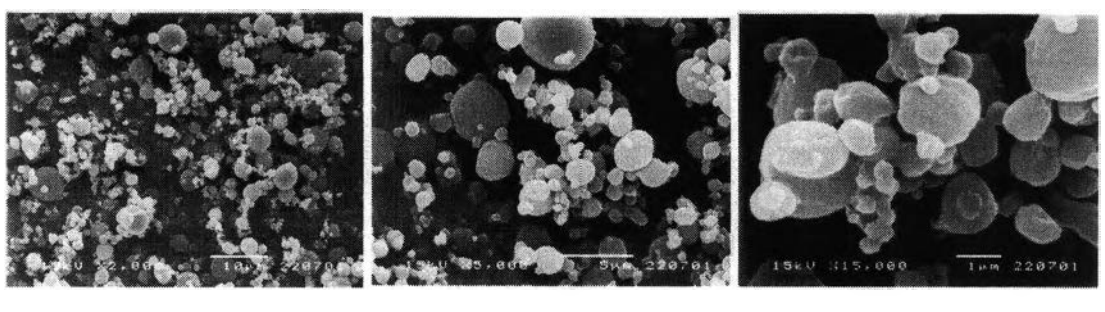

X 2000 **X 5000** **X 15000**

Figure 4-22 SEM photomicrographs of rifampicin-L-PLA microparticles produced at operating pressure of 2000, 2500 and 3000 psi.

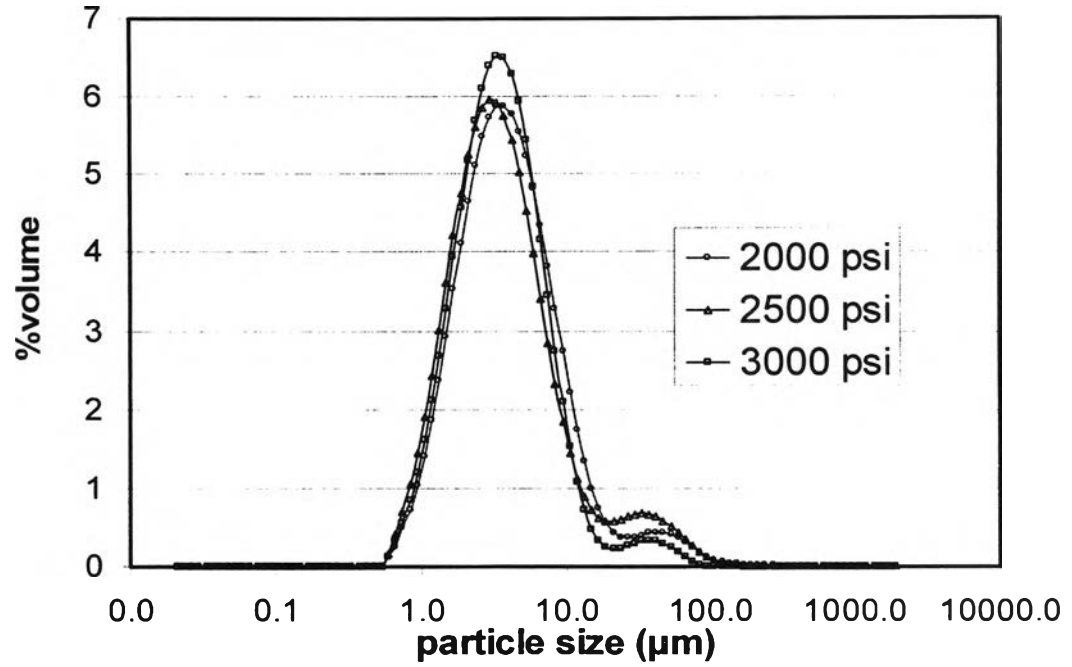

Figure 4-23 Effect of pressure on particle size distribution by volume of rifampicin-L-PLA microparticles.

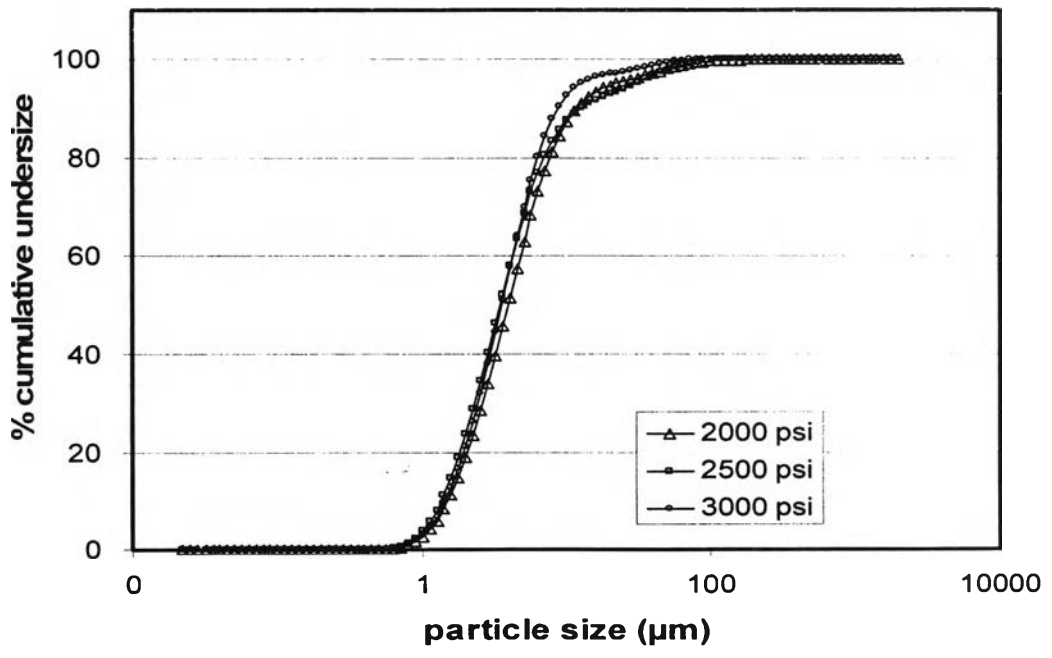

Figure 4-24 Effect of pressure on percent cumulative undersize of rifampicin-L-PLA microparticles.

Table 4-18 Effect of pressure on particle size of rifampicin-L-PLA microparticles.

Pressure (psi)	**$D_{10\%}$** (μm)	**$D_{50\%}$** (μm)	**$D_{90\%}$** (μm)	**Span**
	average (SD)	average (SD)	average (SD)	average (SD)
2000	1.52 (0.02)	3.91 (0.39)	11.83 (2.71)	2.61 (0.46)
2500	1.36 (0.01)	3.40 (0.04)	12.52 (0.77)	3.29 (0.25)
3000	1.44 (0.02)	3.48 (0.04)	8.73 (0.36)	2.09 (0.10)

Table 4-19 Effect of pressure on % particle size of 1-5 μm and < 5 μm rifampicin-L-PLA microparticles.

Pressure (psi)	**% Particle** 1-5 μm	**% Particle** < 5 μm
	average (SD)	average (SD)
2000	56.42 (4.12)	59.00 (3.79)
2500	61.44 (2.68)	65.20 (2.69)
3000	62.79 (3.09)	65.83 (3.22)

The study of Bleich et al. (1993 and 1994) did not find tendency of carbon dioxide density (related to pressure) on particle size if the polymer (Resomer L206) was sprayed from dichloromethane solution into supercritical carbon dioxide at a range of density from 500 to 810 kg/m^3. The results of Thies et al. (1998) showed a distinct dependence between particle size and carbon dioxide density. Microparticles manufactured at a carbon dioxide density of 560 kg/m^3 had a mean particle size of 6 μm. According to Bleich et al. (1994), a further increase in density did not affect the particle size. The particle size increased if the density was lowered below 560 kg/m^3. However, at a carbon dioxide extraction density lower than 250 kg/m^3, the particles showed a constant size in the range of 50 μm. Below a density of 180 kg/m^3, no particles could be formed. The solubility of dichloromethane in the carbon dioxide was too low to dissolve the injected liquid. Thus, conglutinated film like polymer structures were found on the bottom of the column. The morphology of the particles sprayed in moderately compressed (438 kg/m^3) and highly compressed (689 kg/m^3) carbon dioxide was nearly equal. Particles produced at a low carbon dioxide density (201 kg/m^3) showed cracks and holes.

Boutin et al. (2004) could produce co-precipitates of diuron (herbicide) and L-PLA microparticles when increasing the pressure to 14.5 MPa. The formation of rather spherical particles at diuron concentration of 1.5 %wt was occurred whereas pressure of 10 MPa provided larger diuron needle and L-PLA microparticles. One possible interpretation of this result lied on the influence of the pressure upon the droplet size. Increasing the pressure from 10 to 14.5 MPa at 308 K resulted in an increase in the carbon dioxide density from 720 to 805 kg/m^3. The size of the droplets depended either on the interfacial tension between the organic solution and the supercritical phase or on the density of CO_2. In this case, the modification of the anti-solvent density induced a better dispersion of the organic solution in CO_2 and hence a decrease in the droplet size, and as a consequence the acceleration of the mass transfer phenomena. Thereby, supersaturation within the liquid phase was reached more quickly what prevented diuron crystals from growing and allowed the formation of microspheres composed of herbicide embedded in the polymer at higher concentrations.

2.5 Effect of Solution Concentration

The solution concentration of rifampicin (30%) and polymer (70%) in methylene chloride was varied from 1 % to 3 % w/v. Solutions were sprayed at operating pressure of 2500 psi and temperature of 40 °C while maintaining all other variables constant. The effect of increasing the concentration from 1 % to 3 % w/v on the precipitation of drug and L-PLA in the SAS process was to increase the $D_{50\%}$ of the microparticles to 4.5 μm.

The morphology of microparticles obtained from various solution concentrations is shown in Figure 4-25. The characteristics of the rifampicin-polymer microparticles were found slightly sensitive to solution concentration changes in the system. The microparticles produced from solution concentration of 1 % to 3 % w/v were spherical. Figure 4-26 and 4-27 show the particle size distribution by volume and percent cumulative undersize curves of rifampicin-L-PLA microparticles at various solution concentrations, respectively. The volume particle size distribution curve of rifampicin-L-PLA microparticles at operating solution concentration of 3 % w/v was slightly shifted to the right and border than those of 1 % and 2 % w/v. The particle size distribution obtained at different solution concentrations of rifampicin and polymer in methylene chloride are reported in Table 4-20. It was shown that by increasing the solution concentration the volumetric median diameter increased and the particle size distribution enlarged. Their distributions were ranging from 1.3 to 16 μm and the span increased with increasing concentration. By one-way ANOVA tests (Table 5-12 in Appendix), the volumetric median diameter produced at solution concentration of 3 % w/v was significantly different from those produced at solution concentration of 1 % and 2 % w/v ($p<0.05$). As present in Table 4-21 reports, it was observed that the 1-5 μm size of microparticles using of 1 % and 2 % w/v solution were more than 60 %, as those of 3 % w/v was less than 50 %.

Tu and co-worker (2002) reported similar effect of increasing the solution concentration from 0.6 to 2 % w/v on the slight increase in size of the precipitation of L-PLA in the ASES process. However at concentrations above 2 % w/v, fibers were produced. It confirmed the observations by Randolph et al. (1993), fiber formation at solution concentrations exceeding 4 %w/v L-PLA in methylene chloride was found. Similar observations were also reported for the polystyrene/toluene/CO_2 system, where a critical composition of approximately 5 % w/v was reported (Dixon et al. 1993).

1% w/v

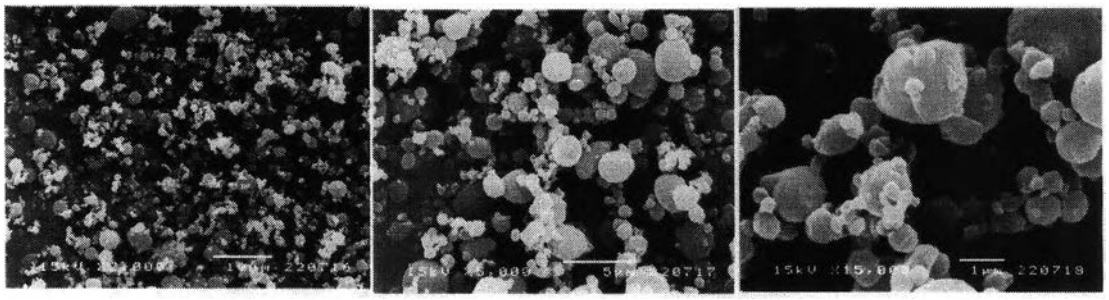

X 2000 **X 5000** **X 15000**

2% w/v

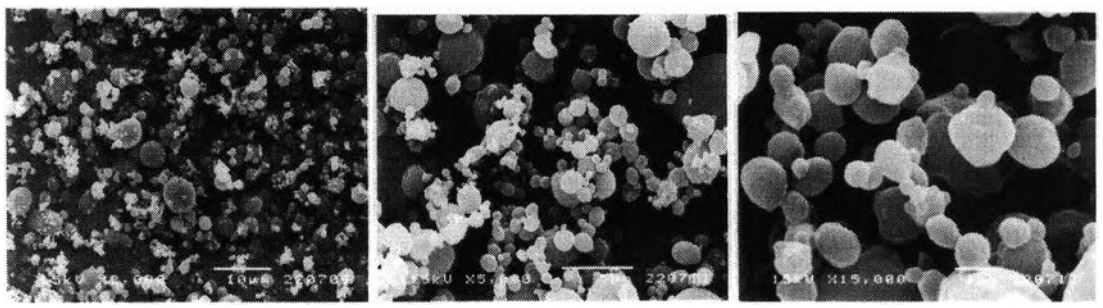

X 2000 **X 5000** **X 15000**

3% w/v

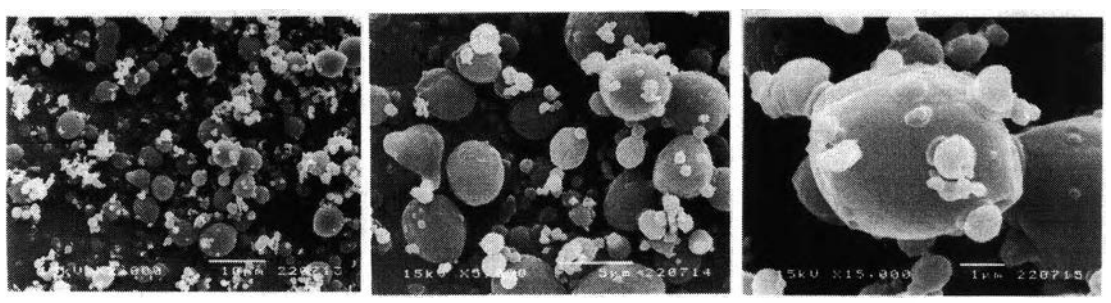

X 2000 **X 5000** **X 15000**

Figure 4-25 SEM photomicrographs of rifampicin-L-PLA microparticles produced from 1 %, 2 % and 3 % w/v solution.

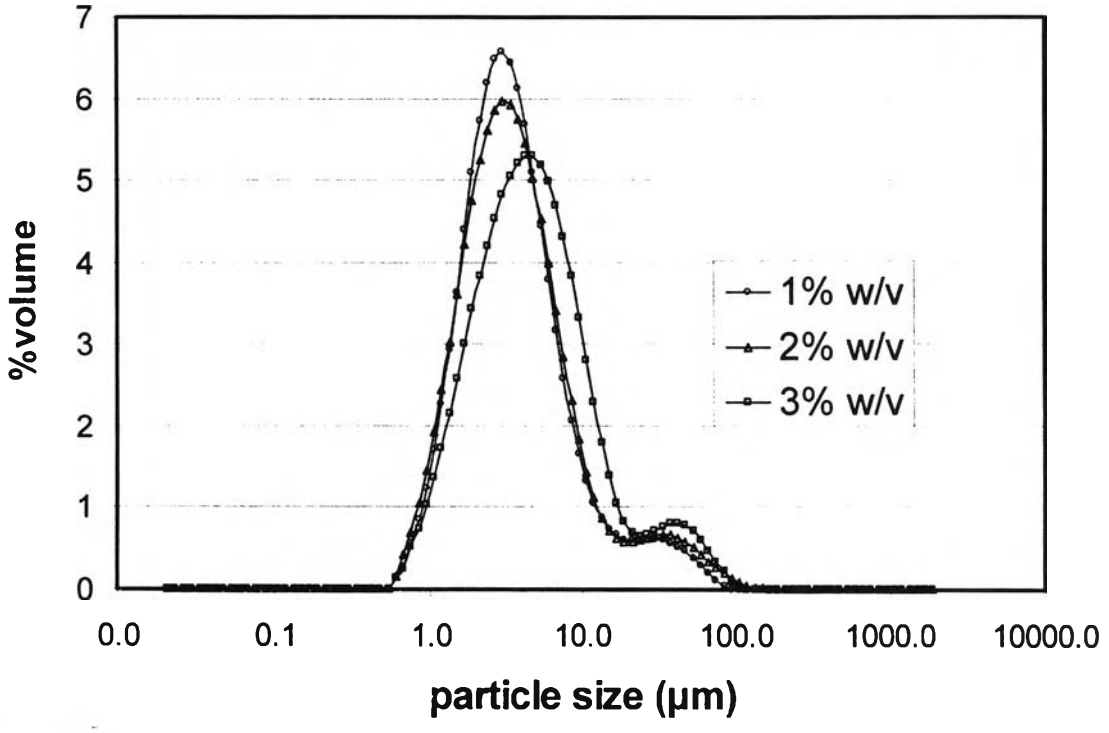

Figure 4-26 Effect of concentration of solution on particle size distribution by volume of rifampicin-L-PLA microparticles.

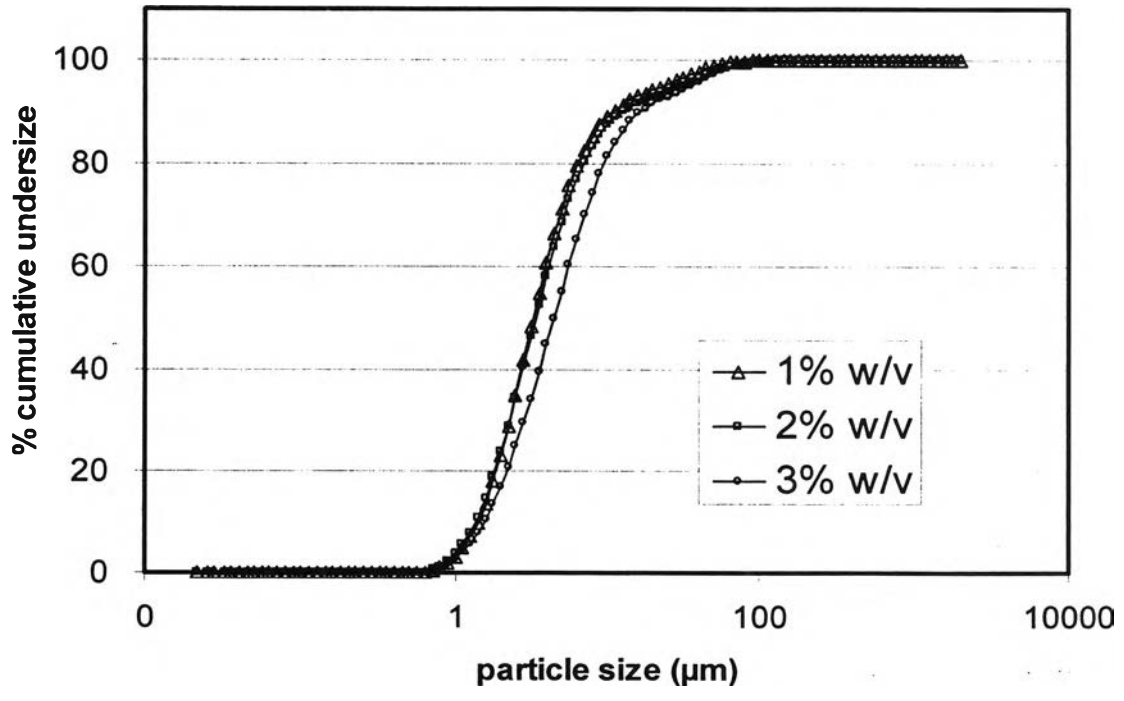

Figure 4-27 Effect of concentration of solution on percent cumulative undersize of rifampicin-L-PLA microparticles.

Table 4-20 Effect of concentration of solution on particle size of rifampicin-L-PLA microparticles.

Conc.	$D_{10\%}$ (μm)	$D_{50\%}$ (μm)	$D_{90\%}$ (μm)	Span
	average (SD)	average (SD)	average (SD)	average (SD)
1% w/v	1.42 (0.05)	3.28 (0.04)	10.84 (0.59)	2.88 (0.18)
2% w/v	1.36 (0.01)	3.40 (0.04)	12.52 (0.77)	3.29 (0.25)
3% w/v	1.56 (0.04)	4.50 (0.23)	16.46 (2.41)	3.31 (0.48)

Table 4-21 Effect of concentration of solution on % particle size of 1-5 μm and < 5 μm of rifampicin-L-PLA microparticles.

Conc.	% Particle 1-5 μm	% Particle < 5 μm
	average (SD)	average (SD)
1% w/v	64.95 (2.93)	68.00 (2.87)
2% w/v	61.44 (2.68)	65.20(2.69)
3% w/v	48.93 (2.42)	51.57 (2.39)

Taki et al. (2001) concluded that the main parameters controlling the encapsulation of diuron by L-PLA were the absolute concentrations of the two components, rather than the ratio of these concentrations. The concentration of each component had an upper limit, 3 % w/v for L-PLA and 0.1 % w/v for diuron and the encapsulation was successful when the two concentrations were below these thresholds. If two concentrations were above these thresholds, the crystals of diuron and the L-PLA microparticles or fibers were instead obtained. This experiment carried out at 10 MPa, 308 K and with a solution flow rate of 30 ml h−1. For other values of the pressure, the respective concentrations remained the main parameters controlling the encapsulation but the thresholds were slightly shifted towards higher values as the pressure was increased.

However, the microparticles processed from the absolute concentration of 3 % w/v of rifampicin and L-PLA consistently provided the discrete microparticles in this study, their particle size were slightly larger than those of 1 % and 2 %w/v. The more concentrated solution was not processed in this experiment.

2.6 Effect of Solution Feed Rate

The solution feed rate was varied from 0.4 to 0.6 ml/min. Solutions were sprayed at operating pressure of 2500 psi and temperature of 40 °C while maintaining all other variables constant. The effect of increasing the feed rate from 0.4 to 0.6 ml/min on the precipitation of drug and L-PLA in the SAS process was the tendency of slight increasing particle size.

The morphology of microparticles obtained from various solution feed rate is illustrated in Figure 4-28. The characteristics of the rifampicin-polymer microparticles were found no sensitive to solution feed rate changes in the system. The microparticles produced from solution feed rate of 0.4 to 0.6 ml/min were spherical. Figure 4-29 and 4-30 depict the volume particle size distribution and % cumulative undersize curves of rifampicin-L-PLA microparticles at various the solution feed rate, respectively. The volume particle size distribution and % cumulative undersize curves of rifampicin-L-PLA microparticles produced all solution feed rate were similar. The particle size distribution and the % particle size of 1-5 μm and < 5 μm of rifampicin-L-PLA microparticles obtained at different feed rate of solution were listed in Table 4-22 and Table 4-23, respectively. Their distributions were ranging from 1.3 to 12 μm. By one-way ANOVA tests (Table 5-13 in Appendix), the median particles size produced at solution feed rate of 0.5 ml/min was significantly different from those produced at solution feed rate of 0.6 ml/min ($p<0.05$). It was observed that the percent particle size of 1-5 μm of microparticles obtained at feed rate of 0.4 and 0.5 ml/min were higher than 60 %, as those of 0.6 ml/min was less than 56 %.

The different results were reported by Tu et al. (2002) that for the L-PLA system, an increase in feed rate of solution resulted in the production of smaller particles. In addition to microspheres, irregularly shaped clusters of polymer were also precipitated at high feed rate. In an atomization process, smaller droplets were generated in the spray when the solution was sprayed at a higher velocity. As feed rate increased and smaller droplets were formed, the higher surface area and higher rates of mass transfer resulted in the precipitation of smaller particles due to higher levels of supersaturation in the droplets. These amorphous particles could have been formed from higher rates of shear as a result of the higher velocities experienced by the liquid stream as it passed through the capillary.

0.4 ml/min

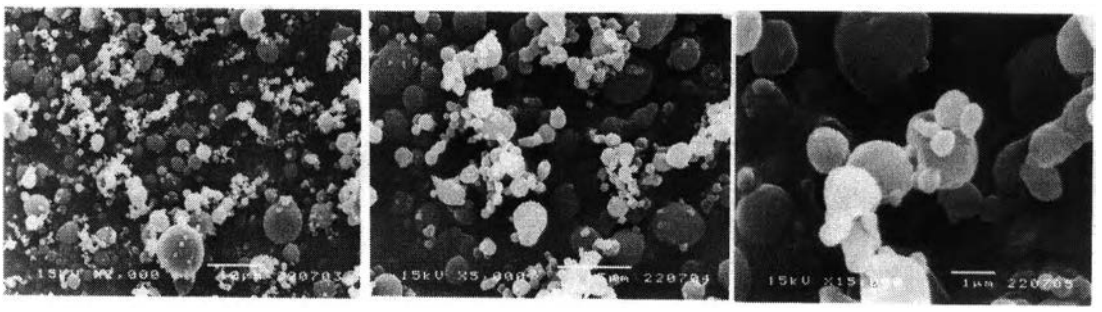

X 2000 **X 5000** **X 15000**

0.5 ml/min

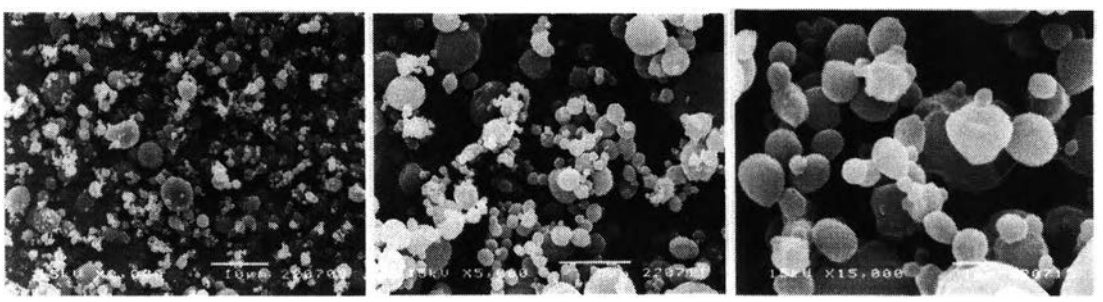

X 2000 **X 5000** **X 15000**

0.6 ml/min

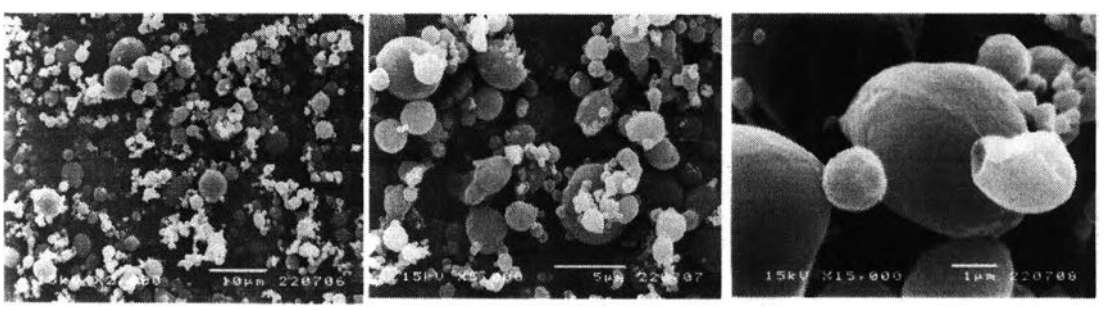

X 2000 **X 5000** **X 15000**

Figure 4-28 SEM photomicrographs of rifampicin-L-PLA microparticles produced from solution feed rate of 0.4, 0.5 and 0.6 ml/min.

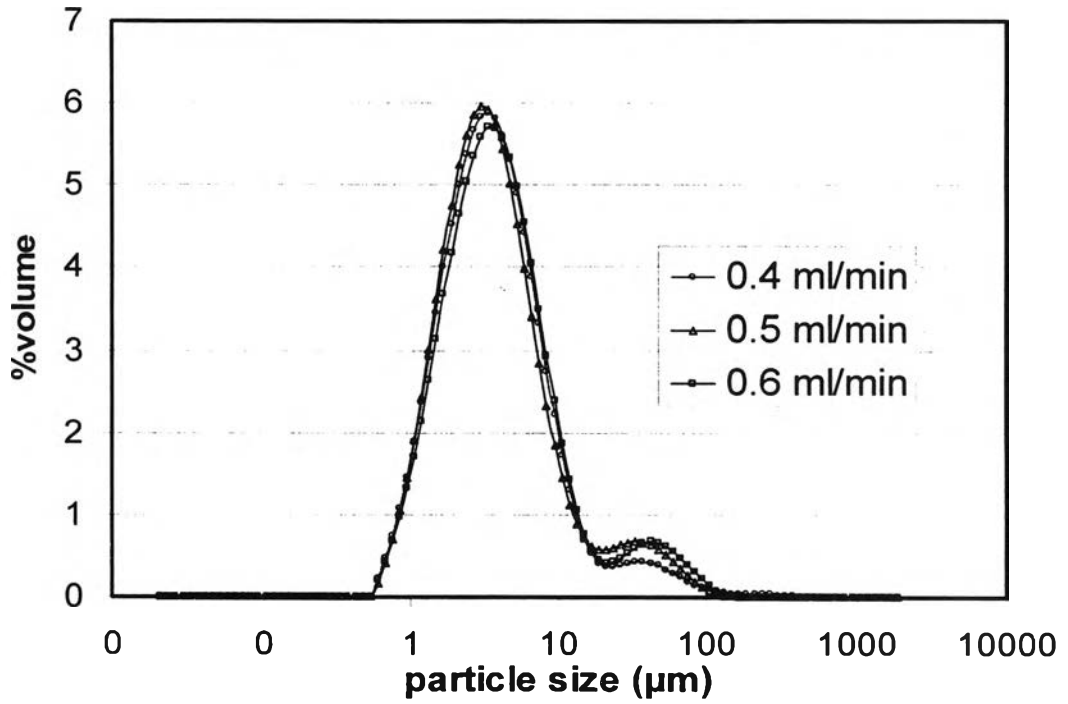

Figure 4-29 Effect of solution feed rate on particle size distribution by volume of rifampicin-L-PLA microparticles.

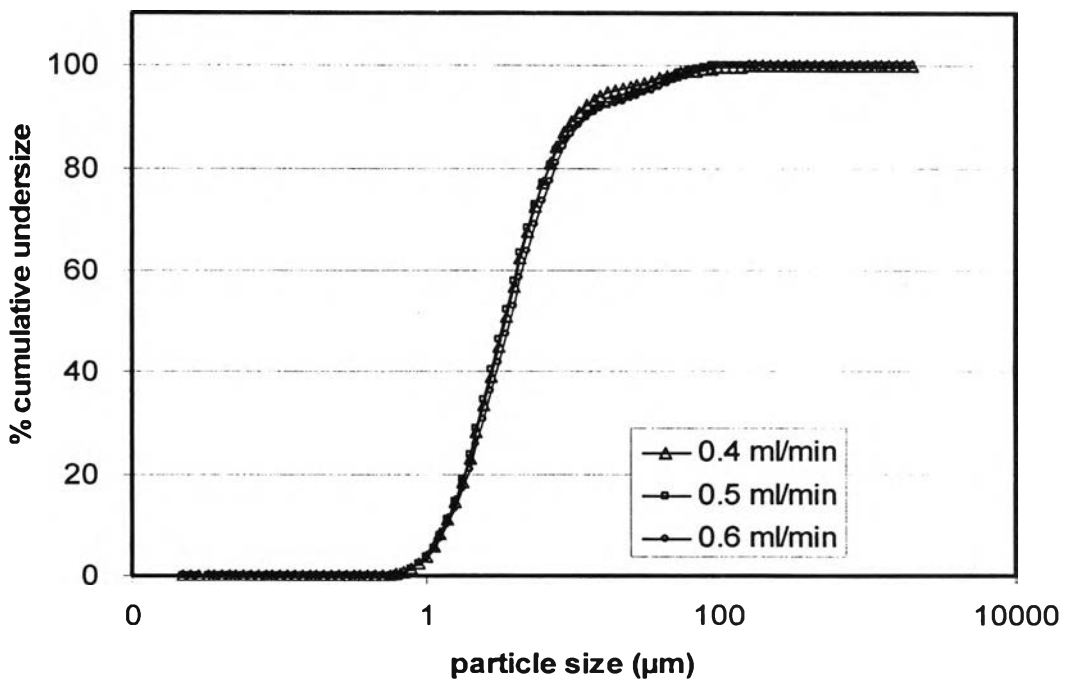

Figure 4-30 Effect of solution feed rate on percent cumulative undersize of rifampicin-L-PLA microparticles.

Table 4-22 Effect of solution feed rate on particle size of rifampicin-L-PLA microparticles.

Feed rate (ml/min)	**$D_{10\%}$** (μm)	**$D_{50\%}$** (μm)	**$D_{90\%}$** (μm)	**Span**
	average (SD)	average (SD)	average (SD)	average (SD)
0.4	1.36 (0.02)	3.49 (0.14)	10.55 (0.81)	2.64 (0.17)
0.5	1.36 (0.01)	3.40 (0.04)	12.52 (0.77)	3.29 (0.25)
0.6	1.41 (0.01)	3.75 (0.04)	12.91 (0.56)	3.07 (0.13)

Table 4-23 Effect of solution feed rate on % particle size of 1-5 μm and < 5 μm of rifampicin-L-PLA microparticles.

Feed rate (ml/min)	**% Particle** 1-5 μm	**% Particle** < 5 μm
	average (SD)	average (SD)
0.4	60.12 (2.51)	64.11 (2.44)
0.5	61.44 (2.68)	65.20 (2.69)
0.6	56.85 (2.24)	60.46 (2.14)

2.7 Reproducibility of Supercritical Fluid Technique in Preparation Polymer-Drug Loaded Microparticles

This experiment was performed to investigate the consistency of supercritical antisolvent process. The formulation containing 30% rifampicin and 70% L-PLA was selected, because it provided spherical and discrete microparticles with high drug loading. The operation parameters as follows; 2% solution of rifampicin and L-PLA in methylene chloride, supercritical carbon dioxide pressure of 2500 psi, temperature of 40 °C and solution feed rate of 0.5 ml/min were chosen for production the L-PLA rifampicin loaded microparticles because it provided the suitable microparticles properties for powder inhalation such as median particle size less than 5 μm, the high percentage of particle size between 1 to 5 μm. The consistency of production of the microparticles was investigated by preparing three consecutive batches.

Figure 4-31 and 4-32 display the particle size distribution by volume and percent cumulative undersize curves of rifampicin-L-PLA microparticles of three consecutive batches, respectively. The particle size distribution by volume and percent cumulative undersize curves of rifampicin-L-PLA microparticles of all batches were similar. The particle size distribution and the % particle size of 1-5 μm and < 5 μm of rifampicin-L-PLA microparticles obtained from all batches are listed in Table 4-23 and Table 4-24, respectively. Their distributions ranged from 1.3 to 12 μm. By one-way ANOVA tests (Table 5-14 in Appendix), the volumetric median diameter of three consecutive batches were not significantly difference. It was observed that the percent particle size of 1-5 μm of microparticles obtained from three consecutive batches were more than 60% (Table 4-24). It was shown that the supercritical process of this study was reproducibility.

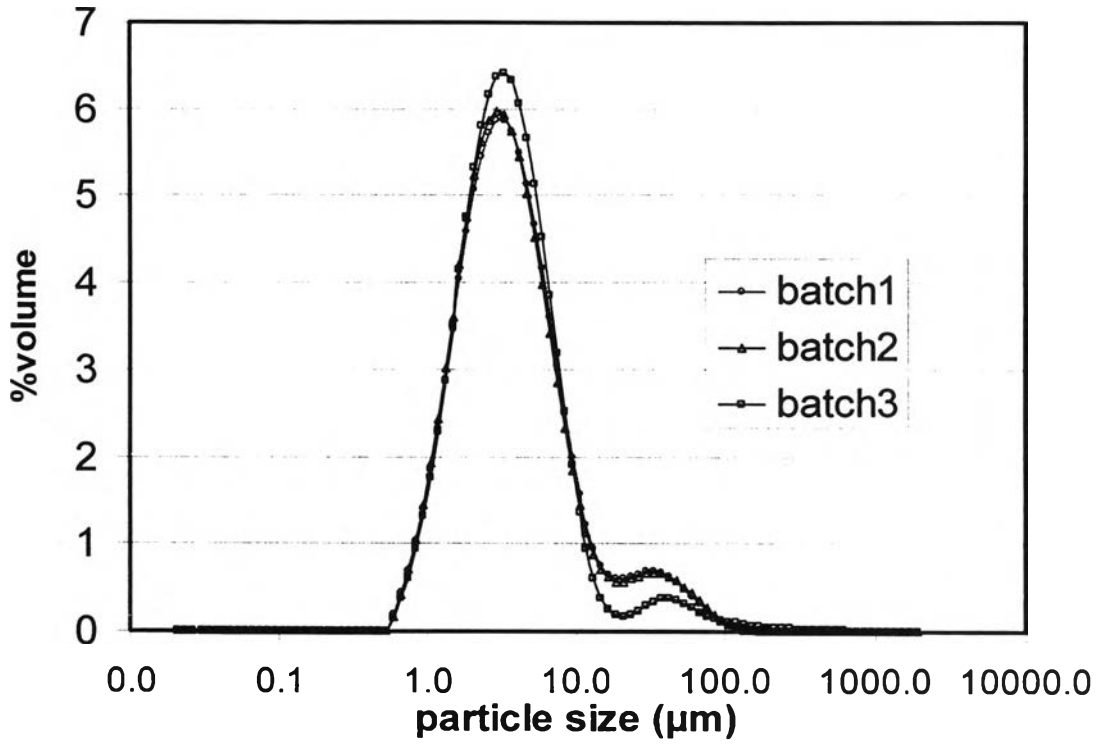

Figure 4-31 The particle size distribution by volume of rifampicin-L-PLA microparticles produced from three consecutive batches.

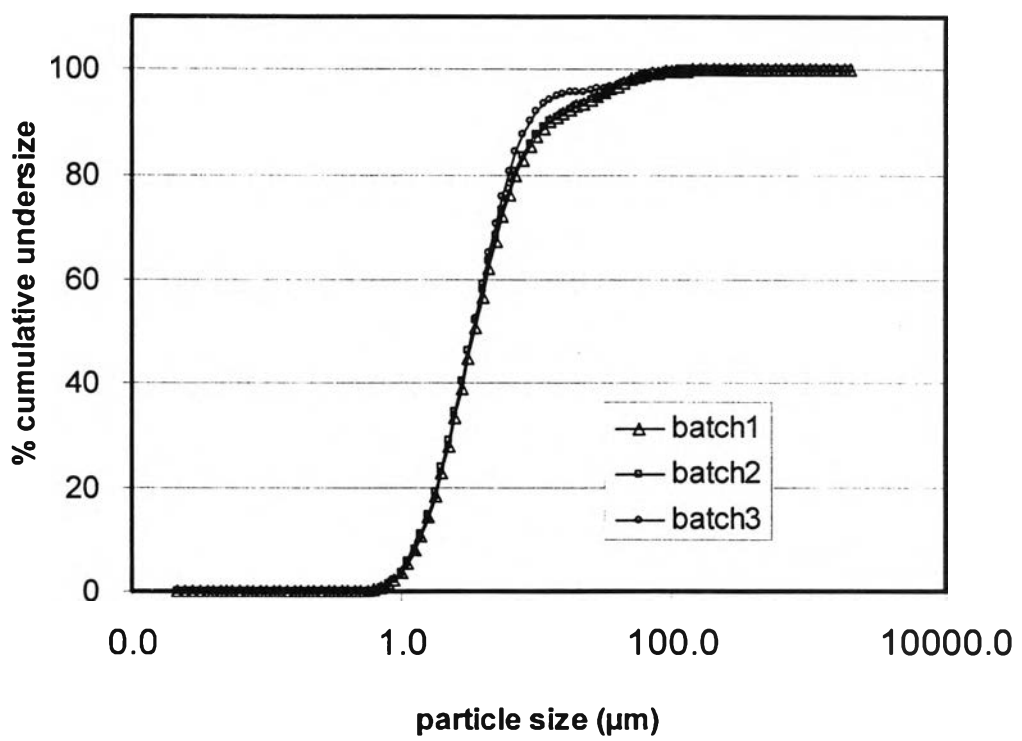

Figure 4-32 The percent cumulative undersize of rifampicin-L-PLA microparticles produced from three consecutive batches.

Table 4-24 Reproducibility on particle size of rifampicin-L-PLA microparticles produced from three consecutive batches.

Batch No.	$D_{10\%}$ (μm)	$D_{50\%}$ (μm)	$D_{90\%}$ (μm)	Span
	average (SD)	average (SD)	average (SD)	average (SD)
1	1.37 (0.02)	3.50 (0.18)	12.60 (0.58)	3.21 (0.19)
2	1.36 (0.01)	3.40 (0.04)	12.52 (0.77)	3.29 (0.25)
3	1.40 (0.04)	3.39 (0.13)	10.38 (4.39)	2.62 (1.19)

Table 4-25 Reproducibility on % particle size of 1-5 μm and < 5 μm of rifampicin-L-PLA microparticles produced from three consecutive batches.

Batch No.	% Particle 1-5 μm	% Particle < 5 μm
	average (SD)	average (SD)
1	60.05 (0.52)	63.79 (0.55)
2	61.44 (2.68)	65.20 (2.69)
3	63.40 (1.08)	66.77 (0.87)

2.8 *In vitro* Drug Release of Rifampicin-L-PLA Microparticles

The dissolution profiles of the microparticles in PBS pH 7.4 are shown in Figure 4-33. Processed rifampicin produced by SAS technique had slightly higher dissolution rate than raw material rifampicin. It is possible that SAS process decreased the particle size and gave needle-like crystals which dissolved faster than larger polygonal particles of unprocessed rifampicin. The dissolution release rate was decrease by the increase percent polymer content in drug loaded microparticles. When the amount of polymer used for preparing microparticles was reduced to 60 % L-PLA, the release was significantly increased. It might be due to the amount of drug entrapped in microparticles of 60 % polymer content was lower than those of 70 % and 80 % polymer content. The initial burst release did not occur in 70 % and 80 % L-PLA rifampicin microparticles. This opposite result was found when the microparticles prepared by the other method, such as solvent evaporation and spray drying method (O'Hara et al. 2000), the initial burst release were approximately 10-20 %. The standard deviations of each point on dissolution curves were rather high because of the poor wettability of microparticles. The dissolution data revealed that drug release from PLA matrix displayed two phases, suggesting different mechanisms of drug release. The faster release probably represented the release of poorly entrapped and surface-associated rifampicin. Consequently, the faster release is not controlled by drug diffusion within the polymer matrix. The drug release during the slower release phase might result from drug diffusion through the polymer matrix. As the process of erosion was slow, a gradual but continuous release occurred.

Fu et al. (2001) who investigated the degradation profiles of the PLA microspheres by GPC. They showed a slight near-linear decrease in the polymer molecular weight over an experimental duration of 1 week. This slight decrease in PLA molecular weight indicated that the drug release from the polymer was much faster than the polymer weight loss. This suggested that the drug was able to diffuse through the aqueous channel in the polymer matrix rather than polymer surface erosion.

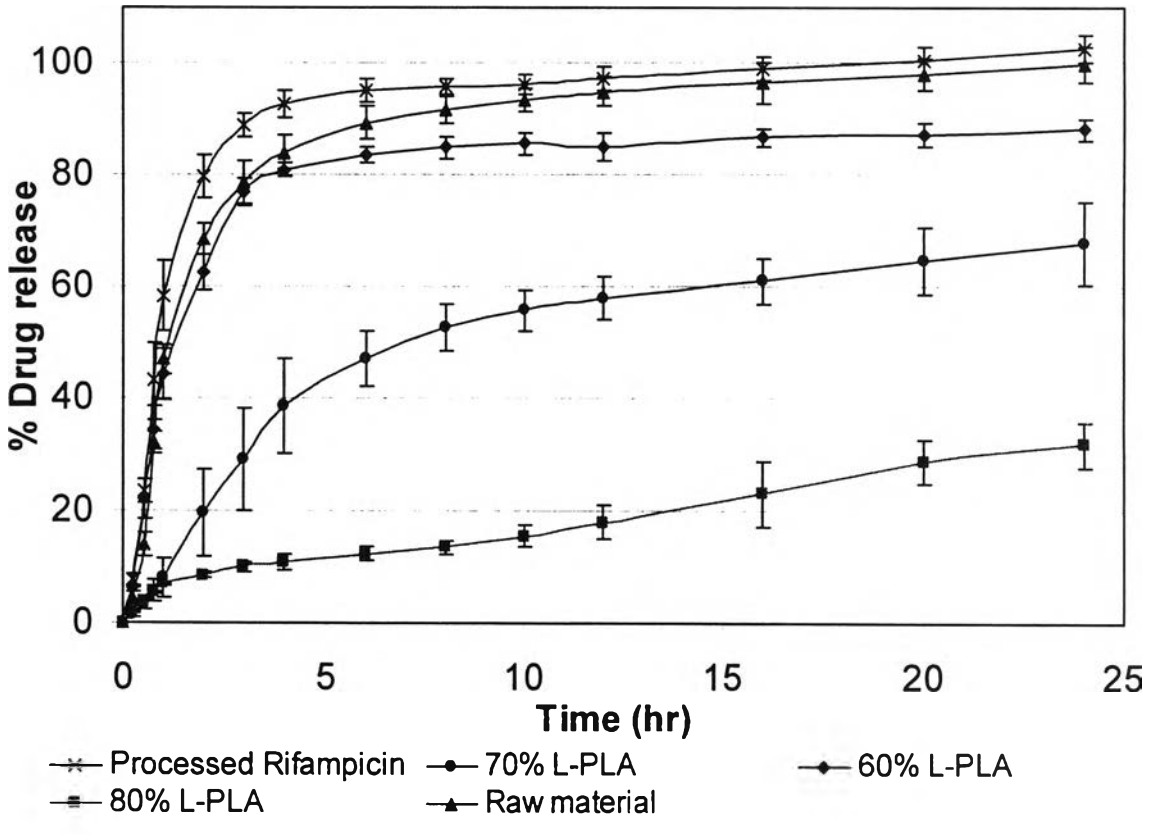

Figure 4-33 Dissolution curves of rifampicin-L-PLA microparticles produced from various polymer content.

Figure 4-34 shows SEM photomicrographs of rifampicin-L PLA microparticles containing 60 %, 70 % and 80 % polymer content after release process. It was observed that those microparticles after release exhibited small pores on the surface of microparticles and their shape did not change. This pore might be occurred after drug diffusion through the polymer matrix.

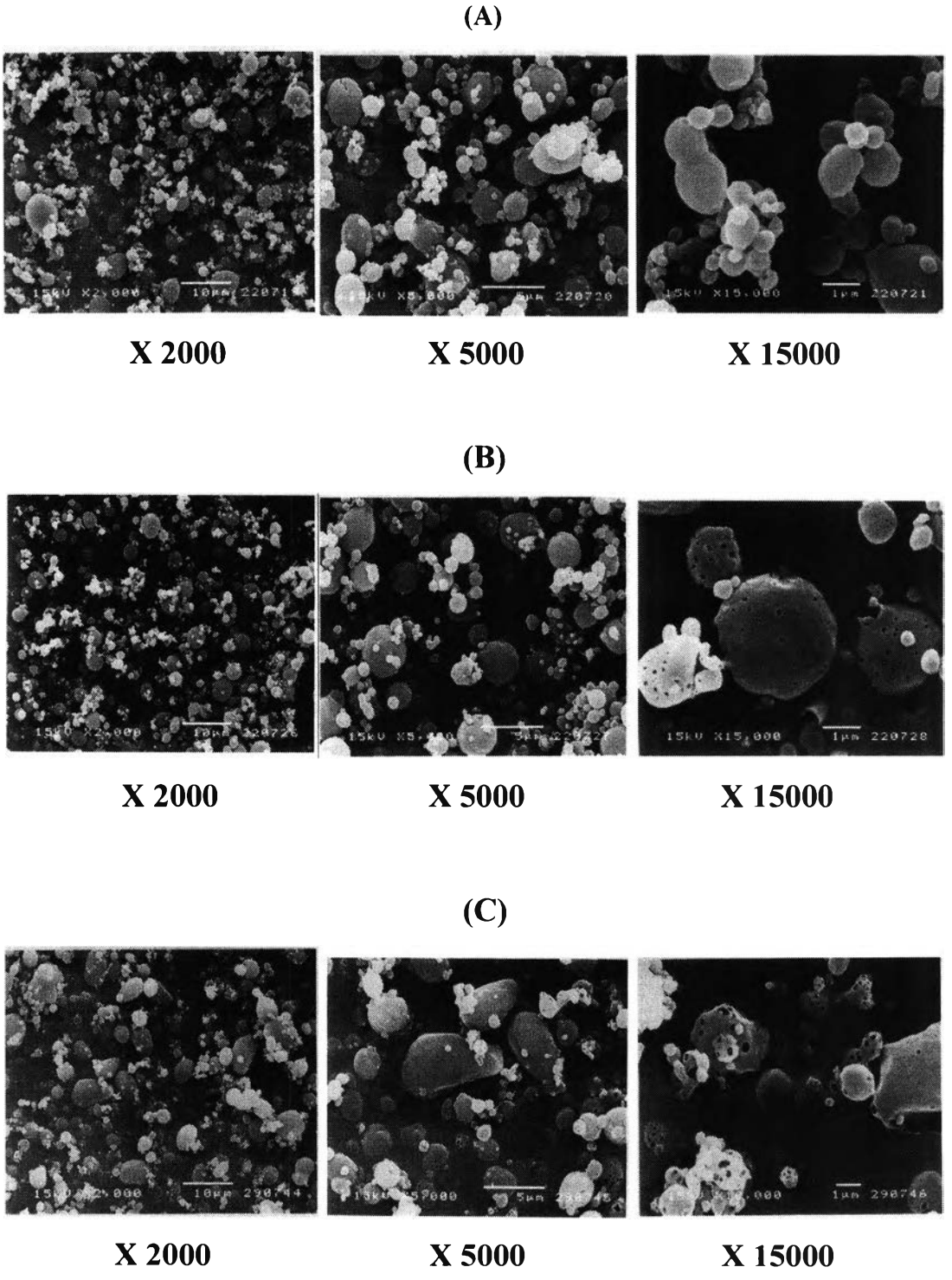

Figure 4-34 SEM photomicrographs of rifampicin-L-PLA microparticles after release processed (A) 80 % L-PLA microparticles (B) 70 % L-PLA microparticles (C) 60 % L-PLA microparticles.

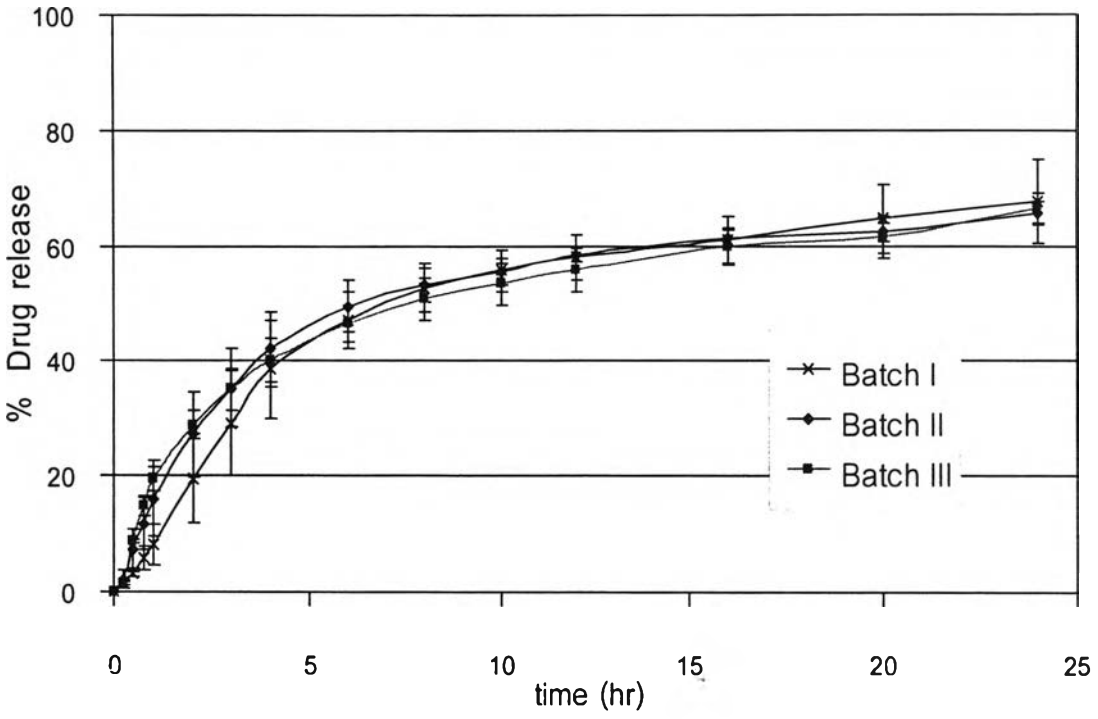

Figure 4-35 Dissolution curves of rifampicin-L-PLA microparticles produced from three consecutive batches.

The dissolution profiles of the microparticles from three consecutive batches are shown in Figure 4-35. Their dissolution curves were slightly different. The difference factor (f_1) and similarity factor (f_2) of each dissolution curves were calculated. The difference factor, f_1, is the average % difference over all time points in the amount of test batch dissolved as compared to the reference batch. The f_1 value is 0 when the test and the reference profiles are identical and increases proportionally with the dissimilarity between the two profiles. The similarity factor (f_2) is a logarithmic transformation of the sum-squared error of differences between the test and reference products.

Difference factor, f_1:

$$f_1 = \left\{ \frac{\sum_{t=1}^{n} w_t |R_t - T_t|}{\sum_{t=1}^{n} w_t R_t} \right\} \times 100\%$$

Similarity factor, f_2:

$$f_2 = 50 \log\left\{ \left[1 + \frac{1}{n}\sum_{t=1}^{n} w_t (R_t - T_t)^2 \right]^{-0.5} \times 100 \right\}$$

n represents the number of time points, w_t is the optional weight factor, R_t the dissolution value of the reference method at time t, while T_t the dissolution value of the test method at time t. f_1 value indicates the percent difference between two profiles at each time point and is a measurement of the relative error between them. The similarity value (f_2), however, is a measurement of the similarity between the dissolution profiles. In general, to ensure sameness between the profiles, f_1 should be in the range of 0–15, and f_2 in the range of 50–100. To calculate the fit factors, the mean dissolution values from both profiles at each time interval were used, including only one pull point at greater than 85% level of drug release in order to avoid bias in the similarity assessment (Shah et al. 1998).

Table 4-26 Difference factor and similarity factors of three consecutive batches

Batch	Difference factor (f_1)	Similarity factor (f_2)
Batch I / Batch II	8.59	68.56
Batch I / Batch III	10.79	63.49
Batch II / Batch III	4.74	81.86

Table 4-26 reports difference factor (f_1) and similarity factor (f_2) of three batches. The difference factor (f_1) and similarity factors (f_2) calculated from the dissolution profiles of rifampicin biodegradable microparticles which were produced in same conditions. Comparing the dissolution profiles of Batch I / Batch II, the difference factor (f_1) and similarity factor (f_2) value obtained were 8.59 and 68.56, respectively. Batch I and batch II had similar dissolution profiles. For dissolution profiles of Batch I / Batch III and Batch II / Batch III, the difference factor (f_1) and similarity factor (f_2) value obtained were 10.79 and 4.74, 63.49 and 81.86, respectively. It was shown that reproducible product character could be achieved.

2.9 *In vitro* Drug Deposition of Rifampicin-L-PLA Microparticles

The small particles could not be handled in the pharmaceutical production or in an inhaler, as the particles would adhere to most surfaces due to van der Waals and electrostatic forces. This problem can be solved by using large carriers, about 30- to 300-μm (most often 50- to 150-μm), such as lactose or glucose, which are blended with the smaller drug particles. The surface of the carrier particles has energy-rich sites and the small drug particles adhere to these sites on the carrier particle during blending. First, the most energy-rich sites are covered with drug particles and eventually also the less energy-rich sites. The properties of the resulting, ordered mixture pharmaceutical formulation, allow the powder to be handled in the production process, in the inhaler, and at inhalation (Figure 4-36). The adhesion of the small particles to the carrier may not be too strong as they should detach during inhalation. The roughness of the carrier and the time and speed of mixing may have a significant effect on the adhesion of the small particles to the carrier particles.

Drug particles are theoretically stripped from the surface of the lactose particles, to which they loosely attach, during the generation process. This process is illustrated schematically in Figure 4-37. Thus, the drug particles are dispersed and can traverse the upper respiratory tract while the excipient particles do not pass beyond the mouth-piece of the device or the mouth and throat of the patient (Borgstrom et al. 2002).

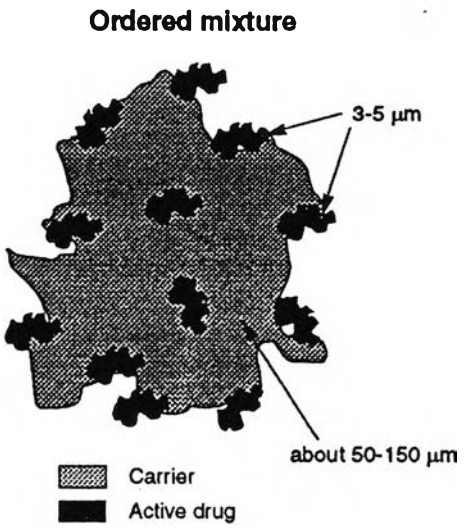

Figure 4-36 An ordered mixture, the active drug particles are small size, while the lactose components are large size. (Borgstrom et al. 2002).

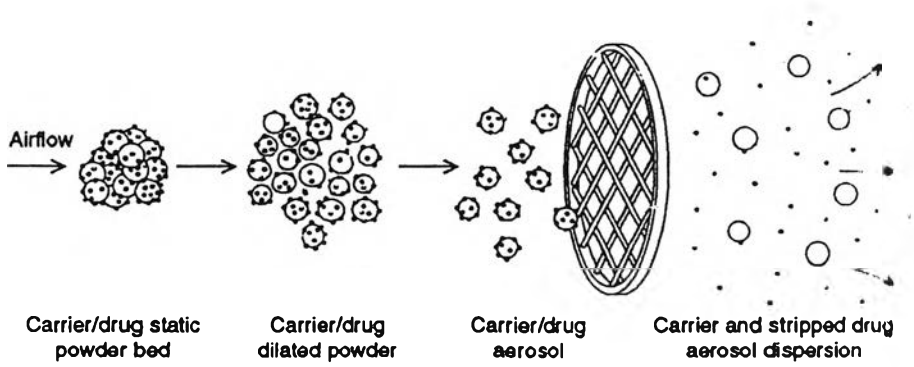

Figure 4-37 A schematic diagram of the deaggregation of an order mixture formula. (Borgstrom et al. 2002).

The respiratory tract is subdivided into air conducting zones and generations of bifurcating passageways. Because of the bifurcation leading to inertial impaction and sedimentation, only particles of aerodynamic diameter below 5 μm are able to reach the deep lung alveoli region which consists of the majority of blood vessels and targeted for drug delivery. Submicron particles are likely to be exhaled, thus a narrow particle size distribution between 1 and 5 μm was required for efficient drug delivery (Shekunov and York 2000). Dry powder inhaler (DPI) formulations are often used an excipient (typically crystalline lactose) to provide easily fluidized, consistent portions of inhalation powder. In this case, size and surface properties of the excipient crystals are also important.

In this experiment, dry powder inhaler (DPI) formulations consisted of inhalation grade lactose as a carrier and microparticles producing from 70 % L-PLA and 30 % rifampicin by SAS process. Figure 4-38 shows the morphology of the carrier. The lactose exhibited polygonal shape with rough surface. Those microparticles were used in DPI formulations due to the high percent particles of 1-5 μm in size. Moreover, those microparticles showed no aggregation, had narrow size distribution and a sustained release property in vitro. The two different size of lactose were mixed in formulations: lactose having less than 45 μm in size and lactose having 45 to 90 μm in size. Figure 4-39 shows SEM photomicrographs of formulation containing 70 % L-PLA rifampicin loaded microparticles and lactose (< 45 μm) in 1: 2 ratio (Formula I). Figure 4-40 shows SEM photomicrographs of formulation containing 70 % L-PLA rifampicin loaded microparticles and lactose (45-90 μm) in 1:2 ratio (Formula II). Their photographs exhibit microparticles which adhered on the surface of lactose as in the order mixture model. Those formulas were tested to find the percent of fine faction and aerodynamic diameter.

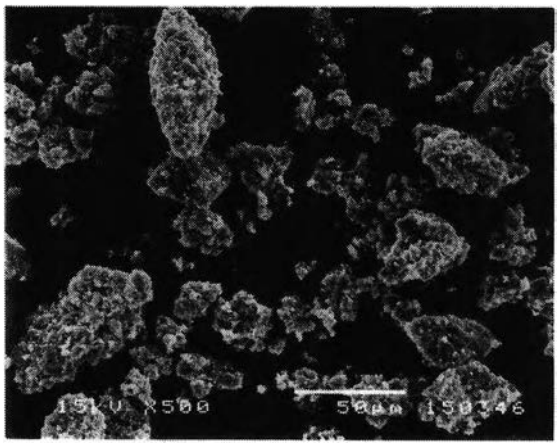

X 500

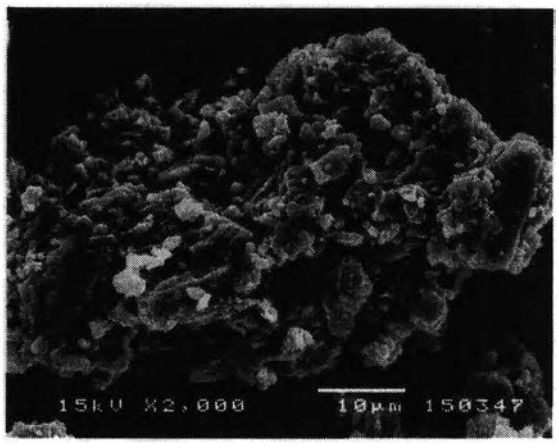

X 2000

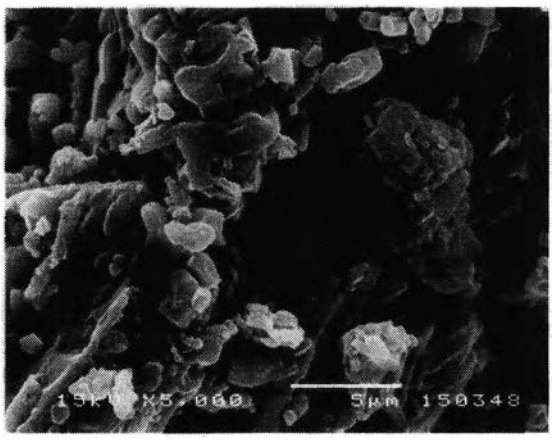

X 5000

Figure 4-38 SEM photomicrographs of inhalation lactose used in formulations at different magnifications.

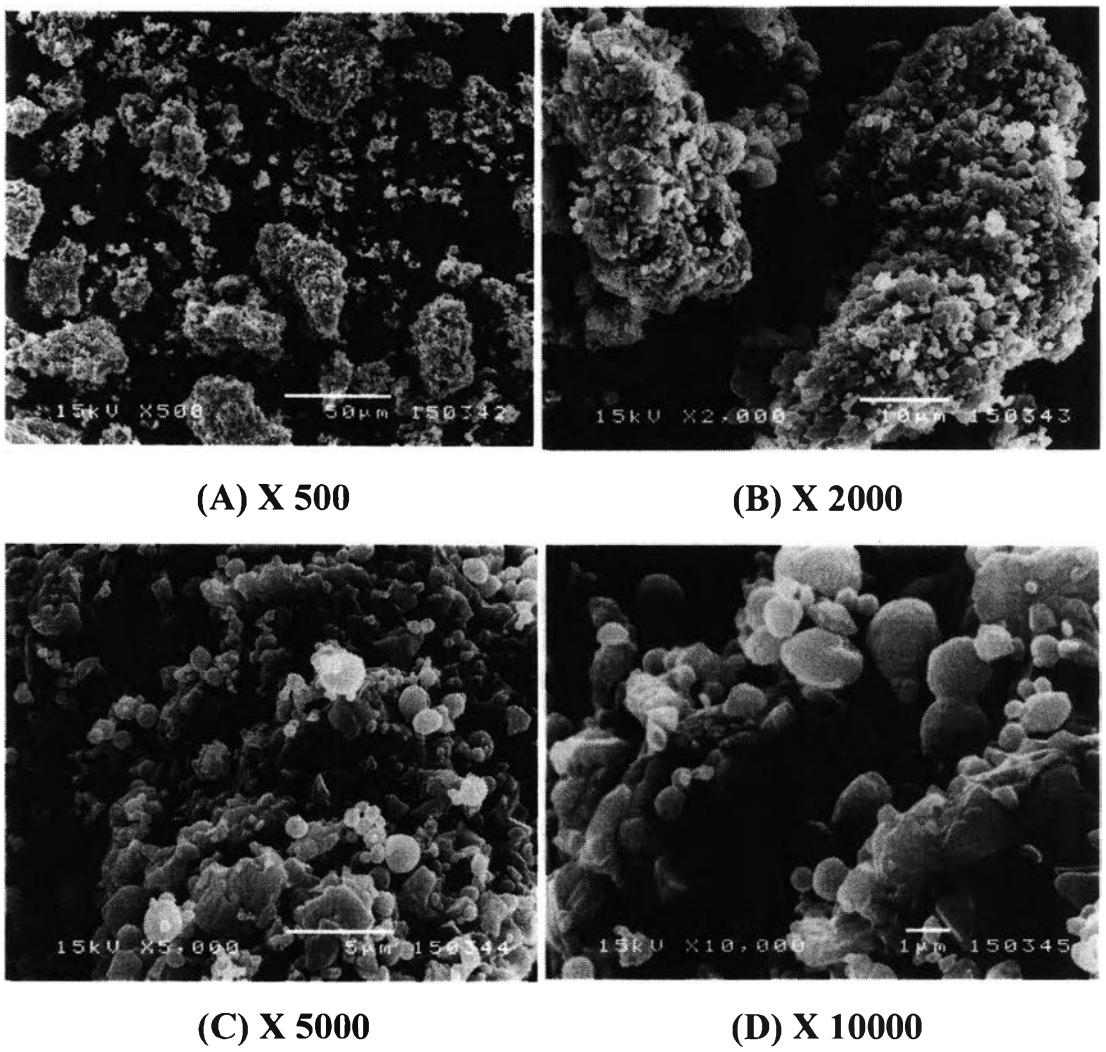

(A) X 500 **(B) X 2000**

(C) X 5000 **(D) X 10000**

Figure 4-39 SEM photomicrographs of formulation containing 70% L-PLA rifampicin loaded microparticles and lactose (< 45µm) in 1: 2 ratio at different magnifications.

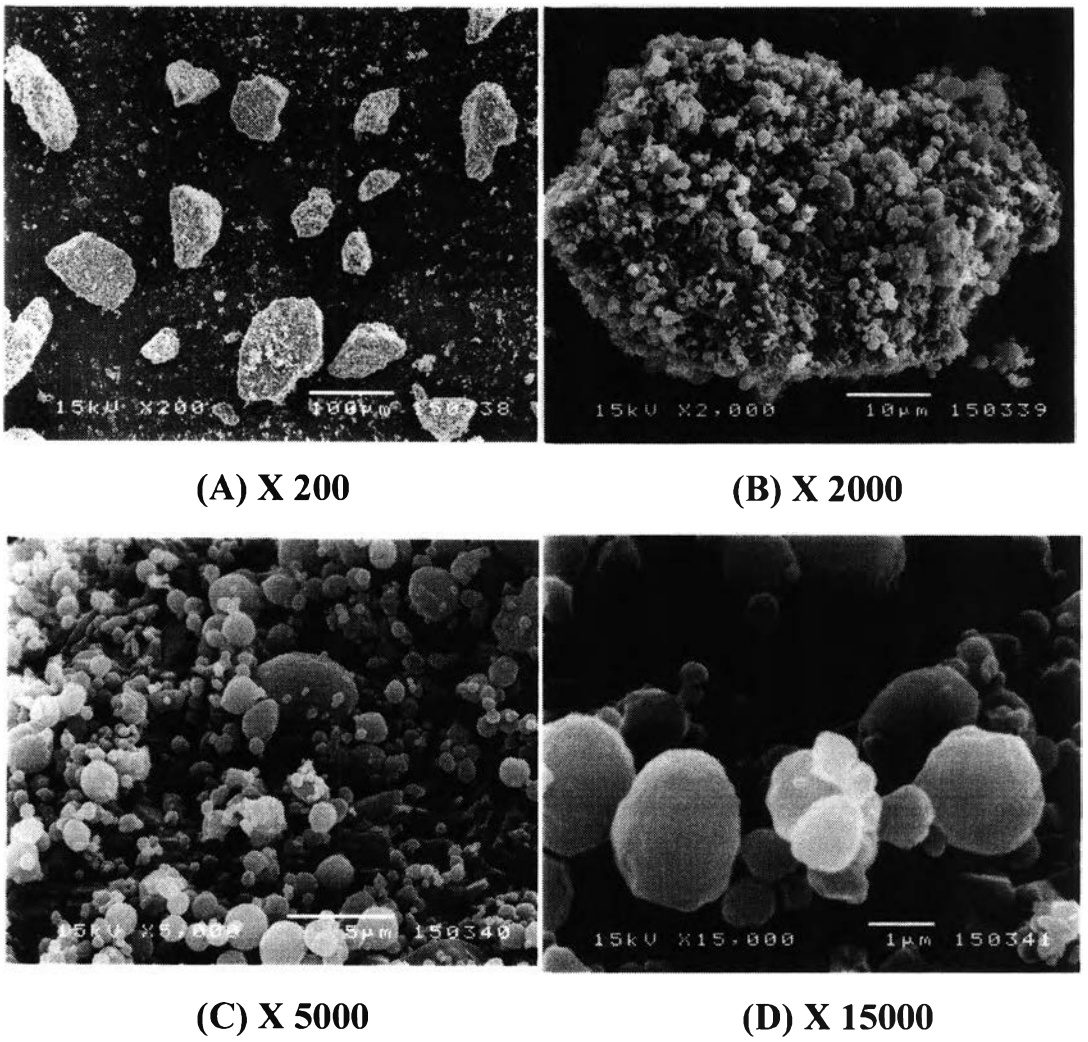

Figure 4-40 SEM photomicrographs of formulation containing 70% L-PLA-rifampicin loaded microparticles and lactose (45-90 µm) in 1: 2 ratio at different magnifications.

The reason for including suitably sized carriers with the micronised drug was to make it less cohesive since the final formulation in an aerosol must flow well so that a reproducible dose would be dispensed from the reservoir. Drug particles detached from the carrier particles if the forces imparted by inhalation exceed the interparticulate forces between drug and carrier particles.

The formula consisting of smaller lactose (< 45μm) provided higher percent fine particle fraction than those of larger lactose (45-90 μm). As shown in Table 4-27, the percent fine faction were 31.24 % and 22.96 % for formulation having smaller lactose (< 45μm) and 45-90 μm lactose, respectively. This result was similar to pervious reports that large carrier particles were shown to exert stronger adhesion forces on drug particles than smaller carriers (Staniforth et al. 1982) and the in vitro respirable fractions of salbutamol from smaller lactose particles have been shown to be higher than those from larger lactose particles (Ganderton and Kassem 1992). The respirable fraction of the drug depends upon the strength of the interaction between drug and carrier particles and the physical properties of both drug and carrier have been shown to influence these interactions (Hickey et al., 1994). Strong adhesion forces resulted in lower amounts of drug detaching from carrier particles.

In addition, Steckel and Muller (1997) pointed out that deposition was found to be highly dependent on the dry powder formulation and fine particle fractions from 10 up to 40 % were observed. At 9 % budesonide in the mixture, they found that a low carrier particle size (< 32 μm) resulted in the highest fine particle fractions (27.48 %) and the medium carrier particle size (63-90 μm) provided fine particle fractions of 23.69 %.

Table 4-27 Percent deposition and fine particle fraction (FPF) of each formula with different lactose size.

% deposition	+Lactose < 45μm average (SD)	+ Lactose 45-90μm average (SD)
Throat	21.16 (2.55)	26.76(5.45)
Presaparator	15.87 (3.28)	10.96(2.71)
Stage 0 (6.2-7.1 μm)*	10.02(0.78)	5.21(0.72)
Stage 1 (4.0-6.2 μm)	10.80(1.11)	7.86(0.35)
Stage 2 (3.2-4.0 μm)	7.59(1.09)	6.14(0.29)
Stage 3 (2.3-3.2 μm)	6.95(0.31)	5.90(0.49)
Stage 4 (1.4-2.3 μm)	3.53(1.05)	1.93(0.88)
Stage 5 (0.7-1.4 μm)	0.71(0.67)	0.53(0.70)
Stage 6 (0.5-0.8 μm)	0.64(0.71)	0.16(0.02)
Stage 7 (0.3-0.5μm)	1.01(0.85)	0.44(0.03)
% Fine particle fraction[a]	31.24(4.88)	22.96(0.96)

[a] Particle size less than 6.2 μm when used flow rate at 60 l/min.
* Aerodynamic diameter of each stage. (Srichana et al. 1998)

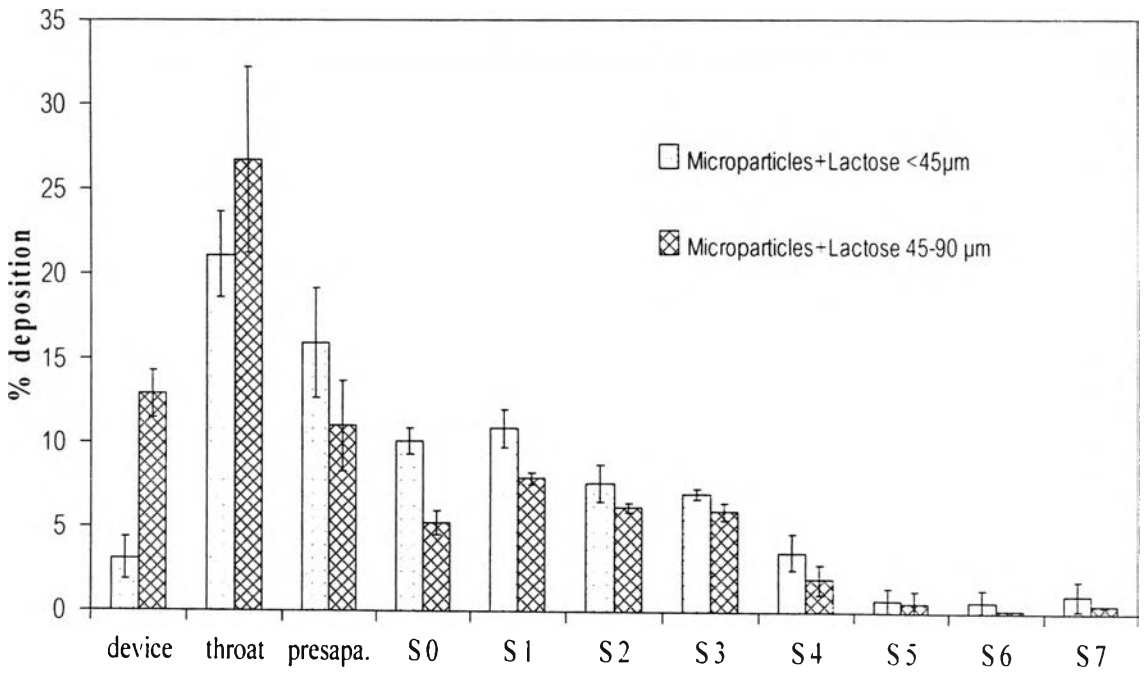

Figure 4-41 Percent drug deposition of formulation containing 70% L-PLA rifampicin loaded microparticles with lactose (< 45μm) in 1: 2 ratio and with lactose (45-90μm) in 1: 2 ratio.

Figure 4-41 shows the results of formulation containing 70% L-PLA rifampicin loaded microparticles with lactose (< 45 μm) in 1:2 ratio and lactose (45-90 μm) in 1:2 ratio where the mass fraction of rifampicin deposited on the device, the throat, preseparator and each stage of the Anderson cascade impactor were shown as a percentage of drug initially contained in the formulation. It was observed that formulation containing smaller lactose could carry out the drug particles to the higher stage than those of larger lactose.

The Andersen cascade impactor permitted direct determination of the drug mass distribution of different aerodynamic size intervals. The percentage particle size distributions of drug depositing on various stages were transformed to a Z-score to obtain the normal distribution. The mass median diameter corresponded to a Z-score of 0 and the geometric standard deviation (G.S.D.) was obtained using the size at Z-score = 1 divided by the size obtained at Z-score = 0 (calculation detail see Table 5-18 and Figure 5-1 in Appendix A).

Table 4-28 summarizes mass median aerodynamic diameter (MMAD) and geometric standard deviation (GSD) of both formulations. The mass median aerodynamic diameter and geometric standard deviation (GSD) of Formula I and Formula II were 4.86 μm, 4.29 μm, 0.63 and 0.66, respectively. The mass median aerodynamic diameters of preparation of both formulations were significantly statistical difference ($p< 0.05$) (Table 5-19 in Appendix).

Although, smaller carrier in formulation higher amount of drug penetrated to the lower stage. The formulation containing small lactose provided larger mass median aerodynamic diameters than those of large lactose. The formulation containing large lactose lost percent particles in device and throat more than those of small lactose (Figure 4-41). It was possible that the microparticles adhered to the larger carrier particles could not detach and deposited with the carrier particles in the device and throat, whereas the rest of the small microparticles were distributed in the impactor according to the aerodynamic properties of the drug-carrier agglomerates. The large value of MMAD for small lactose suggested that those small microparticles were carried out to lower stage.

Table 4-28 Mass median aerodynamic diameter (MMAD) and geometric standard deviation (GSD) of formula I and II.

No.	Formula I		Formula II	
	MMAD	GSD	MMAD	GSD
Sample 1	4.97	0.63	4.61	0.65
Sample 2	4.48	0.65	4.62	0.65
Sample 3	4.89	0.63	4.00	0.66
Sample 4	4.99	0.61	3.98	0.65
Sample 5	4.96	0.63	4.23	0.66
Average (SD)	4.86(0.21)	0.63(0.02)	4.29 (0.31)	0.66 (0.01)

The volume median diameter (VMD) of the microparticles using in those formulation was 3.4 μm. It was shown that the VMD of the same sample determined by laser diffraction was smaller than those of determined by using cascade impactor (MMAD = 4.86 μm) and this discrepancy is probably due to the different principles employed in these methods. The Malvern instrument calculated particle size from the scattering angle of a laser beam induced by the particles dispersed in a liquid (as employed in this study, although the particles may also be dispersed in a gaseous medium) whereas using cascade impactor measured the size of a particle based upon the time required to travel in an air stream across a fixed distance. Both methods, however, confirmed that the L-PLA rifampicin loaded microparticles was of a suitable size to be used in dry powder inhaler formulations.

3. Physicochemical Characterization of Rifampicin and Microparticles

3.1 X-ray Diffraction

Rifampicin exhibits polymorphism due to its complex structure and exists in two polymorphic forms, i.e. form I and form II (Agrawal et al. 2004). It also exists as hydrates and various solvates, which eventually convert into amorphous form at room temperature or after desolvation (Henwood et al. 2001). Agrawal et al. (2004) reported that characteristic peaks of form I were 13.65° and 14.35° 2θ and main X-ray diffractogram (XRD) peaks of form II at 11.10° and 9.93° 2θ. In report of Henwood et al. (2000), the main peaks characteristic of form II at 19.92°, 15.89° and 12.71° 2θ were present in the X-ray diffractogram. In addition, Gallo and Radaelli (1976) also reported XRD pattern of form II.

Unprocessed rifampicin provided XRD peaks at 7.90°, 9.34°, 11.18°, 12.68°, 15.72° and 19.96° 2θ (Figure 4-42, see detail in Appendix Table 5-20). It is possible that raw material rifampicin was form II. The different XRD pattern was found in the X-ray diffractogram of processed rifampicin (Table 5-21 in Appendix). However, a sharp drop in peak intensity counts from about 25,000–5,000 to 7,000–1,500 indicated that less crystalline form was present in this powder. XRD pattern of processed 70% L-PLA with drug was similar with XRD pattern of 100% L-PLA but it had low peak intensity counts (8,000 cps) at 16.34° 2θ comparison with 13,000 cps of 100 % L-PLA at 16.5° 2θ. The XRD pattern of physical mixture of 70 % L-PLA with drug showed both peak of rifampicin form II at 11.10°, 12.7° and 19.9° 2θ and peak of L-PLA at 16.42° 2θ (10,200 cps) (see detail in Appendix Table 5-20–Table 5-24).

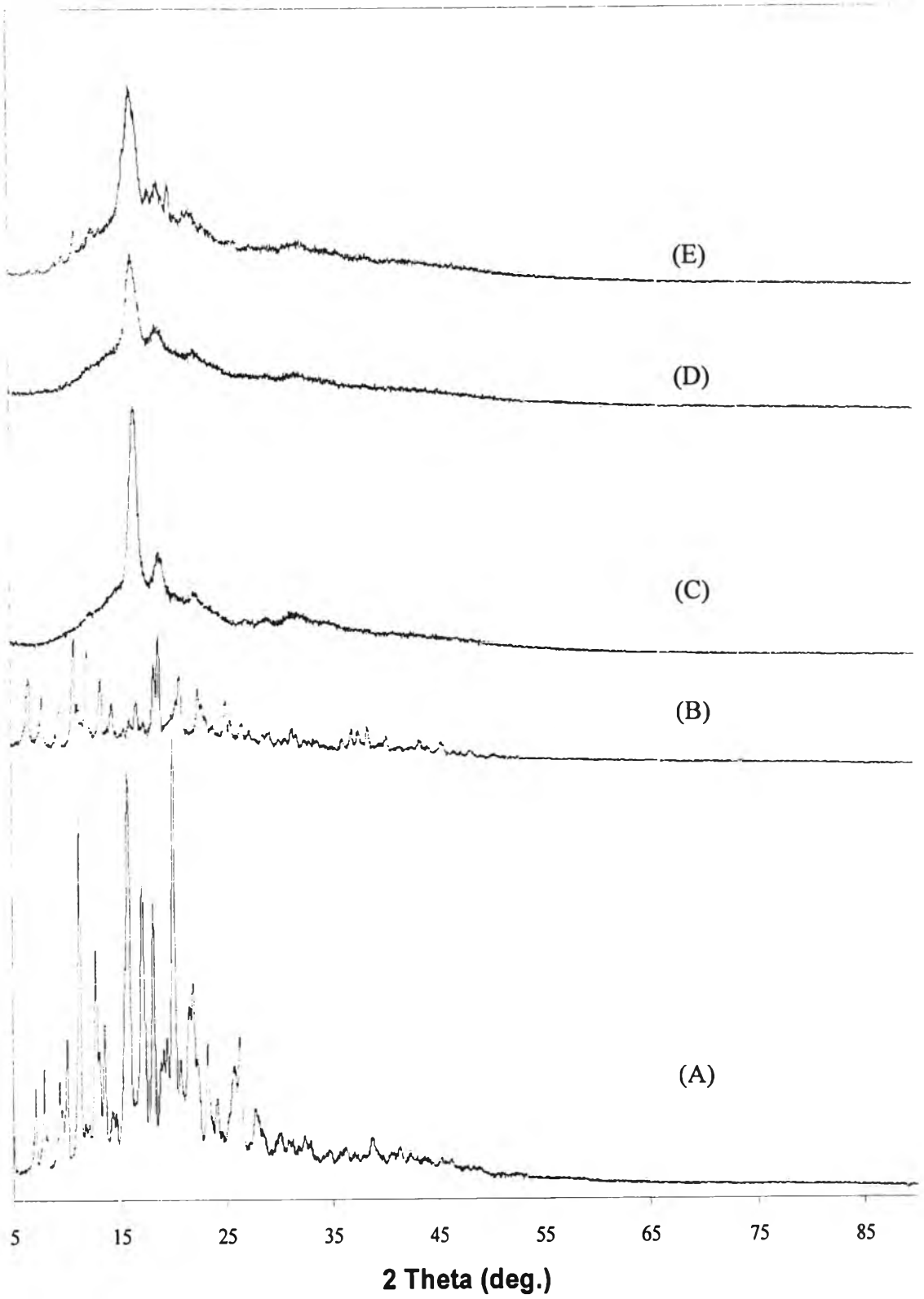

Figure 4- 42 X-ray diffractograms of rifampicin (A), processed rifampicin (B), 100% L-PLA (C), processed 70% L-PLA with drug (D) and physical mixture of 70% L-PLA with drug (E)

3.2 Fourier Transformed Infrared Spectroscopy (FTIR)

Rifampicin exhibits polymorphism due to its complex structure (Figure 4-43) and exists in two polymorphic forms, i.e. form I and form II (Agrawal et al. 2004). The IR spectra of the various forms of rifampicin were previously reported (Gallo and Radaelli 1976, Henwood et al. 2000 and 2001, Agrawal et al. 2004). Three distinct regions in the IR spectrum of rifampicin were identified as characteristic IR vibrations due to the amide moiety, chromophore, and the ansa (pharmacophore C_{20} to C_{27}) chain (Figure 4-43).

The relationship an important part of the ansa chain was the acetyl group at C_{25}, which exhibited bands in three regions of the spectrum corresponding to ν C=O, ν asym C–O–C, and ν sym C–O–C. For rifampicin from II, the ν C_{11}=O in choromophore and ν C_{25}=O in ansa chain are indicated by a 1735 cm^{-1} and 1715 cm^{-1} frequency, respectively (Henwood et al. 2001). In study of Agrawal et al. (2004), double peak due to furanone and acetyl C=O at 1734 and 1712 cm^{-1} was used as a characteristic of form II. In this study, it was found that unprocessed rifampicin had similar double peak due to furanone and acetyl C=O at 1734 and 1712 cm^{-1} in FTIR spectra (Figure 4-44). So, unprocessed rifampicin was characterized as rifampicin form II (see detail in Appendix, Figure 5-2 - Figure 5-6).

Henwood et al. (2001) reported that FTIR spectra of amorphous form I and II had peaks of ν C_{11}=O in choromophore at 1,650 and 1652 cm^{-1} and ν C_{25}=O in ansa chain at 1710 and 1725 cm^{-1}, respectively. FTIR spectra of processed rifampicin contained peak at 1650 and 1722 cm^{-1} (see detail in Appendix, Figure 5-3). The FTIR of processed rifampicin was not corresponding to previous FTIR reports. The absorption band of the –C=O functional group (1759 cm^{-1}) of L-PLA was shown in spectra of physical mixture, processed 70 %L-PLA with drug and pure L-PLA. FTIR spectra of L-PLA, processed 70% L-PLA with drug and physical mixture of 70 % L-PLA with drug were identical.

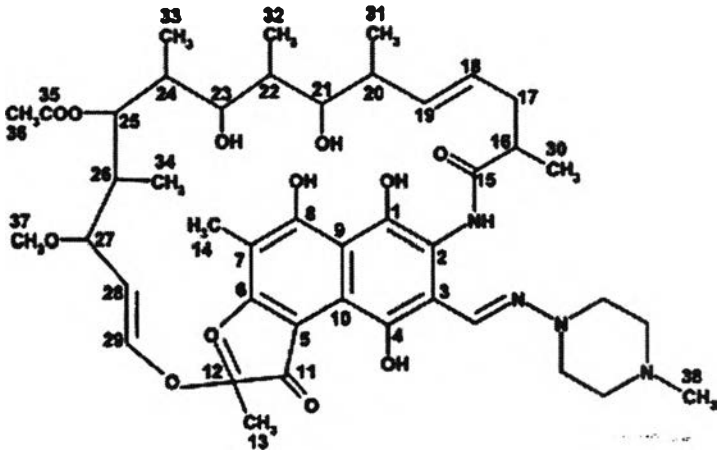

Rifampicin MW= 822.95

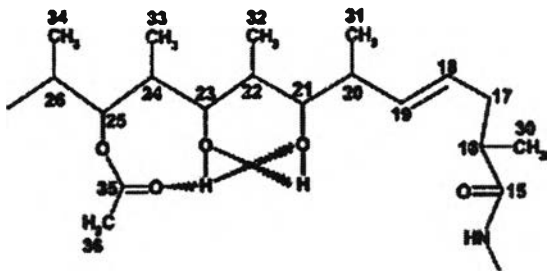

Rifampicin Ansa Chain

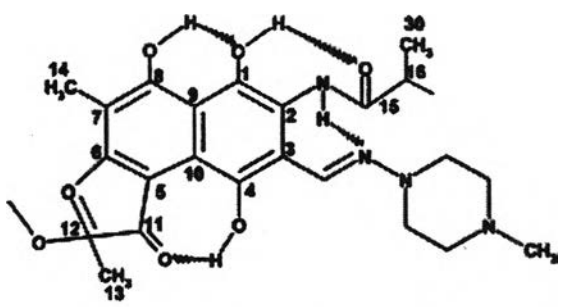

Rifampicin Chromophore

Figure 4-43 Molecular structures of rifampicin, with the chromophore and ansa chain showing the various hydrogen-bonding possibilities.

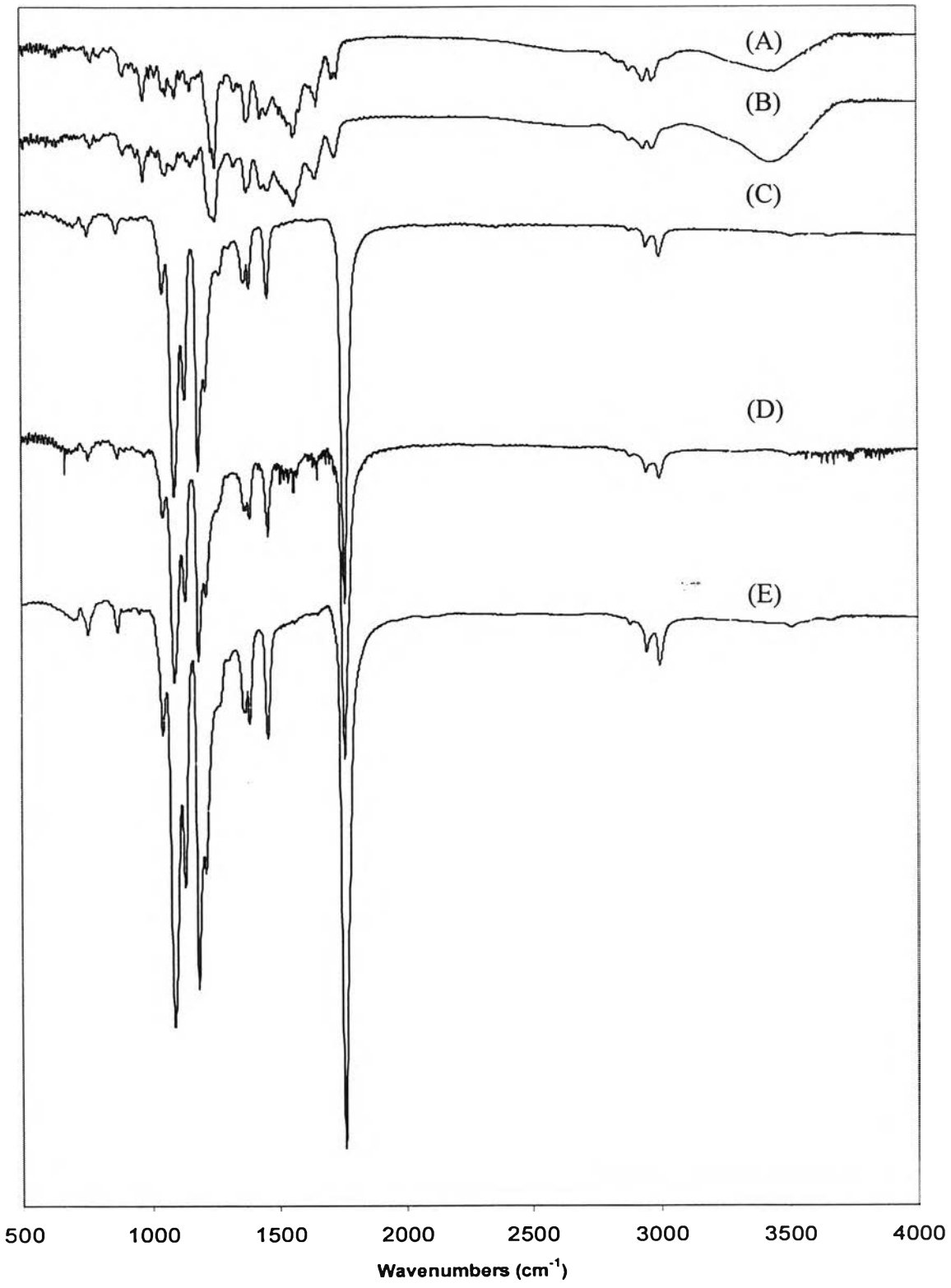

Figure 4-44 IR spectra of rifampicin (A), processed rifampicin (B), 100 % L-PLA (C), processed 70 % L-PLA with drug (D) and physical mixture 70% L-PLA with drug (E).

3.3 Differential Scanning Calorimetry

Differential scanning calorimetry (DSC) thermogram of form I directly shows decomposition as indicated by sharp exotherm at 255–266 °C. Form II shows endotherm at 180–197 °C immediately followed by recrystallization to form I (exotherm at 197–223 °C) which is a characteristic of solid–liquid–solid transition and finally decomposed at 247–266 °C (Figure 4-45 a). DSC thermogram unprocessed rifampicin (Figure 4-46) was comparable with that reported for form II (Agrawal et al. 2004) The powder showed an endotherm at 188–193 °C, corresponding to melting of the powder. It was immediately followed by an exotherm, which corresponded to recrystallization of the melt. The melt decomposed exothermally at around 250 °C.

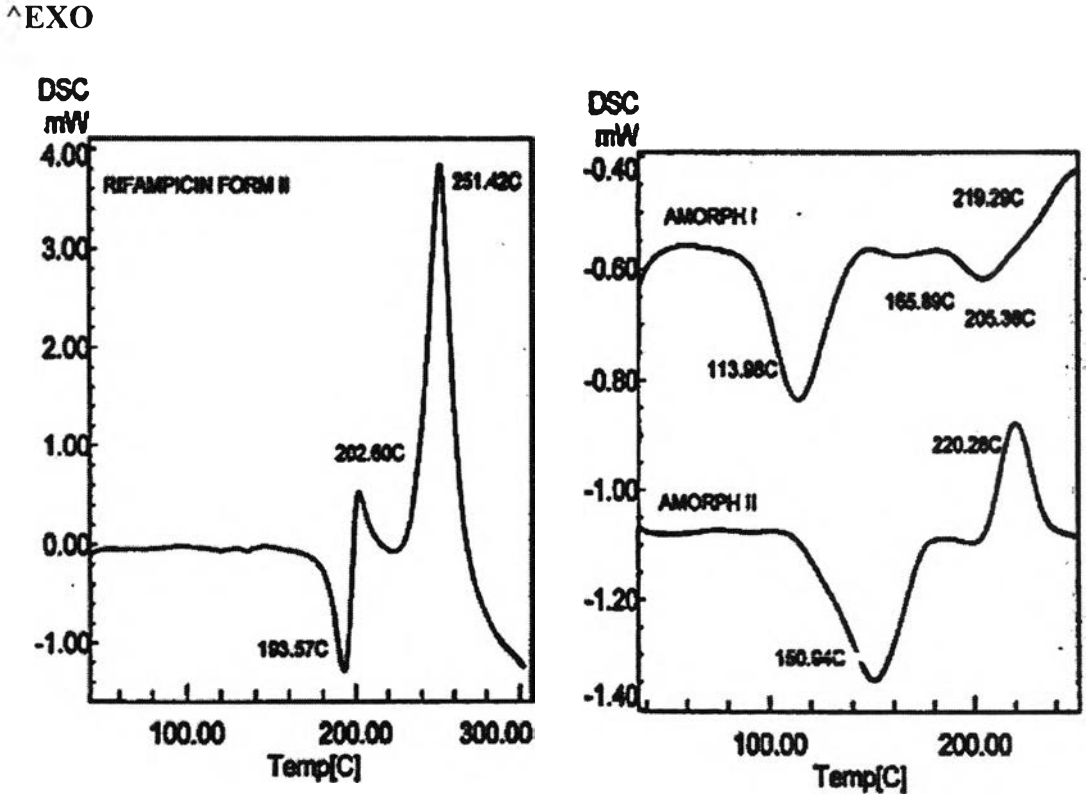

(a) **(b)**

Figure 4-45 DSC thermograms of rifampicin form II (a) and amorphous I and II (b) (Henwood et al. 2001).

In the thermogram of an amorphous form I, endotherm at 114 °C and decomposition at 219 °C–243 °C were seen. The second amorphous (II) displayed endotherm at 151°C, with a large exotherm at 188 °C–220 °C (Figure. 4-45(b)) (Henwood et al. 2001). Thermogram of processed rifampicin (Figure. 4-46) showed distinct endotherm at a lower temperature (160–170 °C). The temperature at which decomposition occurred was around 250 °C. DSC thermogram of processed rifampicin was not corresponding to that of rifampicin in the previous reports (Henwood et al, 2001 and Agrawal et al. 2004).

DSC thermogram of processed 100 % L-PLA showed melting temperature (T_m) at 180 °C. DSC thermogram of processed 70 % L-PLA with drug showed endotherm of L-PLA at 180 °C and exothermal of rifampicin decomposed at around 250 °C. DSC thermogram of physical mixture 70 % L-PLA with drug (Figure 4-46) was comparable with processed 70 % L-PLA with drug.

The thermograms of L-PLA depicted the melting temperature (T_m). As can be seen from the thermograms, T_m of L-PLA remained within 170–180 °C. T_m of processed 70%-L-PLA, physical mixture and pure L-PLA were 172.44 °C, 176.26 °C and 176.75 °C, respectively. T_g of processed 70 % L-PLA with drug was obviously 66.12 °C where as T_g of physical mixture and pure L-PLA exhibited a flatter thermal change which remained within 60–70 °C.

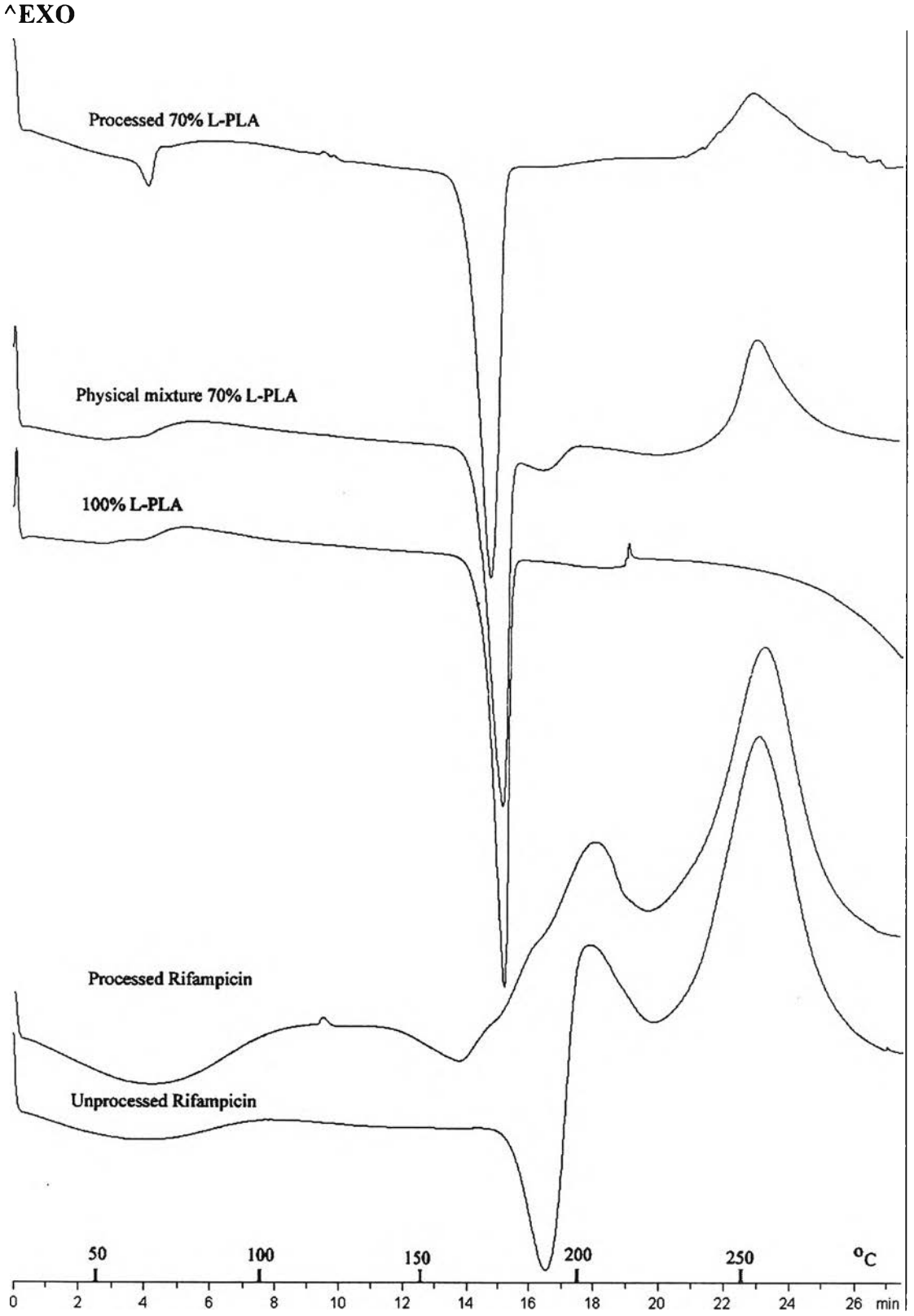

Figure 4-46 DSC thermograms of rifampicin, processed rifampicin, 100 % L-PLA, physical mixture 70 % L-PLA with drug and processed 70 % L-PLA with drug

4. Effect of Processing on Stability of Rifampicin

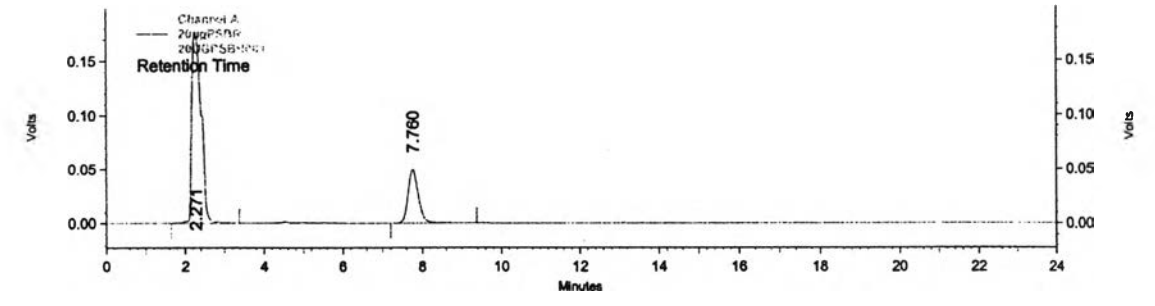

(A)

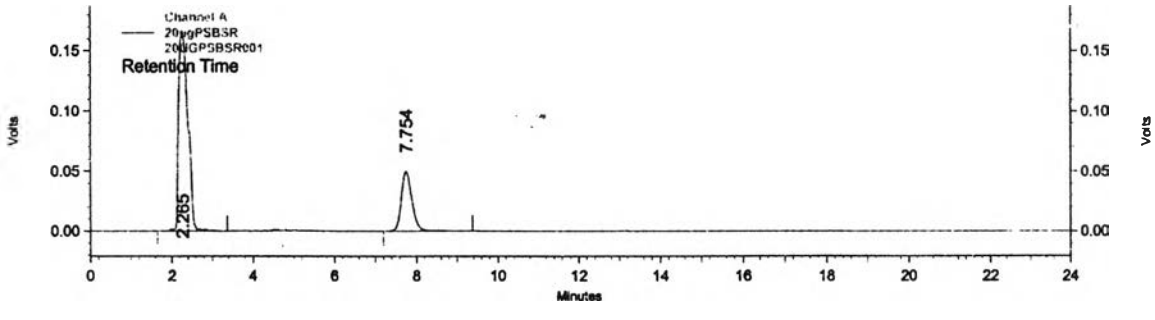

(B)

Figure 4-47 HPLC chromatograms of rifampicin (A) and processed rifampicin (B).

Processed rifampicin was tested by HPLC to assess if any decomposition occurred due to SAS processing. The typical results of HPLC analysis are shown in Figure 4-47. The two traces were referred to unprocessed and processed rifampicin. The characteristic peak of rifampicin was the same in the two traces, no other peaks, related to decomposition products, were present. % Rifampicin contents of unprocessed rifampicin and processed rifampicin in Table 4-29 were not significantly statistical difference (Table 5-25 in Appendix).

Table 4-29 Percent rifampicin content of unprocessed rifampicin and processed rifampicin.

Sample	% Rifampicin content
Unprocessed rifampicin	100.09
Unprocessed rifampicin	100.66
Unprocessed rifampicin	100.69
Average (SD)	100.48 (0.34)
Processed rifampicin	100.19
Processed rifampicin	100.32
Processed rifampicin	100.12
Average (SD)	100.21 (0.10)

5. Determination of Residual Methylene Chloride Content in the Microparticles.

Amount of residual organic solvent after production was important because the toxicity of methylene chloride which was classified as class 2 solvent: suspect animal carcinogens or possible cause of other irreversible toxicity, such as neurotoxicity or teratogenicity. The United Stated Pharmacopeia indicated the limits for dichloromethane in preparation was less than 500 ppm (USP).

The calibration curve of methylene chloride concentration and area of peak by GC method was depicted in Figure 4-46. Amount of residual dichloromethane in preparation of 70 % L-PLA rifampicin loaded microparticles was lower than the USP limits (Table 4-29). It was revealed that those microparticles contained only 11.82 ppm of methylene chloride.

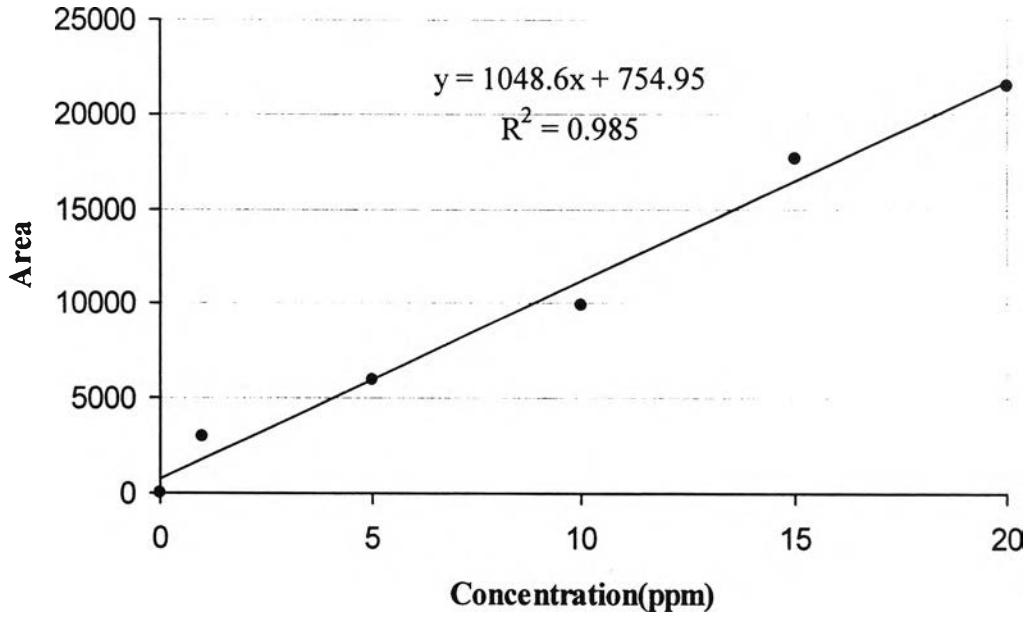

Figure 4-48 Calibration curve of dichloromethane concentration and peak area determination with GC method.

Table 4-30 Residual dichloromethane of 70% L-PLA rifampicin loaded microparticles prepared by SAS technique.

No.	Area	Concentration (ppm)	Weight of sample (mg)	Residual dichloromethane (ppm)
Sample 1	5,788	4.80	11.20	11.36
Sample 2	4,903	3.96	9.80	10.70
Sample 3	6,211	5.20	10.30	13.39
			Average	11.82
			SD	1.40

6. Effect of molecular weight of L-PLA

Using high molecular weight of L-PLA above 150,000 (L-PLA M3, Fluka) in preparation, it was found that fibers were formed (Figure 4-49). It was possible that the higher viscosity of high molecular weight polymer obstructed the formation of droplets from nozzle. In the similar result, increasing percentage of polymer in formulation caused the formation of fibers; Randolph et al (1993) observed fiber formation at solution concentrations exceeding 4 %w/v. L-PLA in methylene chloride. Similar observation was also reported for the polystyrene/toluene/CO_2 system, where a critical composition of approximately 5 % w/v was reported (Dixon et al. 1993).

Polymer of Fluka	Molecular weight
L-PLA M1	~67,400 Da
L-PLA M2	~101,700 Da
L-PLA M3	~152,000 Da

Where polymer concentration in the starting solution was maintained constant, the spray globule size increased with polymer MW due to enhanced intermolecular forces between polymer chains (Bodmeier and Chen 1988), until a limiting Mw was reached, where no microspheres, result due to insufficient force to break up the stream of feed solution.

Figure 4-50 and 4-51 show the particle size distribution by volume and percent cumulative undersize of rifampicin-L-PLA microparticles produced from various molecular weights of polymer, respectively. It was shown that products of L-PLA M1 and L-PLA M2 almost overlapped and had narrow particle size distribution. But the product of L-PLA M3 had very large diameter and broad distribution curve.

L-PLA M1

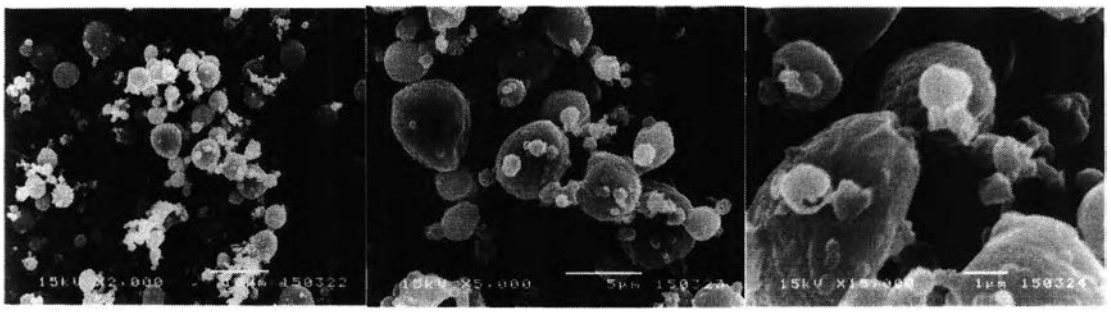

X 2000 **X 5000** **X 15000**

L-PLA M2

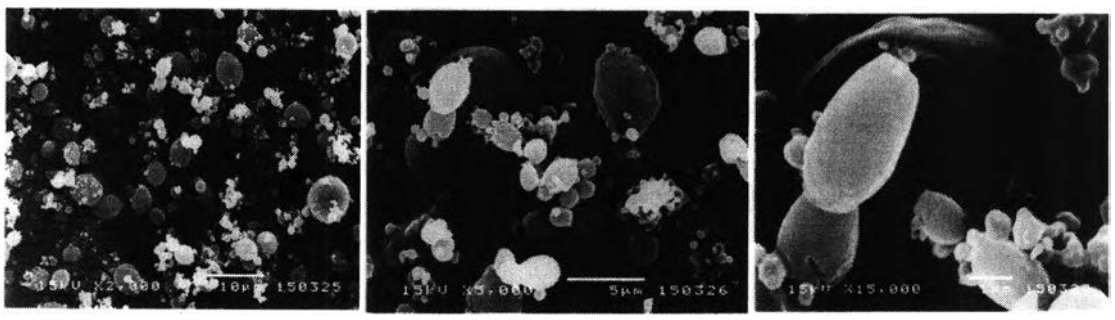

X 2000 **X 5000** **X 15000**

L-PLA M3

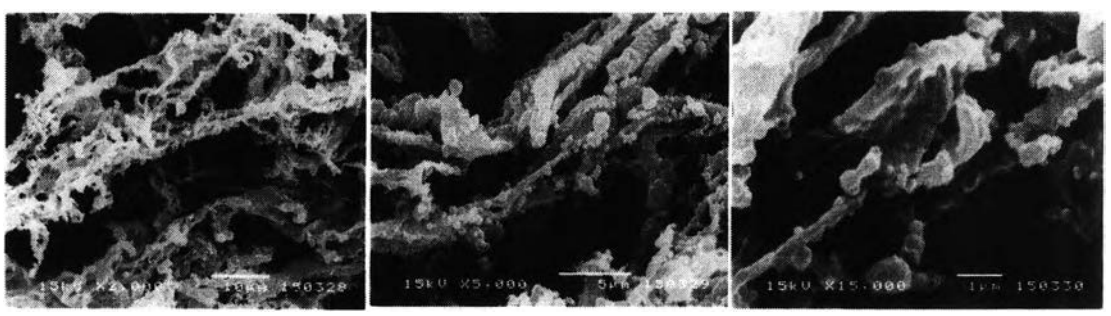

X 2000 **X 5000** **X 15000**

Figure 4-49 SEM photomicrographs of rifampicin-L-PLA microparticles produced from various molecular weights of polymer.

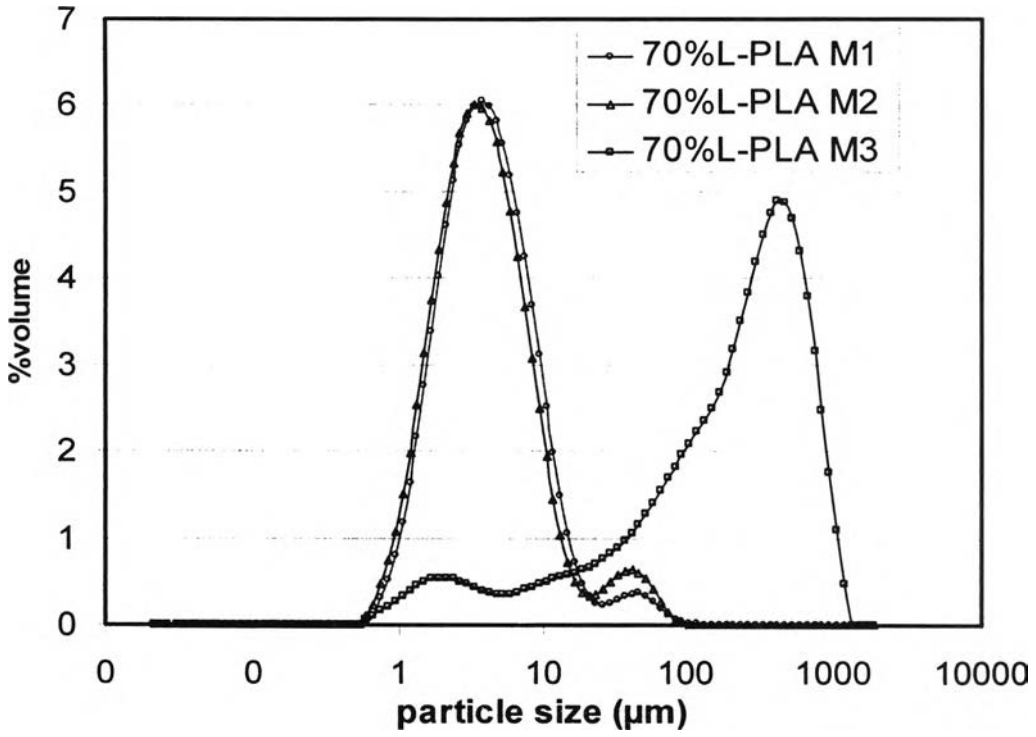

Figure 4-50 The particle size distribution by volume of rifampicin-L-PLA microparticles produced from various molecular weights of polymer.

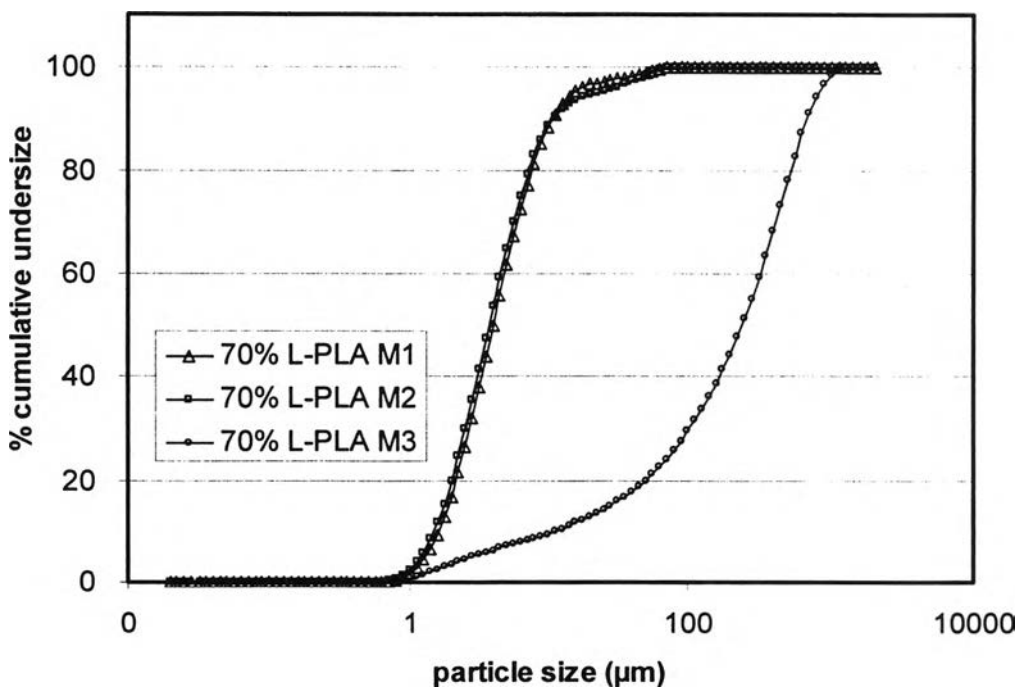

Figure 4-51 The percent cumulative undersize of rifampicin-L-PLA microparticles produced from various molecular weights of polymer.

Table 4-31 and Table 4-32 summarize the effect of polymer molecular weight on particle size and % particle size of 1-5 μm and < 5 μm of rifampicin-L-PLA microparticles, respectively. The microparticles having size 1-5 μm using L-PLA M1 and L-PLA M20 % were approximately 57 % and the volume median diameter of microparticles were 3.99 μm and 3.73 μm, respectively. The size of L-PLA M1 and L-PLA M2 microparticles was very smaller than size of L-PLA M3 microparticles. The particles sizes of L-PLA M1 and L-PLA M2 loaded microparticles were comparable to L-PLA of Sigma microparticles. It was no statistically significant difference on $D_{50\%}$ of the microparticles generating from L-PLA M1, L-PLA M2 and L-PLA of Sigma (Table 5-26 in Appendix).

Table 4-31 Effect of polymer molecular weight on particle size of rifampicin-L-PLA microparticles.

MW	**$D_{10\%}$** (μm)	**$D_{50\%}$** (μm)	**$D_{90\%}$** (μm)	**Span**
	average (SD)	average (SD)	average (SD)	average (SD)
70% L-PLA M1	1.62(0.07)	3.99(0.10)	10.85(0.92)	2.31(0.25)
70% L-PLA M2	1.49(0.03)	3.73(0.18)	11.73(3.18)	2.72(0.74)
70% L-PLA M3	11.19(1.43)	243.16(3.96)	684.03(71.13)	2.77(0.27)

Table 4-32 Effect of polymer molecular weight on % particle size of 1-5 μm and < 5 μm of rifampicin-L-PLA microparticles.

MW	**% Particle** 1-5 μm	**% Particle** < 5 μm
	average (SD)	average (SD)
70% L-PLA M1	56.16(2.71)	57.89(2.23)
70% L-PLA M2	58.54(2.51)	61.13(2.63)
70% L-PLA M3	6.00(0.31)	6.81(0.33)

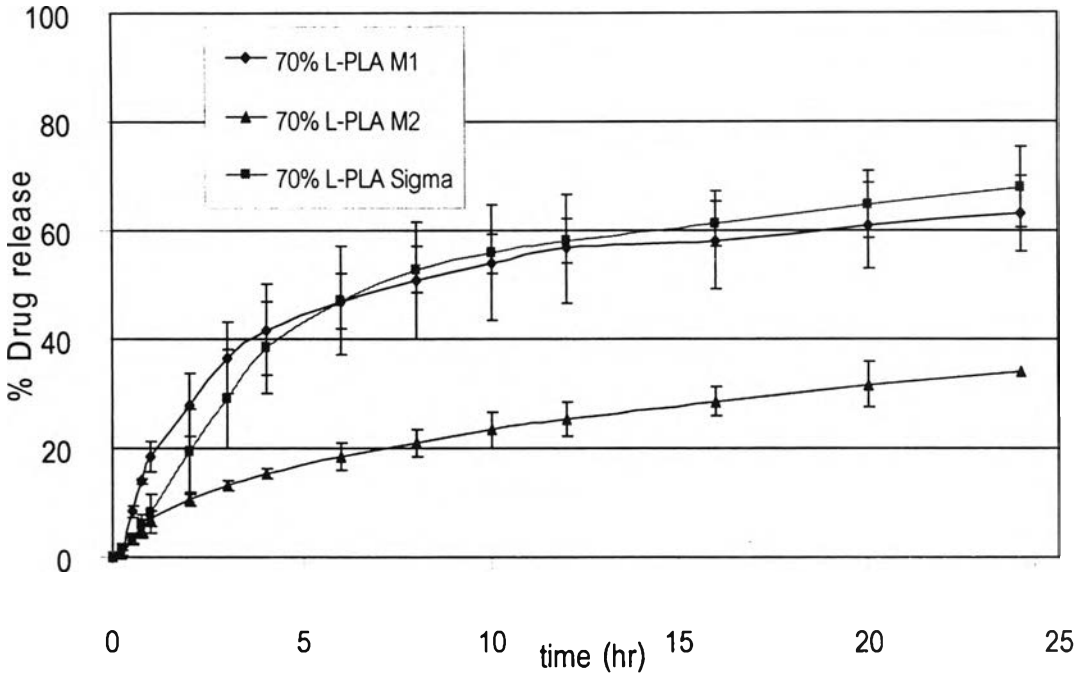

Figure 4-52 Dissolution curve of rifampicin-L-PLA microparticles produced from various molecular weights of polymer.

Figure 4-52 shows dissolution curve of rifampicin-L-PLA microparticles produced from various molecular weights of polymer. The dissolution rate of 70 % L-PLA M1 rifampicin loaded microparticles was dramatically higher than those of 70 % L-PLA M2 rifampicin loaded microparticles. It might be possible that water difficultly penetrated into the matrix because the high molecular weight of L-PLA M2 had poor wettability and higher hydrophobicity than L-PLA M1.

Figure 4-53 shows SEM photomicrographs of 70 % L-PLA M1 and 70 % L-PLA M2 rifampicin loaded microparticles after release process. It was observed that those microparticles after release exhibited smaller pore on surface of microparticles and their shape were not changed. This pore might occur after drug diffusion through the polymer matrix.

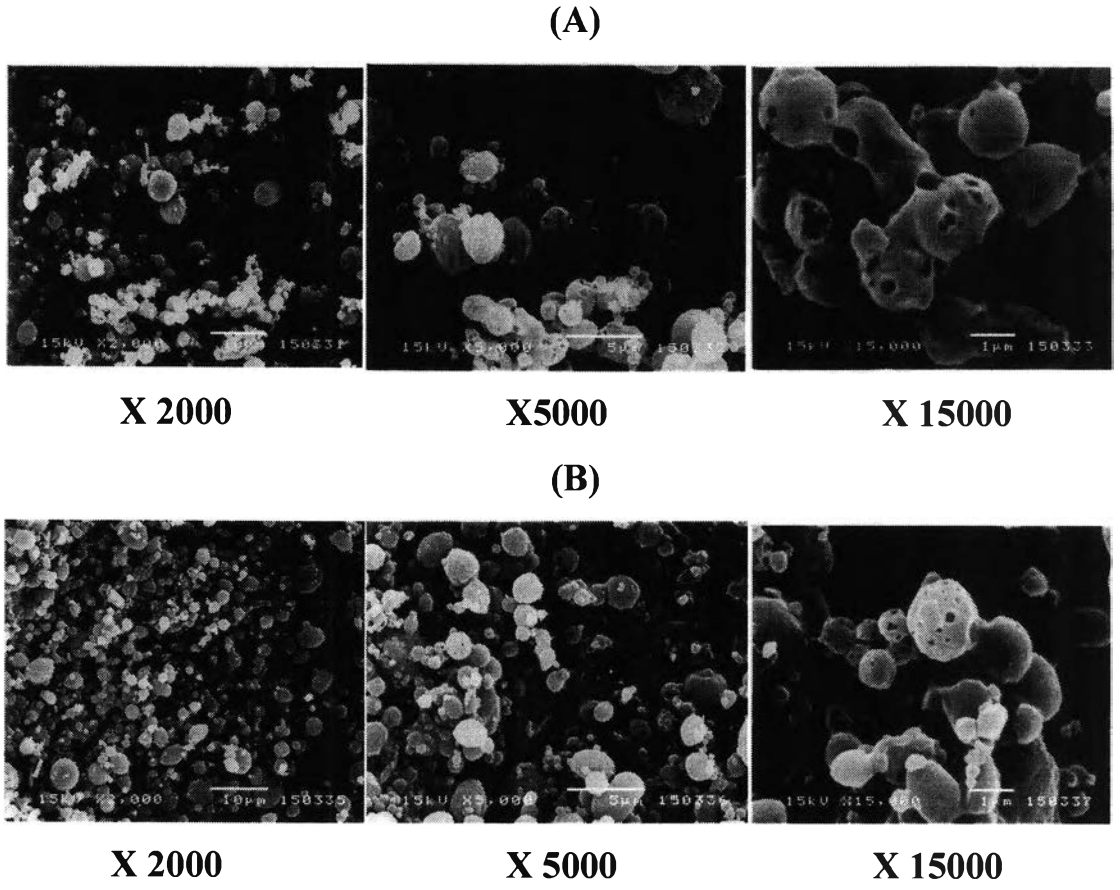

Figure 4-53 SEM photomicrographs of rifampicin-L-PLA microparticles after drug release process from various molecular weights of polymer (A) 70 % L-PLA M1 (B) 70 % L-PLA M2.

Table 4-33 Difference factor and similarity factor of dissolution profiles of L-PLA rifampicin microparticles from different polymer molecular weights.

Batch	Difference factor (f_1)	Similarity factor (f_2)
70% L-PLA M1/ 70% L-PLA M2	56.05	55.50
70% L-PLA M2/ 70% L-PLA sigma	53.81	52.22
70% L-PLA M1/ 70% L-PLA sigma	11.09	89.55

Table 4-33 reports difference factor (f_1) and similarity factor (f_2) of L-PLA rifampicin microparticles from different polymer molecular weights and different source. The molecular weight of L-PLA from Sigma was 85,000-160,000 Da whereas those of L-PLA M1 and L-PLAM2 from Fluka were approximately 67,400 Da and 101,700 Da, respectively. The molecular weight of L-PLA from Sigma and L-PLAM2 from Fluka were comparable. But their dissolution profiles were distinctly different. The dissolution profiles of L-PLA M1 / L-PLA (Sigma) drug loaded microparticles; the difference factor (f_1) and similarity factor (f_2) value obtained were 11.09 and 89.55, respectively. It was indicated that those dissolution profiles were similar. Comparing the dissolution profiles of L-PLA M2 / L-PLA (Sigma) drug loaded microparticles; the difference factor (f_1) and similarity factor (f_2) value obtained were 53.81 and 52.22, respectively. It was indicated that those dissolution profiles were different. For dissolution profiles of L-PLA M1 / L-PLA M2 drug loaded microparticles; the difference factor (f_1) and similarity factor (f_2) value obtained were 56.05 and 55.50, respectively. This data also indicated that those dissolution profiles were different. These results were shown that not only molecular weight of polymer but also source of polymer influenced the characteristic of microparticles.

7. Bactericidal Efficacy of the Drug-Loaded Microparticles Against *Mycobacterium Tuberculosis*.

The rifampicin, biodegradable polymer (L-PLA) and rifampicin L-PLA loaded microparticles preparing by SAS process were tested for their clinical antimycobacterial activity against isolates of *Mycobacterium tuberculosis* H37Rv and other mycobacteria. *Mycobacterium tuberculosis* isolated from 5 resistant and 20 susceptible to rifampicin patients and *Mycobacterium tuberculosis* (H37Rv), a standard strain were concurrently tested for in vitro susceptibility to rifampicin. In addition, Mycobacterium resisted to rifampicin, *Mycobacterium fortuitum* and *Mycobacterium avium complex*, were also concurrently tested. The cultures were plated on Middlebrook 7H10 agar plates supplemented with OADC. The plates were incubated at 37 °C for 28 days and counted the colony growth.

A formulation containing 60% L-PLA and 40% rifampicin had good core loadings (24%) and size 4 μm by volume but their release of drug was premature and too fast. Formulation containing 70% L-PLA and 30% rifampicin was acceptable because it had good core loadings (16.1%) and size 3.4 μm by volume and with MMAD ~ 4.8μm. In addition, it showed that sustained in vitro release during 24 hours. It was used this experiment.

The strain of bacteria and its number used in this experiment is shown in Table 4-34. Table 4-35 illustrates the number of colony of *Mycobacterium* growth in 28 days in a code for reading results in Table 4-36 and Table 4-37. Table 4-36 and Table 4-37 contain data of bactericidal efficacy of rifampicin, rifampicin-polymer microparticles and polymer against *M. Tuberculosis* on agar at 28 days by using dimethyl formamide and method as a solvent, respectively.

Table 4-34 The strain of bacteria used in experiment.

Sample	Strain of bacteria
No.1	*Mycobacterium fortuitum*
No.2	*Mycobacterium avium complex*
No.3 - 7	*Mycobacterium tuberculosis* Rifampicin resistant strains
No.8 - 27	*Mycobacterium tuberculosis* Rifampicin sensitive strains
No.28 -30	*Mycobacterium tuberculosis* Standard strain (H37Rv)

Table 4-35 The number of colony of *Mycobacterium* growth in 28 days.

Code in Table	Number of colony growth
1 – 50	actual count
1+	51 - 100
2+	101 -200
3+	201 - 500
4+	>500

Table 4-36 Bactericidal Efficacy of rifampicin, rifampicin-polymer microparticles and polymer against *M. Tuberculosis* on agar at 28th day.

No. / Colony number	Control	Rifampicin (DM**) (μg/ml)			Rifampicin +Polymer (DM) (μg/ml)			Polymer (DM) (μg/ml)		
		0.5	1.0	2.0	0.5	1.0	2.0	0.5	1.0	2.0
1	4+	4+	4+	4+	4+	4+	4+	4+	4+	4+
2	4+	4+	4+	4+	4+	4+	4+	4+	4+	4+
3	3+	3+	3+	3+	3+	3+	3+	3+	3+	3+
4	2+	2+	2+	2+	2+	2+	2+	2+	2+	1+
5	1+	1+	50	10	1+	50	-	1+	50	30
6	2+	2+	2+	2+	2+	1+	50	2+	2+	30
7	2+	2+	2+	2+	2+	2+	2+	2+	2+	2+
8	3+	60	-	-	20	-	-	3+	3+	3+
9	4+	50	-	-	-	-	-	2+	2+	2+
10	4+	30	-	-	20	-	-	4+	4+	4+
11	4+	14	-	-	4	-	-	4+	4+	4+
12	2+	20	-	-	20	-	-	2+	2+	20
13	1+	-	-	-	-	-	-	1+	1+	1+
14	3+	34	-	-	30	-	-	3+	3+	3+
15	2+	20	-	-	20	-	-	2+	2+	2+
16	2+	1+	-	-	4	-	-	2+	2+	2+
17	4+	1+	-	-	80	-	-	4+	4+	4+
18	4+	1+	-	-	80	-	-	4+	4+	4+
19	3+	12	-	-	6	-	-	3+	3+	3+
20	4+	1+	-	-	50	-	-	4+	4+	4+
21	4+	40	-	-	30	-	-	4+	4+	4+
22	2+	-	-	-	-	-	-	2+	2+	2+
23	2+	-	-	-	-	-	-	2+	2+	2+
24	4+	50	-	-	50	-	-	4+	4+	4+
25	4+	60	-	-	20	-	-	4+	4+	4+
26	1+	22	-	-	30	-	-	3+	3+	3+
27	2+	10	-	-	-	-	-	2+	2+	2+
28	2+	-	-	-	-	-	-	2+	2+	2+
29	2+	-	-	-	-	-	*	2+	2+	2+
30	6	*	*	*	*	*	*	*	*	*

- no growth of bacteria *no data obtained because of failure of bacterial growth

** used dimethyl formamide as a solvent

Table 4-37 Bactericidal Efficacy of rifampicin, rifampicin-polymer microparticles and polymer against *M. Tuberculosis* on agar at 28th day.

No. / Colony number	Control	Rifampicin (Me**) (μg/ml)			Rifampicin +Polymer (Me) (μg/ml)			Polymer (Me) (μg/ml)		
		0.5	1.0	2.0	0.5	1.0	2.0	0.5	1.0	2.0
1	4+	4+	4+	4+	4+	4+	4+	4+	4+	4+
2	4+	4+	4+	4+	4+	4+	4+	4+	4+	4+
3	3+	3+	3+	3+	3+	3+	3+	3+	3+	3+
4	2+	2+	2+	2+	2+	2+	2+	2+	2+	2+
5	1+	50	50	4	50	-	-	50	50	30
6	2+	2+	1+	1+	2+	1+	1+	2+	2+	50
7	2+.	2+	2+	2+	2+	2+	-	2+	2+	2
8	3+	60	-	-	20	-	-	3+	3+	3+
9	4+	50	-	-	-	-	-	2+	2+	2+
10	4+	30	-	-	30	-	-	4+	4+	4+
11	4+	35	-	-	14	-	-	4+	4+	4+
12	2+	50	-	-	2	-	-	2+	2+	2+
13	1+	-	-	-	-	-	-	1+	1+	1+
14	3+	12	-	-	36	-	-	C	3+	3+
15	26	40	-	-	20	-	-	2+	2+	2+
16	2+	2	-	-	11	-	-	2+	2+	2+
17	4+	1+	-	-	70	-	-	4+	4+	-
18	4+	1+	-	-	70	-	-	4+	4+	4+
19	3+	18	-	-	-	-	-	3+	3+	-
20	4+	1+	-	-	50	-	-	4+	4+	4+
21	4+	40	-	-	30	-	-	4+	4+	4+
22	2+	4	-	-	-	-	-	2+	2+	2+
23	2+	-	-	-	-	-	-	2+	2+	2+
24	4+	65	-	-	42	-	-	4+	4+	4+
25	4+	1+	-	-	10	-	-	4+	4+	4+
26	3+	30	-	-	20	-	-	3+	3+	3+
27	2+	1	-	-	-	-	-	2+	2+	2+
28	2+	-	-	-	-	-	-	2+	2+	-
29	2+	-	-	-	-	-	-	2+	2+	2+
30	5	*	*	*	*	*	*	*	*	*

- no growth of bacteria *no data obtained because of failure of bacterial growth

** used methanol as a solvent

The rifampicin and rifampicin-polymer microparticles had no inhibitory effect against *Mycobacterium fortuitum, Mycobacterium avium complex* and *Mycobacterium Tuberculosis* rifampicin resistant strains. However rifampicin showed the inhibitory effect against *Mycobacterium Tuberculosis* rifampicin sensitive strains at concentration 1 μg/ml and this result was similar to that of rifampicin-polymer microparticles. But the polymer could not inhibit the growth of all bacteria.

For *Mycobacterium tuberculosis* standard strain (H37Rv) did not grow in the agar plates containing rifampicin as same as rifampicin-polymer microparticles at concentration 0.5 μg/ml. This result indicated that bactericidal efficacy of rifampicin and rifampicin loaded microparticles were equal. Similar findings were also obtained when dimethyl formamide and methanol were used as solvent in Table 4-36 and Table 4-37, respectively. It was shown that the SAS process produced rifampicin loaded microparticles did not change the bactericidal efficacy of rifampicin.